



**CONTRACT NO. A832-133**  
**FINAL REPORT**  
**JUNE 1991**

**Diagnostic Analysis of  
Wind Observations Collected  
during the Southern California  
Air Quality Study**

QC  
9/15  
1991  
1/6/91  
1991

**State of California  
AIR RESOURCES BOARD  
Research Division**



**DIAGNOSTIC ANALYSIS OF WIND  
OBSERVATIONS COLLECTED DURING THE  
SOUTHERN CALIFORNIA AIR QUALITY STUDY**

**FINAL REPORT  
CONTRACT NO. A832-133**

Prepared for:

Research Division  
California Air Resources Board  
1102 Q Street  
P.O. Box 2815  
Sacramento, CA 95812

Submitted by:

Systems Applications International  
101 Lucas Valley Road  
San Rafael, California 94903

Prepared by:

Sharon G. Douglas  
Robert C. Kessler  
Christopher A. Emery  
Janice L. Burtt

**JUNE 1991**



## **Abstract**

One objective of the Southern California Air Quality Study (SCAQS) was to acquire an improved understanding of pollutant transport within the South Coast Air Basin (SOCAB). The complex meteorology of the SOCAB governs the transport of pollutants within the basin and through its boundaries. Thus, a thorough understanding of the mesoscale airflow patterns in the SOCAB is critical to understanding pollutant transport in the basin.

Wind data collected during eight intensive monitoring periods in the 1987 SCAQS were used to analyze the mesoscale airflow patterns in the SOCAB. The SCAQS data base contains the most comprehensive set of surface and upper-air wind data ever assembled for the SOCAB. The data set represents good spatial and temporal resolution of some mesoscale airflow features.

The wind data were analyzed using the SAI Diagnostic Wind Model (DWM). In this model, observational wind data are incorporated into a first-guess field that consists of a domain-mean wind that has been adjusted for terrain effects. The analysis consisted of (1) generation of hourly, gridded wind fields for the 17 SCAQS intensive study days using the DWM, (2) analysis of the mesoscale airflow patterns, and (3) calculation of forward and backward particle trajectories to examine pollutant transport in the SOCAB.



## **Disclaimer**

The statements and conclusions in this report are those of the Contractor and not necessarily those of the California Air Resources Board. The mention of commercial products, their source or their use in connection with material reported herein is not to be construed as actual or implied endorsement of such products.



## **Contents**

1	<b>INTRODUCTION</b>	1
2	<b>GENERATION OF WIND FIELDS AND ANALYSIS OF AIRFLOW PATTERNS</b>	8
	Diagnostic Wind Model	8
	General Procedures	9
	Summer Intensive Monitoring Periods	10
	Autumn Intensive Monitoring Periods	15
3	<b>PARTICLE PATH ANALYSIS</b>	18
	Calculation of Particle Paths	18
	Summer Particle Paths	31
	Autumn Particle Paths	32
	Comparison with Tracer Data	33
	Uncertainty Analysis	34
	<b>References</b>	43
	<b>Appendix A: SCAQS Wind Monitoring Sites</b>	
	<b>Appendix B: SCAQS Diagnostic Wind Analyses</b>	
	<b>Appendix C: Particle Paths</b>	



## 1 INTRODUCTION

One objective of the 1987 Southern California Air Quality Study (SCAQS) was to acquire an improved understanding of pollutant transport within the South Coast Air Basin (SOCAB). The complex meteorology of the SOCAB governs the transport of pollutants within the basin and through its boundaries. Thus, a thorough understanding of the mesoscale airflow patterns in the SOCAB is critical to understanding pollutant transport in the basin.

Wind data collected during eight intensive monitoring periods in the SCAQS were used to analyze the mesoscale airflow patterns in the SOCAB. The SCAQS data base contains the most comprehensive set of surface and upper-air wind data ever assembled for the SOCAB. High spatial and temporal resolution wind measurements are available for 17 intensive study days representing both summer and autumn air-quality episodes:

19 June,  
24-25 June,  
13-15 July,  
27-29 August,  
2-3 September,  
11-13 December,  
3 December, and  
10-11 December.

The data set represents data good spatial and temporal resolution of some mesoscale airflow features. The SCAQS surface wind monitoring sites are listed in Table 1-1; the upper-air wind monitoring sites are listed in Table 1-2. Data availability varied from episode to episode. Plots of the surface and upper-air wind monitoring site locations for each episode are given in Appendix A.

The wind data were analyzed using the Systems Applications International (SAI) Diagnostic Wind Model (DWM) (Douglas et al., 1990). Using this model, observational wind data are incorporated into a first-guess field that consists of a domain-mean wind that has been adjusted for terrain effects. Figure 1-1 illustrates the complex topography of the SCAQS wind analysis domain. This domain is identical to the Urban Airshed Model modeling domain used by the South Coast Air Quality Management District for modeling performed in support of their 1991 Air Quality Management Plan.



TABLE 1-1. SCAQS surface wind monitoring sites.

Site Identifier	Location	UTM-Easting (km)	UTM-Northing (km)
ALHA	Alhambra	394.5	3772.7
ANAH	Anaheim	415.0	3742.5
AZUS	Azusa	414.9	3777.4
BANN	Banning-Allesandro	511.7	3754.0
BARS	Barstow	497.9	3861.1
BU23	Buoy 46023-Point Conception	159.4	3801.4
BU25	Buoy 46025-Catalina Ridge	305.4	3730.7
BURK	Burbank	379.5	3783.0
CASI	BLM-Casitas/Los Padres NF	282.4	3808.9
CELA	Los Angeles-North Main	386.9	3770.1
CHIL	BLM-Chilao/Angeles NF	404.6	3799.0
CHIN	Chino	436.5	3763.4
CI	Santa Catalina Island	368.3	3696.3
CJNS	Cajon Summit	461.7	3799.0
CLAR	Claremont College	435.1	3773.5
CM36	CIMIS-Blythe	726.2	3725.6
CM44	CIMIS-U.C. Riverside	469.0	3758.1
CM50	CIMIS-Thermal	570.3	3723.0
CM55	CIMIS-Palm Desert	557.2	3732.3
CM60	CIMIS-Barstow	489.5	3862.1
CM62	CIMIS-Temecula	479.4	3705.5
COMP	Compton Airport	385.5	3750.3
COST	Costa Mesa-Placentia	413.8	3724.2
CRES	Lake Gregory-Crestline	474.8	3789.0
ELRO	El Rio-Rio Mesa School	302.6	3792.2
ELSN	Elsinore	467.7	3726.0
FONT	Fontana-Arrow Highway	453.4	3773.1

Continued

TABLE 1-1. Continued.

Site Identifier	Location	UTM-Easting (km)	UTM-Northing (km)
GLEN	Glendora-Laurel	421.5	3778.2
HAWT	Hawthorne	373.4	3754.3
HESP	Hesperia-17288 Olives	473.8	3808.4
HF	Henninger Flats	400.6	3784.7
KH	Kellogg Hill	424.2	3771.1
LA	Los Alamitos-SCE Power Plant	398.0	3737.0
LAHB	La Habra	412.1	3754.2
LANC	Lancaster	395.7	3841.5
LBCC	Long Beach City College	394.7	3743.7
LCAN	La Canada	388.2	3786.1
LGBH	North Long Beach	390.0	3743.0
LSAL	Los Alamitos-Orangewood	404.5	3739.8
LYNN	Lynwood	388.2	3754.8
MALI	Malibu	344.0	3766.9
MISS	Mission Hills	365.1	3793.2
NEWL	Newhall-County Fire Station	359.0	3806.0
NORC	Norco-Norconian	447.2	3753.3
NTD	Pt. Mugu Naval Weapons Test Center	304.8	3776.9
OJAI	Ojai-1768 Maricopa Highway	291.4	3813.8
PASA	Pasadena-Wilson	396.1	3777.3
PERI	Perris	478.4	3738.0
PICO	Pico Rivera	402.3	3764.1
PIRU	Piru-2SW	332.4	3807.6
PLSP	Palm Springs-Fire Station	542.5	3745.7
POMA	Pomona	430.7	3769.6
PV	Palos Verdes-San Pedro Hill	376.2	3734.6

Continued

TABLE 1-1. Concluded.

Site Identifier	Location	UTM-Easting (km)	UTM-Northing (km)
RDLD	Redlands-Dearborn	485.3	3768.6
REDO	Redondo Beach	372.0	3745.9
RESE	Reseda	358.7	3785.1
RIAL	Rialto	462.5	3776.0
RIVR	Riverside-Rubidoux	461.5	3762.0
SIMI	Simi Valley-5400 Cochran	344.9	3794.0
SNBO	San Bernardino	474.8	3773.9
SNI	San Nicolas Island	268.4	3682.3
TANB	BLM-Tanbark/Angeles NF	430.1	3784.9
TEME	BLM-Temescal/Los Padres NF	353.1	3816.7
TORO	El Toro	432.0	3725.2
TRON	Trona-Market Street	436.1	3957.3
UPLA	Upland ARB	442.0	3773.6
VCTC	Victorville-Civic Drive	470.7	3818.5
VENI	Venice Beach	364.2	3761.2
VERN	Vernon	387.4	3762.5
WALN	Walnut	422.3	3767.7
WHIT	Whittier	405.3	3754.0
WSLA	West Los Angeles-VA Hospital	365.7	3768.6
WSPR	BLM-Warm Springs/Angeles NF	355.2	3829.1
ZUMA	Zuma Beach	331.3	3765.9

TABLE 1-2. SCAQS upper-air wind monitoring sites.

Site Identifier	Location	UTM-Easting (km)	UTM-Northing (km)
BUR	Burbank/Glendale/Pasadena Airport	374.8	3785.0
DAGG	Daggett SCENES Site	519.8	3858.1
EMUA	El Monte-9528 Telstar	402.1	3770.0
GLUA	Glendora-near SCAQMD site 7000591	421.6	3778.3
LBCC	Long Beach City College	394.7	3743.7
LBCR	Long Beach City College	394.7	3743.7
LMUA	Loyola Marymount University-Engng Bldg	369.4	3760.4
NEED	Needles SCENES Site	718.1	3849.6
NSI	San Nicolas Island	271.7	3679.6
NTD	Pt. Mugu Naval Weapons Test Center	304.8	3776.9
ONT	Ontario International Airport	444.3	3768.4
PSP	Palm Springs	546.0	3742.9
RAL	Rialto	458.9	3756.7
SFUA	Santa Fe Springs	402.0	3755.7
TRM	Thermal Airport	577.6	3720.9
VBG	Vandenberg AFB	173.3	3847.2
YLUA	Yorba Linda County Park	428.7	3754.9

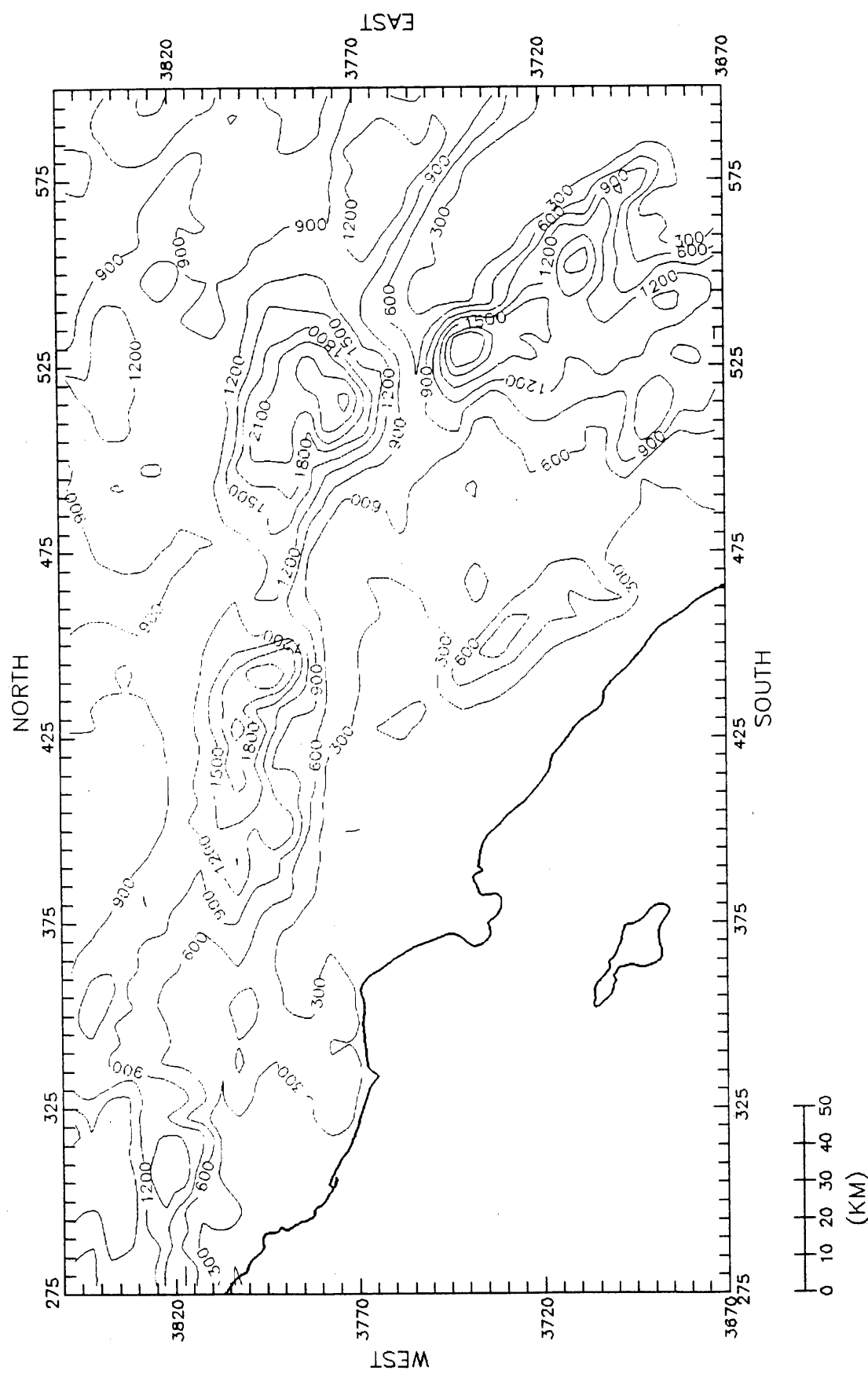


FIGURE 1-1. The SCAQS 1987 analysis domain (axes labeled in zone 11 UTM coordinates; topography contoured in meters).

Our analysis consisted of (1) generation of hourly, gridded wind fields for the 17 SCAQS intensive study days using the DWM, (2) analysis of the mesoscale airflow patterns, and (3) calculation of forward and backward particle trajectories to examine pollutant transport in the SOCAB.

The results of the diagnostic analysis of SCAQS wind observations are presented in this report. The generation of wind fields and the resulting airflow patterns are described in Section 2. The trajectory analysis is presented in Section 3. Plots of the wind fields are given in Appendix B. The trajectory plots are included in Appendix C.

## 2 GENERATION OF WIND FIELDS AND ANALYSIS OF AIRFLOW PATTERNS

### DIAGNOSTIC WIND MODEL

Hourly, gridded wind fields were generated for the 17 SCAQS intensive monitoring days using the Diagnostic Wind Model (DWM) (Douglas et al., 1990). This model incorporates observations where they are available and provides some information on terrain-induced airflows in regions where local observations are absent. The model is formulated in terrain-parallel coordinates. Wind fields are generated using a two-step procedure.

In step 1, a domain-scale mean wind is adjusted for terrain effects. These include the kinematic effects of terrain (lifting and acceleration of the airflow over terrain obstacles), thermodynamically generated slope flows, and blocking effects. Step 1 produces a spatially varying gridded field of  $u$  and  $v$  for each vertical layer within the model domain.

In step 2, observational information is added to the  $(u, v)$  field calculated in step 1 using an objective analysis procedure: observations are used within a user-specified radius of influence while the step 1  $(u, v)$  field is used in subregions where observations are unavailable. The following modified inverse-distance-squared weighting scheme (Ross and Smith, 1986) is used for the interpolation of data:

$$(u, v)_2 = \left\{ \sum_k [r_k^{-2} (u_o, v_o)_k + R^{-2} (u, v)_1] \right\} / \left\{ \sum_k r_k^{-2} + R^{-2} \right\}$$

where  $(u_o, v_o)_k$  denotes an observed wind at station  $k$ ;  $r_k$  is the distance from station  $k$  to a given grid point;  $(u, v)_1$  is the step 1 wind field at the grid point, and  $(u, v)_2$  is the updated wind vector. The parameter  $R$  controls the relative influence of the observations and the step 1 wind field.

Following the interpolation, a five point smoother of the form

$$A_{i,j} = 0.5A_{i,j} + 0.125(A_{i-1,j} + A_{i+1,j} + A_{i,j-1} + A_{i,j+1})$$

is applied to the horizontal wind field to reduce discontinuities that may result from the interpolation. The vertical velocity is calculated by integrating the incompressible conservation of mass equation. Zero-gradient lateral boundary conditions are used.

## GENERAL PROCEDURES

Generation of the SCAQS wind fields involved (1) preprocessing of the wind data for input into the DWM, (2) plotting and quality control checking of the data, (3) specification of the model input parameters, (4) exercise of the DWM, and (5) graphical display of the gridded wind fields. Winds were analyzed at six vertical levels: 10, 100, 300, 600, 1000, and 1500 meters (m) above ground level (agl).

In the preprocessing step the upper-air data were vertically interpolated to the model levels and temporally interpolated to enhance the temporal consistency of the wind fields and to provide hourly input for the DWM.

Following the preprocessing step, the data were plotted and examined for horizontal, vertical, and temporal consistency. Data that failed the quality control checks were eliminated from the model input data set.

The controlling parameters for the DWM include the maximum radius of influence (RMAX) at which a monitoring station can influence the interpolation at a grid point, the weighting parameter for terrain effects (R), the number of stations to be used in the interpolation (NINTRP) , and the number of smoothing passes (NSMTH). Note that the maximum radius of influence is specified independently for the surface level (over land), upper levels (over land), and over-water portions of the domain. The weighting parameter for terrain effects and the number of interpolating stations are specified separately for the surface level and upper levels. In the diagnostic analysis of the SCAQS wind observations these parameters were specified as follows:

RMAX (surface):	20 km
RMAX (aloft):	100 km
RMAX (over water):	150 km
R (surface):	10 km
R (aloft):	50 km
NINTRP (surface):	4
NINTRP (aloft):	3
NSMTH:	4

Tests were performed to examine the sensitivity of the DWM to the various controlling parameters and to select the optimum values of these parameters for the SCAQS wind analysis.

The DWM also requires as input a domain-mean wind and stability information. For this analysis, the domain-mean wind was specified separately for each analysis level and was based upon the average of the level 6 (1500 m agl) wind observations. To account for friction, the speed of the domain-mean wind was reduced for the lower levels by multiplying the average wind speed for level 6 by the following scaling factors:

<u>Level</u>	<u>Scaling Factor</u>
1	0.48
2	0.72
3	0.83
4	0.90
5	0.96
6	1.00

The domain-scale lapse rate was the calculated average of four inland sites. These varied according to data availability.

Six-hourly plots of the level 1 (surface), level 3 (300 m agl), and level 5 (1000 m agl) wind fields for each episode are given in Appendix B.

## **SUMMER INTENSIVE MONITORING PERIODS**

Mesoscale airflow in the SOCAB during the SCAQS summer intensive monitoring periods appears to have two components:

A "basic diurnal cycle" driven by land-water temperature differences and complex terrain, and

A "perturbation" associated with the overlying synoptic flow.

### **19 June 1987**

The surface and upper-air wind monitoring site locations for this intensive monitoring period are indicated on pages A-1 and A-2, respectively. Plots of the diagnostic wind analyses for 19 June are given on pages B-1 through B-12.

The surface early morning airflow pattern on this day is characterized by weak winds over much of the coastal and inland areas with moderate NW winds over the Coachella Valley and offshore. At 300 m agl winds are S over the western half of the domain and W to NW over the eastern half of the domain. The overlying flow at 1000 m is W.

The sea breeze is somewhat slow to appear in the western basin on this day but has begun to develop by 1000 PST. At this time winds at 300 m agl remain S over the western part of the domain and W to NW over the eastern part of the domain. Some S flow is also apparent at 1000 m.

During the afternoon hours, three distinct features are apparent in the surface airflow pattern:

A sea breeze (W flow) develops along the coast between Santa Monica and Palos Verdes and penetrates inland. A branch of the sea breeze penetrates into the San Fernando Valley, resulting in weak SE flow at Burbank and Reseda.

An area of weak (SW) winds forms in the Whittier-La Habra-Pico Rivera area, persists throughout the afternoon, and forms a convergence zone in the central basin with the penetrating westerly flow. The S component of this flow is due to sea breeze development along the coast near Long Beach.

Upslope flow develops along the foothills of the San Gabriel and San Bernardino Mountains (e.g. at Glendora and San Bernardino). Along the eastern foothills the upslope flow is supplanted during the afternoon by the penetrating W flow.

By 1600 PST on 19 June the depth of the upslope flow near Glendora exceeds 600 m. Strong outflow is apparent through the Cajon and Banning passes. Aloft, winds are generally SW with some SE flow near Burbank and NW flow over the Coachella Valley.

Significant onshore flow (3 m/s) persists along the Santa Monica-Palos Verdes coastline through 2200 PST. Features of the afternoon airflow persist aloft through this time.

#### 24-25 June 1987

Surface and upper-air wind monitoring site locations for this intensive monitoring period are indicated on pages A-3 and A-4, respectively. Plots of the diagnostic wind analyses for 24-25 June are given on pages B-13 through B-36.

The airflow patterns on these two days are similar to one another and to the pattern on 19 June. The overlying flow is generally weak below 1000 m agl, with moderate (5 m/s) SE flow at 1500 m agl.

On 24 June, the early morning surface airflow patterns are characterized by very weak winds. At 300 m agl winds in the Coachella Valley are SE. By 1000 PST a well-organized zone of weak S flow extends from Long Beach to Pasadena, this S flow

reaches a depth of 300 m agl. Southeastern flow in the Coachella Valley and E flow through Banning Pass are apparent both at the surface and 300 m agl. S to SE flow dominates at 1000 m agl. The "three-zone" surface airflow pattern is apparent during the afternoon. The wind shifts to W at Banning Pass by 1500 PST. At 300 m agl winds are SW over much of the basin with SE flow at Burbank and in the Coachella Valley. At 1000 m winds are generally SW. At 2200 PST the airflow pattern is characterized by weak unorganized flow at the surface and 300 m agl. Winds at 1000 m are NW over much of the domain but SE over the Coachella Valley.

The airflow on 25 June is similar to that on 24 June. During the early morning hours winds at the surface are very light. Weak SE flow is apparent at 300 m agl. At 1000 m agl winds continue to veer toward N. The sea breeze develops more quickly than on the previous day and winds at Banning Pass become westerly by 1300 PST. Calm winds are observed at Pico Rivera throughout the afternoon. As on 24 June, the afternoon airflow at 300 m agl is characterized by SW flow over the basin, and SE flow at Burbank and over the Coachella Valley. Upward propagation of W flow is generally slower than on 24 June. Winds at 1000 m agl are S to SE. During the evening hours the surface winds become light while at 300 m agl winds over the Coachella Valley become NW. Organized W flow is apparent over the W basin through a depth of at least 300 m agl through 2200 PST.

### 13-15 July 1987

Surface and upper-air wind monitoring sites for this intensive monitoring period are shown on pages A-5 and A-6, respectively. Plots of the diagnostic wind analyses for 13-15 July are given in Figures B-37 through B-72.

Airflow patterns on 13 and 14 July are generally consistent with the basic diurnal cycle described earlier. However, an unusual airflow pattern develops in the Coachella Valley on both days. On 15 July strong SE forcing is associated with a delay in sea breeze development.

The 13 July early morning surface airflow pattern is characterized by light winds and a weak cyclonic eddy over the Santa Monica Bay. Winds aloft are light to moderate and primarily W. The sea breeze develops rapidly on this day and by 1200 PST W flow overwhelms the S sea-breeze flow in the Long Beach Area. W flow appears at Banning Pass by 0800 PST. The surface afternoon airflow is characterized by the "three-zone" airflow pattern described earlier with strong upslope flow along the foothills (> 5 m/s) and significant outflow through Cajon Pass. Observations at Palm Spring (NW winds) and Thermal (SE winds) indicate a convergence zone in the Coachella Valley with a depth of at least 600 m. W flow dominates at 1000 m with S to SE flow over the Coachella Valley. During the evening hours a cyclonic eddy redevelops over the Santa

Monica Bay, winds are weak throughout the basin but airflow into the Coachella Valley is especially strong.

Airflow patterns on 14 July are similar to 13 July with a few exceptions. During the early morning hours the surface airflow is characterized by weak, disorganized flow. There is no eddy apparent over the Santa Monica Bay. The overlying flow is weak and primarily S to SE at 300 m agl but W to NW at 1000 m agl. Sea breeze development is approximately two hours slower on this day than on 13 July. By 1000 PST weak S flow has developed over the Whittier-La Habra-Pico Rivera area and SE flow is apparent at Burbank. A S component to the flow appears at 1000 m. The afternoon surface airflow pattern is similar to that on 13 July but the S upslope flow at Glendora is weaker. S flow develops at Elsinore and several coastal Orange County sites. The Coachella Valley convergence zone reappears at the surface at 1600 PST, two hours later than on the previous day. At 300 and 1000 m agl, W to SW flow dominates over the western two-thirds of the domain. SE flow is apparent over the Coachella Valley. During the evening hours the surface airflow over the central basin is S to SW. W flow components persist along the eastern foothills through 2200 PST.

On the morning of 15 July surface winds are weak but maintain a S component. Moderate SE flow is apparent offshore. The overlying flow is generally E to SE. By 1000 PST the surface airflow pattern is characterized by S flow over the central basin and along the foothills, SE flow in the Coachella Valley, and E flow through Banning Pass. The depth of the S to SE flow is greater than 1000 m agl. During the afternoon a weak sea breeze penetrates inland and winds along the foothills become W. Winds shift from E to NW at Banning Pass at 1600 PST. A weak S flow component persists in the Whittier-La Habra-Pico Rivera area throughout the afternoon. A weak slope/valley circulation develops in the Coachella Valley resulting in SE flow there. At 300 m agl winds are SW to W over the central basin and SE over the Burbank and the Coachella Valley. At 1000 m S to SE flow dominates. W winds persist along the foothills through 2200 PST and weak S to SE flow redevelops at the surface. Remnants of the afternoon airflow pattern persist aloft.

### 27-29 August 1987

The surface and upper-air wind monitoring site locations for this intensive monitoring period are indicated on pages A-7 and A-8, respectively. Plots of the diagnostic wind analyses for 27-29 August are given on pages B-73 through B-108.

On the morning of 27 August surface winds are weak over most land areas and adjacent coastal waters with moderate (5 m/s) NW winds well offshore. Winds aloft are primarily N with weak NE flow at 100-300 m agl over the central basin. By 1000 PST, a "three-zone" airflow pattern has developed at the surface and is somewhat apparent (within the limits of the upper-air network) at 300 m agl. SE flow has developed at 1000 m agl.

This pattern is maintained throughout the afternoon. Within the Coachella Valley a classic daytime slope/valley flow pattern develops, with SE flow extending to a depth of 1000 m. E flow develops at Banning Pass and persists through 1700 PST. W flow over the basin develops upward throughout the afternoon. By 1600 PST, wind at 300 m agl are W to SW over the central basin and SE over Burbank and the Coachella Valley. During the evening hours the features of the mesoscale airflow pattern over land weaken both at the surface and aloft. There is no clearly developed offshore-directed land breeze.

On the morning of 28 August the surface winds are weak and the overlying flow is primarily E. Retardation of the sea breeze by the overlying E flow is apparent by 0900 PST. S flow develops in the Long Beach area. E flow at Banning Pass is substantially stronger than on 27 August. During the afternoon of 28 August, S flow persists at Long Beach and develops in the Whittier-La Habra-Pico Rivers area. SE flow is observed along the Orange County coast. E flow through Banning Pass persists throughout the day. W wind components along the Santa Monica-Palos Verdes coastline are weaker than on the previous day and NW flow fails to develop at San Nicolas Island. W flow over the central basin disrupts the SE flow aloft. During the evening hours the airflow features weaken. W flow along the foothills does not persist as long as on the previous day.

The early morning airflow pattern on 29 August is characterized by SE flow both at the surface and aloft. Sea breeze development on this day is slower than on either of the previous two days. S flow again develops in the Long Beach area and appears to be stronger than on the previous day. Although the sea breeze is weaker, winds at Banning Pass shift from E to SW by 1300 PST. This shift occurs at 1800 on 27 and 28 August. SE flow persists aloft with limited upward development of the W sea breeze flow. W flow persists in the western basin area through 2200 PST and SE flow persists aloft.

## 2-3 September 1987

The surface and upper-air monitoring site locations for this intensive monitoring period are indicated on pages A-9 and A-10, respectively. Plots of the diagnostic wind analyses for 2-3 September are given on pages B-109 through B-132.

The first day of this period is probably the most "anomalous" of the summer SCAQS intensive measurement days. Overlying easterly forcing during the morning hours prevents development of W flow along the foothills and inhibits upward development of the sea breeze over the western and central portions of the basin. The easterly forcing appears to reverse rather abruptly on the afternoon of 2 September. Unusual winds are also observed at Burbank on 2 September. During the late morning and afternoon Burbank experiences an unusual wind shift from SE to W through a depth of 1000 m. On 3 September, the overlying airflow is W and the airflow patterns are more typical.

On the morning of 2 September, strong downslope flow results in N to NE winds at several sites along the foothills of the San Gabriel Mountains. At 300 m strong NE winds are apparent over the central basin. The overlying flow is E. By 1000 PST, the sea breeze appears as W flow along the Santa Monica-Palos Verdes coast and S flow in the Long Beach area. The surface analysis indicates a band of S flow from Costa Mesa to Azusa. W flow has not developed along the eastern foothills. Winds are SE in the Coachella Valley and E through Banning Pass. E flow aloft continues and intensifies. During the early afternoon hours, a relatively strong sea breeze penetrates inland to Azusa while winds in the Whittier-La Habra-Pico Rivera area remain weak. The sea breeze weakens considerably after mid-afternoon. Between 1200 and 1500 PST, the wind at Burbank shifts from SE to W through a depth of 600-1000 m. By 1600 PST the overlying flow has shifted from SE to W. Onshore flow continues at the surface through 2200 PST while the winds weaken considerably. Although the overlying W flow persists in general, 300 m agl winds at Burbank become SE.

The early morning airflow on 3 September is characterized by weak winds at the surface, SE flow at 300 m agl, and primarily W flow at 1000 m agl. Although the major surface airflow features appear to develop as on previous days, upward development of the pattern is limited. Strong S flow is apparent by 1200 PST between 100 and 300 m agl over the central and western basin. By 1600 PST, the sea breeze has penetrated well inland. Imbedded in the sea breeze is a persistent calm area in the vicinity of Lynwood. S flow persists at 100-300 m agl over the central and western basin while flow at this level offshore remains NW. At 1000 m agl W flow continues. This general pattern persists through 2200 PST but weakens considerably, especially at the surface.

#### AUTUMN INTENSIVE MONITORING PERIODS

The mesoscale airflow patterns in the SOCAB during the SCAQS autumn intensive monitoring periods exhibit a weaker "diurnal cycle" than the summer airflow patterns. Synoptic forcing also appears to be stronger.

##### 11-13 November 1987

The surface and upper-air wind monitoring site locations for this intensive monitoring period are plotted on pages A-11 and A-12, respectively. Plots of the diagnostic wind analyses for 11-13 November are given on pages B-133 through B-168.

During the early morning hours of 11 November NE surface winds are apparent over most of the region. Surface wind speeds are very light over the basin and somewhat stronger along the foothills and the coast. At 300 m agl winds are light and generally E. At 1000 m agl winds are W to SW over the western half of the domain and SE over the eastern half of the domain. Weak E to NE surface flow persists throughout most of the

morning in the first 300 m. An apparent anticyclonic eddy (SE flow at Long Beach, weak S flow at Burbank, W flow at El Monte) develops between 600 and 1000 m agl on this morning. A weak sea breeze forms around 1200 PST, penetrating only to the central basin. There is no apparent turning of the sea breeze into the San Fernando Valley. W to NW flow develops offshore and is deflected around the Palos Verdes Hills. This W flow is also apparent at 300 m agl. Downslope flow components along the foothills are apparent by 1600 PST. At this time the 1000 m agl winds are weak and N. The sea breeze rapidly dissipates and NE flow develops at several coastal sites indicating a land breeze. NW flow is maintained offshore. The nighttime airflow pattern aloft is characterized by weak N winds at 300 m agl and weak W winds at 1000 m agl.

The surface airflow pattern on the morning of 12 November is generally similar to that on 11 November. E flow over land is apparent through a depth of 300 m, while NW flow persists offshore. The overlying flow is W. The afternoon surface airflow pattern is more similar to a typical summer afternoon pattern than the previous day. Turning of the sea breeze into the San Fernando Valley is apparent and W flow develops along the foothills of the San Gabriel and San Bernardino Mountains by 1400 PST. Airflow at 300-600 m agl appears to veer continuously from E to W at most inland sites during the afternoon. NW flow through a depth of 1000 m is apparent over the Coachella Valley. Surface winds become light and disorganized during the evening hours. Unlike the previous day, NE flow does not develop at the coastal sites and NW flow weakens offshore. W winds persist aloft.

On 13 November surface winds are very light through the early morning hours, with E flow components apparent immediately offshore. The overlying flow is WNW but becomes S over the central basin by 1000 PST. As on the previous two days, a sea breeze becomes apparent at the surface by noon. W flow components over the basin and foothill areas are stronger than on the previous two days, both at the surface and aloft. Significant W flow also develops in Banning Pass. Moderate to strong W winds are apparent aloft. During the afternoon and evening hours SE winds are apparent at Burbank between 300 and 600 m agl. Intense W flow develops offshore and propagates inland during the evening hours. W flow continues aloft with some S to SE flow between 100 and 600 m agl at Burbank and El Monte.

### 3 December 1987

The surface and upper-air wind monitoring site locations for this intensive monitoring period are plotted on pages A-13 and A-14, respectively. Plots of the diagnostic wind analyses for 3 December are given on pages B-169 through B-180.

The early morning surface airflow pattern on 3 December is characterized by weak NE winds over the inland areas and a weak cyclonic eddy offshore. The overlying flow is S to SE. Surface winds remain light and variable through most of the morning. Moderate

E flow is apparent over the western and central basin between 300 and 600 m agl. A sea breeze develops around 1200 PST, reaching a depth of 300 m and penetrating only approximately 30 km inland. S to SE flow persists above 300 m agl. The sea breeze weakens during the evening hours and N flow through a depth of 300 m develops at Long Beach. E flow components intensify at 600 m agl and above.

### 10-11 December 1987

The surface and upper-air wind monitoring site locations for this intensive monitoring period are plotted on pages A-15 and A-16, respectively. Plots of the diagnostic wind analyses for 10-11 December are given on pages B-181 through B-204.

On 10 December the early morning surface airflow pattern is weak and disorganized. Weak NE flow is apparent over much of the basin between 100 and 600 m agl. The overlying flow at 1000 m is N. The surface airflow over the basin is weak throughout the morning hours while NW flow develops offshore. Winds aloft remain N. A weak sea breeze is apparent by 1200 PST; the sea breeze penetrates only about 30 km inland and is limited to a depth of approximately 300 m. There is no apparent turning of the sea breeze into the San Fernando Valley. Elsewhere in the basin the surface airflow remains weak. By 1600 PST the sea breeze has weakened. At this time winds aloft are predominantly W to NW at 300 m agl and N at 1000 m agl. During the evening hours surface airflow over the basin becomes weak and disorganized while E flow develops at Palos Verdes. Strong N winds appear aloft (300-600 m agl) at Burbank, LMU, and Long Beach, however, winds at this level further to the east remain light.

On 11 December the early morning surface airflow pattern is similar to that on 10 December. Relatively strong ( $> 10$  m/s) NNW winds persist at 600-1000 m agl at Burbank and LMU. E wind in the 100-300 m agl appear at LMU and Long Beach. Throughout the morning the surface winds remain light and N winds over Burbank weaken considerably. A sea breeze is apparent by 1200 PST but is weaker than on the previous day and reaches a depth of only 100 m or less. Significant N winds (3-6 m/s) develop between San Bernardino and Elsinore and in the western San Fernando Valley. NE flow is observed in Ventura County. Winds aloft continue to be primarily N, however, E flow is apparent over the Long Beach area at 1000 m agl. Surface airflow over the central and western basin becomes very weak during the evening hours. Strong N to NE flow develops at the coast west of Santa Monica, while N flow persists in the western San Fernando Valley and in the San Bernardino/Riverside area. The overlying flow is N to NE.

### **3 PARTICLE PATH ANALYSIS**

A series of forward and backward particle paths (trajectories) were calculated using the SCAQS DWM wind fields. The particle paths will be used by other SCAQS investigators in their examination of pollutant transport within the SOCAB. The forward particle paths can be used to estimate the transport of pollutants from known source locations. The backward particle paths can be used to estimate potential source areas. The particle paths can also be used to estimate the residence time of certain pollutants in the SOCAB as a whole or in subregions.

#### **CALCULATION OF PARTICLE PATHS**

Two-dimensional particle paths were computed using the DWM wind fields as follows:

Starting (ending) points for a given number of forward (backward) particle paths were specified.

Using a time interval of 15 minutes, the hourly, gridded DWM wind fields were linearly interpolated in time and then interpolated in space to each particle position using an inverse-distance-squared weighting scheme.

The particles were then advected horizontally for the specified time interval.

The distance traveled by each particle during each time interval was integrated. The new position of the particle was reported at hourly intervals.

Forward and backward particle paths were calculated for the SCAQS intensive monitoring periods for several vertical levels and a variety of origination and destination points. The origination (destination) locations and times for the summer and autumn particle paths are listed in Tables 3-1 and 3-2, respectively. Most of the particle paths originated (ended) at one of the SCAQS wind monitoring sites listed in Tables 1-1 and 1-2. Additional sites are identified in Table 3-3. Note that for some sites in Tables 3-1 and 3-2 a new particle path was initiated at the particle's 1000 PST location but at a higher level.

Additional forward particle paths were calculated for comparison with the SCAQS tracer data (England et al., 1989; Horrell et al., 1989). The initiation times and locations correspond to the tracer releases and are given in Tables 3-4 and 3-5.

TABLE 3-1a. Summer particle paths: forward particle paths.

Start Date	Start Time (PST)	Origination Site	Level(s)
6/24	0500	LBCC	1,3
		CELA	1,3
6/24	0700	LBCC	1,3
		CELA	1,3
6/24	1000	LBCC	1,3
		CELA	1,3
6/24	1500	LBCC	1,3
		CELA	1,3
6/24	2100	LBCC	1,3
		CELA	1,3
6/25	0500	HHRA	5
		PADA	4,5
		FULA	5
6/25	0700	FULA	5
7/13	0500	LBCC	1,3
		CELA	1,3
7/13	0700	LBCC	1,3
		CELA	1,3
7/13	1000	LBCC	1,3
		CELA	1,3
		EMTA	2,4
7/13	1500	LBCC	1,3
		CELA	1,3
7/13	2100	LBCC	1,3
		CELA	1,3
7/14	0500	LBCC	1,3
		CELA	1,3
7/14	0700	LBCC	1,3
		CELA	1,3
7/14	1000	LBCC	1,3
		CELA	1,3
7/14	1500	LBCC	1,3
		CELA	1,3
7/14	2100	LBCC	1,3
		CELA	1,3

Continued

TABLE 3-1a. Concluded.

Start Date	Start Time (PST)	Origination Site	Level(s)
8/27	0500	LBCC	1,3
		CELA	1,3
8/27	0700	LBCC	1,3
		CELA	1,3
8/27	1000	LBCC	1,3
		CELA	1,3
8/27	1500	LBCC	1,3
		CELA	1,3
8/27	2100	LBCC	1,3
		CELA	1,3
8/28	0500	LBCC	1,3
		CELA	1,3
8/28	0700	LBCC	1,3
		CELA	1,3
8/28	1000	LBCC	1,3
		CELA	1,3
8/28	1500	LBCC	1,3
		CELA	1,3
8/28	2100	LBCC	1,3
		CELA	1,3
9/2	0500	LBCC	1,3
		CELA	1,3
		HHRA	1,2
9/2	0700	LBCC	1,3
		CELA	1,3
		FULA	1,2
9/2	1000	LBCC	1,3
		CELA	1,3
		HHRA*	4,5
		FULA*	4,5
9/2	1500	LBCC	1,3
		CELA	1,3
9/2	2100	LBCC	1,3
		CELA	1,3
9/3	0700	RIVA	1,2
9/3	1000	RIVA*	4,5

\* A new particle path was initiated at the particle's 1000 PST location but at a higher level.

TABLE 3-1b. Backward particle paths.

End Date	End Time (PST)	Destination Site	Level(s)
6/24	1500	CABA	2,3
		EMTA	4,5
		BURA	1,2,3,4
		HHRA	4
		FULA	4,5
6/24	1800	RIVA	3
6/25	0500	CLAR	1,3
		RIVR	1,3
		HHRA	5
		PADA	4,5
		FULA	5
6/25	0700	CLAR	1,3
		RIVR	1,3
		FULA	5
6/25	1000	CLAR	1,3
		RIVR	1,3
6/25	1500	CLAR	1,3
		RIVR	1,3
		CABA	2,3
		EMTA	4
		BURA	4
		RIVA	4,5
6/25	1600	RIVA	4,5
6/25	2100	CLAR	1,3
		RIVR	1,3
7/13	1000	EMTA	2,4
7/13	1500	CABA	2,3
		EMTA	4,5
		RIVA	2,4
		RIVA	2,4
7/13	1600	CLAR	1,3
7/14	0500	RIVR	1,3
7/14	0700	CLAR	1,3
		RIVR	1,3
7/14	1000	CLAR	1,3
		RIVR	1,3
		BUR	1,2,3
		CLAR	1,3
7/14	1500	RIVR	1,3
		CABA	2,3
		EMTA	4
		BURA	2,3,4
		RIVA	2
7/14	1600	RIVA	2

Continued

TABLE 3-1b. Continued.

End Date	End Time (PST)	Destination Site	Level(s)
7/14	2100	CLAR	1,3
		RIVR	1,3
7/15	0500	CLAR	1,3
		RIVR	1,3
7/15	0700	CLAR	1,3
		RIVR	1,3
7/15	1000	CLAR	1,3
		RIVR	1,3
7/15	1500	CLAR	1,3
		RIVR	1,3
7/15	2100	CLAR	1,3
		RIVR	1,3
8/27	1000	CABA	2
		EMTA	2,3
		BURA	1,2,3
8/27	1500	CABA	2
8/28	0500	CLAR	1,3
		RIVR	1,3
8/28	0700	CLAR	1,3
		RIVR	1,3
8/28	1000	CLAR	1,3
		RIVR	1,3
8/28	1500	CLAR	1,3
		RIVR	1,3
8/28	2100	CLAR	1,3
		RIVR	1,3
8/29	0500	CLAR	1,3
		RIVR	1,3
8/29	0700	CLAR	1,3
		RIVR	1,3
8/29	1000	CLAR	1,3
		RIVR	1,3
8/29	1500	CLAR	1,3
		RIVR	1,3
8/29	2100	CLAR	1,3
		RIVR	1,3
9/2	1000	PADA	3
9/2	1100	PADA	3
9/2	1500	EMTA	2
		RIVA	2

Continued

TABLE 3-1b. Concluded.

End Date	End Time (PST)	Destination Site	Level(s)
9/2	1600	RIVA	2
9/3	0500	CLAR	1,3
		RIVR	1,3
9/3	0700	CLAR	1,3
		RIVR	1,3
9/3	1000	CLAR	1,3
		RIVR	1,3
		CABA	2
		BURA	1,2,3,4
9/3	1500	CLAR	1,3
		RIVR	1,3
9/3	2100	CLAR	1,3
		RIVR	1,3

TABLE 3-2a. Autumn particle paths: forward particle paths.

Start Date	Start Time (PST)	Origination Site	Level(s)
11/11	0300	LBCC	1,3
		CELA	1,3
11/11	0700	LBCC	1,3
		CELA	1,3
11/11	0900	FULA	1,2
11/11	1200	LBCC	1,3
		CELA	1,3
11/11	1500	LBCC	1,3
		CELA	1,3
11/11	2100	LBCC	1,3
		CELA	1,3
11/12	0300	LBCC	1,3
		CELA	1,3
11/12	0700	LBCC	1,3
		CELA	1,3
		FULA	1,2
11/12	1000	FULA*	4,5
11/12	1200	LBCC	1,3
		CELA	1,3
11/12	1500	LBCC	1,3
		CELA	1,3
11/12	2100	LBCC	1,3
		CELA	1,3
11/13	0500	ONTA	1,2,3
11/13	1000	ONTA*	4,5
12/3	0300	LBCC	1,3
		CELA	1,3
12/3	0700	LBCC	1,3
		CELA	1,3
		FULA	1,2
12/3	1000	FULA*	4,5
12/3	1200	LBCC	1,3
		CELA	1,3
12/3	1500	LBCC	1,3
		CELA	1,3
12/3	2100	LBCC	1,3
		CELA	1,3
12/10	0300	LBCC	1,3
		CELA	1,3
12/10	0700	LBCC	1,3
		CELA	1,3

Continued

TABLE 3-2a. Concluded.

Start Date	Start Time (PST)	Origination Site	Level(s)
12/10	1200	LBCC	1,3
		CELA	1,3
		FULA	1,2,3
12/10	1500	LBCC	1,3
		CELA	1,3
12/10	2100	LBCC	1,3
		CELA	1,3
12/11	0500	ONTA	1,2
12/11	0700	FULA	1,2
12/11	1000	ONTA*	4,5
		FULA*	4,5

\* A new particle path was initiated at the particle's 1000 PST location but at a higher level.

TABLE 3-2b. Backward particle paths.

End Date	End Time (PST)	Destination Site	Level(s)
11/11	1500	HHRA	3,4
11/12	0300	LBCC	1,3
		CELA	1,3
		RIVR	1,3
11/12	0700	LBCC	1,3
		CELA	1,3
		RIVR	1,3
11/12	1200	LBCC	1,3
		CELA	1,3
		RIVR	1,3
11/12	1500	LBCC	1,3
		CELA	1,3
		RIVR	1,3
		HHRA	3,4
		PADA	3
		FULA	3,4
11/12	2100	LBCC	1,3
		CELA	1,3
		RIVR	1,3
11/13	0300	LBCC	1,3
		CELA	1,3
		RIVR	1,3
11/13	0700	LBCC	1,3
		CELA	1,3
		RIVR	1,3
11/13	1200	LBCC	1,3
		CELA	1,3
		RIVR	1,3
		ONTA	3,4
		EMTA	4,5
11/13	1500	LBCC	1,3
		CELA	1,3
		RIVR	1,3
11/13	2100	LBCC	1,3
		CELA	1,3
		RIVR	1,3
12/3	0300	LBCC	1,3
		CELA	1,3
		RIVR	1,3
12/3	0700	LBCC	1,3
		CELA	1,3
		RIVR	1,3

Continued

TABLE 3-2b. Concluded.

End Date	End Time (PST)	Destination Site	Level(s)
12/3	1200	LBCC	1,3
		CELA	1,3
		RIVR	1,3
12/3	1500	LBCC	1,3
		CELA	1,3
		RIVR	1,3
		PADA	3
12/3	2100	LBCC	1,3
		CELA	1,3
		RIVR	1,3
12/11	0300	LBCC	1,3
		CELA	1,3
		RIVR	1,3
12/11	0700	LBCC	1,3
		CELA	1,3
		RIVR	1,3
12/11	1200	LBCC	1,3
		CELA	1,3
		RIVR	1,3
12/11	1500	LBCC	1,3
		CELA	1,3
		RIVR	1,3
		PADA	1,2,3,4
		BURA	1,2,3
11/13	2100	LBCC	1,3
		CELA	1,3
		RIVR	1,3

TABLE 3-3. Additional particle path initiation (destination) points.

Site Identifier	Location	UTM Easting (km)	UTM Northing (km)
BURA	Burbank Airport	374.9	3785.9
CABA	Cable Airport	437.0	3775.1
EMTA	El Monte Airport	404.7	3771.7
FULA	Fullerton Airport	409.1	3748.5
HHRA	Hawthorne Airport	376.8	3754.7
ONTA	Ontario Airport	443.5	3768.6
PADA	PADDR Intersection	381.0	3717.5
RIVA	Riverside Airport	458.4	3748.5

TABLE 3-4. Forward particle paths calculated for comparison with the SCAQS tracer data.

Start Date	Start Time	Origination Site	Levels
6/25	0300	LAGS	1,3
	0600	"	1,3
	0900	"	1,3
	1200	"	1,3
	1500	"	1,3
7/15	0500	VRNN	1
	0800	VRNN	1
8/28	0600	LAGS	1,3
	1000	"	1,3
	1300	"	1,3
	1500	"	1,3
9/3	0500	VRNN	1
	0800	VRNN	1
11/11	1600	LAGS	3
		ESGS	3
		VRNN	1
	1900	LAGS	3
		ESGS	3
		VRNN	1
11/12	0600	ESGS	3
		VRNN	1
12/10	0900	ESGS	3
		VRNN	1
	0600	LAGS	3
		ESGS	3
		VRNN	1
	0900	LAGS	3
		ESGS	3
		VRNN	1
	1600	VRNN	1

TABLE 3-5. SCAQS tracer release sites.

Site Identifier	Location	UTM Easting (km)	UTM Northing (km)
ESGS	El Segundo	369.0	3753.6
LAGS	Los Alamitos	398.0	3737.0
VRNN	VRNN	387.4	3762.5



The particle paths were calculated for up to a three-day period. In general, forward particle paths were calculated through the end of the monitoring period or until the particle was advected out of the domain. Backward particle paths were calculated through the beginning of the intensive monitoring period or until the particle left the domain.

Selected plots of the forward and backward particle paths are given in Appendix C.

## SUMMER PARTICLE PATHS

Forward particle paths (levels 1 and 3) originating from Central Los Angeles (CELA) and Long Beach City College (LBCC) at 0700 PST on 24 June, 13 and 14 July, 27 and 28 August, and 2 September are shown on pages C-1 through C-12.

The surface-level particle paths originating at CELA indicate northward advection from this site on all days. The particle path initiated on 27 August indicates that the initial northward advection is followed by westward advection on the following day; the particle path initiated on 2 September indicates that the initial northward advection is followed by eastward advection on the following day. In all cases the residence time in the central Los Angeles basin is less than 12 hours.

The surface-level particle paths originating at LBCC are carried northward and eastward, usually exiting the Los Angeles basin through Cajon Pass. On 24 June and 14 July, however, the particles are carried across the San Gabriel Mountains (with the upslope flow). Considerable eastward transport is indicated by the particle paths initiated on 2 September after 1800 PST. Residence time in the Los Angeles basin varies from day to day and is especially long for the particle path initiated on 27 August (approximately 30 hours). Particle paths initiated on 13 July and 28 August also indicate some recirculation and a significant residence time within the Los Angeles basin.

The level 3 particle paths also indicate northward transport from CELA on most days. Advection into the San Fernando Valley, which may be partly due to the SE flow produced by the turning of the sea breeze into the valley, is more pronounced on certain days (14 July, 28 August, and 2 September). Level 3 particle paths originating at LBCC show mostly northwestward transport. Recirculation over the Los Angeles basin is indicated for the 2 September particle path.

Backward particle paths (levels 1 and 3) culminating at Claremont College (CLAR) and Riverside-Rubideaux (RIVR) at 1500 PST on 25 June, 14 and 15 July, 28 and 29 August, and 2 September are shown on pages C-13 through C-24.

The surface-level backward particle paths originate over water on all days; the particles are carried eastward and northward into the Los Angeles basin. On 14 July and 28 August, the particle paths indicate primarily eastward transport. There is some indication that particles arriving at the destination sites on 28 August may have originated in the South Central Coast Air Basin (SCCAB). On 25 June, 15 July, and 3 September, the particle paths indicate primarily northeastward transport. On 29 August, northward transport is indicated.

The level 3 backward particle paths also indicate transport from the W, SW, or SE on the intensive monitoring days. The over-water segments of the particle paths indicate eastward advection on 14 and 15 July and 27 and 28 August, and northward advection on 25 June and 3 September. Again there is some indication that particles arriving at the destination sites on 28 August may have originated in the SCCAB. Almost all of the particle paths indicate that the particles are carried onshore between Long Beach and Laguna Beach and advected northeastward to CLAR and RIVR. An exception to this occurs on 28 August. On this day the particles are carried onshore near Redondo Beach and are recirculated over the Los Angeles basin for approximately 24 hours before arriving at the destination sites.

## AUTUMN PARTICLE PATHS

Forward particle paths (levels 1 and 3) originating at CELA and LBCC at 0700 PST on 11 and 12 November, 3 and 10 December are presented on pages C-25 through C-32.

The autumn particle paths exhibit more day-to-day variability than the summer particle paths, indicating more variability in the autumn airflow patterns. Because both the CELA and LBCC locations are affected by the land-breeze/sea breeze circulations, all of the surface-level particle paths show some recirculation in the western basin. Particle paths initiated on 11 and 12 November eventually indicate eastward transport.

The level 3 particle paths also differ among episodes, but are all affected by the sea-breeze circulation. Particle paths initiated on 11 November show eastward transport from CELA and southward transport from LBCC. Northeastward transport at this level is indicated by the 12 November particle paths. The particle paths initiated on 3 December illustrate local recirculation by the sea breeze. On 10 December, southward advection is indicated.

Backward particle paths culminating at CELA, LBCC and RIVR at 1500 PST on 12 and 13 November, 3 and 11 December are presented on pages C-33 through C-40.

The surface-level particle paths indicate that particles arriving at CELA at 1500 PST on all four days follow a southward then eastward course. Particles arriving at LBCC are affected by some combination of onshore advection and local recirculation. The particle

paths culminating at Riverside indicate a variety of possible transport patterns: eastward transport on 12 and 13 November, northwestward transport on 3 December, and southeastward transport on 11 December.

The level 3 backward particle paths for 12 November illustrate recirculation aloft by the evolving airflow patterns while the particle paths for 13 November indicate primarily eastward advection. The particle paths for 3 December are clearly affected by the SE that occurs on this day; the resulting particle paths indicate northwestward transport. The particle paths for 11 December indicate southward advection and recirculation by the sea breeze.

## COMPARISON WITH TRACER DATA

Forward particle paths originating from El Segundo (ESGS), Los Alamitos (LAGS), and Vernon (VRNN) at times corresponding to the SCAQS tracer release times are shown on pages C-41 through C-76. For ground-level tracer releases the particle paths were calculated using level 1 (10 m agl winds); for stack releases the particle paths were calculated using level 3 (300 m agl) winds. A qualitative comparison with the observed tracer data is provided here.

Surface-level particle paths originating at LAGS on 25 June indicate northward transport during the morning and afternoon hours. The level-3 particle paths indicate that material is transported out of the basin through Cajon and Banning Passes by the upper-level winds. Both of these indicated transport patterns are supported by observed tracer data.

Surface-level particle paths originating at VRNN on 15 July indicate northward transport and exhibit good qualitative agreement with the tracer data.

Both the surface-level and level-3 particle paths originating at LAGS on 28 August indicate primarily northeastward transport. Most of the particles are eventually advected through Cajon Pass. This is consistent with observed tracer at Redlands, San Bernardino, and Crestline.

Surface-level particle paths originating at VRNN on the morning of 3 September do not agree with the tracer data. While the particle paths indicate northeastward transport, the tracer data indicate northwestward transport.

Surface-level particle paths originating at VRNN on the afternoon of 11 November indicate westward transport and a long residence time in the central basin. The level-3 particle paths originating at LAGS and ESGS show southeastward transport and recirculation by the sea breeze. Surface-level particle paths originating at VRNN on the following morning again show net westward transport and a long residence time in the central basin, but the level-3 particle paths indicate northward transport with recirculation

by the sea breeze. The surface-level particle paths are consistent with the tracer data. Tracer was observed over the north-central basin and along the foothills on the morning of 13 November.

The surface-level particle paths originating at VRNN on the morning of 10 December indicate relatively stagnant conditions with a weak sea breeze circulation. Some net transport toward the south is indicated. Particle paths originating at VRNN on the afternoon of 10 December show little movement throughout the following day. The long residence time in the basin is in qualitative agreement with the tracer data. Tracer was observed in the basin on the following day. The dispersion indicated by the widespread tracer concentrations, however, cannot be represented by a single particle path. The level 3 particle paths originating at LAGS and ESGS on the morning of 10 December show southward transport and recirculation by the sea breeze.

## UNCERTAINTY ANALYSIS

A simple analysis was performed in an attempt to quantify the degree of uncertainty inherent in the particle paths. The uncertainty analysis was similar to an analysis described by Moore et al. (1989).

Three major forms of error in the particle path calculations can be identified. The first two result from errors in the wind fields. The most fundamental of these is measurement error, as measurements can only be regarded as approximations of the true winds. Regardless of the accuracy of interpolation techniques, measurement error will always affect the final wind field. The second type of error results from the interpolation of these measurements and the parameterizations and approximations in the diagnostic wind model. This error will be greatest in data-sparse areas. The third type of error results from the use of two-dimensional wind fields. The two-dimensional particle paths do not incorporate the effects of vertical motion which may be a significant source of error considering the mesoscale regimes present in the study area.

The particle path uncertainty in this analysis is the result of all sources of error and is therefore very difficult to estimate. A "lower bound" on the uncertainty was assumed to result from measurement error alone. Here we use a "lower bound" uncertainty estimate to illustrate the effects of measurement error on the particle path calculations. Several assumptions were made in order to estimate this uncertainty. First, average bias for all instruments was assumed to be very small. Second, instrument precision was assumed to be constant over the region. Third, measurement error (speed and directional error) was assumed to be normally distributed around zero. The standard deviation about the mean was based on observational data.

For this uncertainty analysis 20 particle paths were initiated from a single site at a single time. For each 15-minute particle path segment,  $u$  and  $v$  were calculated as described in

the previous section. Small random wind components (representing the measurement error) were then added to the interpolated wind. The smaller components were determined by randomly selecting wind speed and direction error from two separate normal probability density functions (PDF). To do this, a uniform random number generator was used to find two error probabilities  $P_s$  and  $P_d$  between 0 and 1. An inverse normal PDF routine was then used to find the speed or direction error that results in error probability  $P_s$  or  $P_d$ , respectively. Commercial statistical software from IMSL<sup>1</sup> was used to generate uniform random and inverse normal PDF values.<sup>1</sup>

The PDFs possess means of zero, and standard deviations equal to the root mean square error (RMSE) of the measurements. For simplicity, RMSE values for speed and direction were taken from those specified by Moore et al. (1989),; namely 0.2 m/s and 10 degrees, respectively. Random error components were determined for each 15-minute segment of every particle path. The resulting divergence in the particle paths represents a lower limit to the uncertainty inherent in the particle-path calculations.

Plots illustrating the effect of the "lower-bound" uncertainty on the particle path calculations are given for one summer and one winter episode in Figures 3-1 and 3-2, respectively. The summer particle-path bundles (Figure 3-1) were initiated at CELA and LBCC at 0700 PST on 14 July. The winter particle paths (Figure 3-2) were initiated at CELA and LBCC at 0700 PST on 12 November. The bundles were calculated for levels 1 and 3. In general, the bundles indicate that the airflow patterns do not vary abruptly in space or time. The winter particle paths are less divergent than the summer particle paths.

While plots of the particle path bundles qualitatively indicate the degree of lower-limit uncertainty, a quantitative summary of the uncertainty can be obtained via hourly estimates of RMSE of all particle positions relative to that with "zero" error. The RMSE can be obtained from

$$RMSE = \left[ \frac{1}{M} \sum_{j=1}^M d_j^2 \right]^{\frac{1}{2}}$$

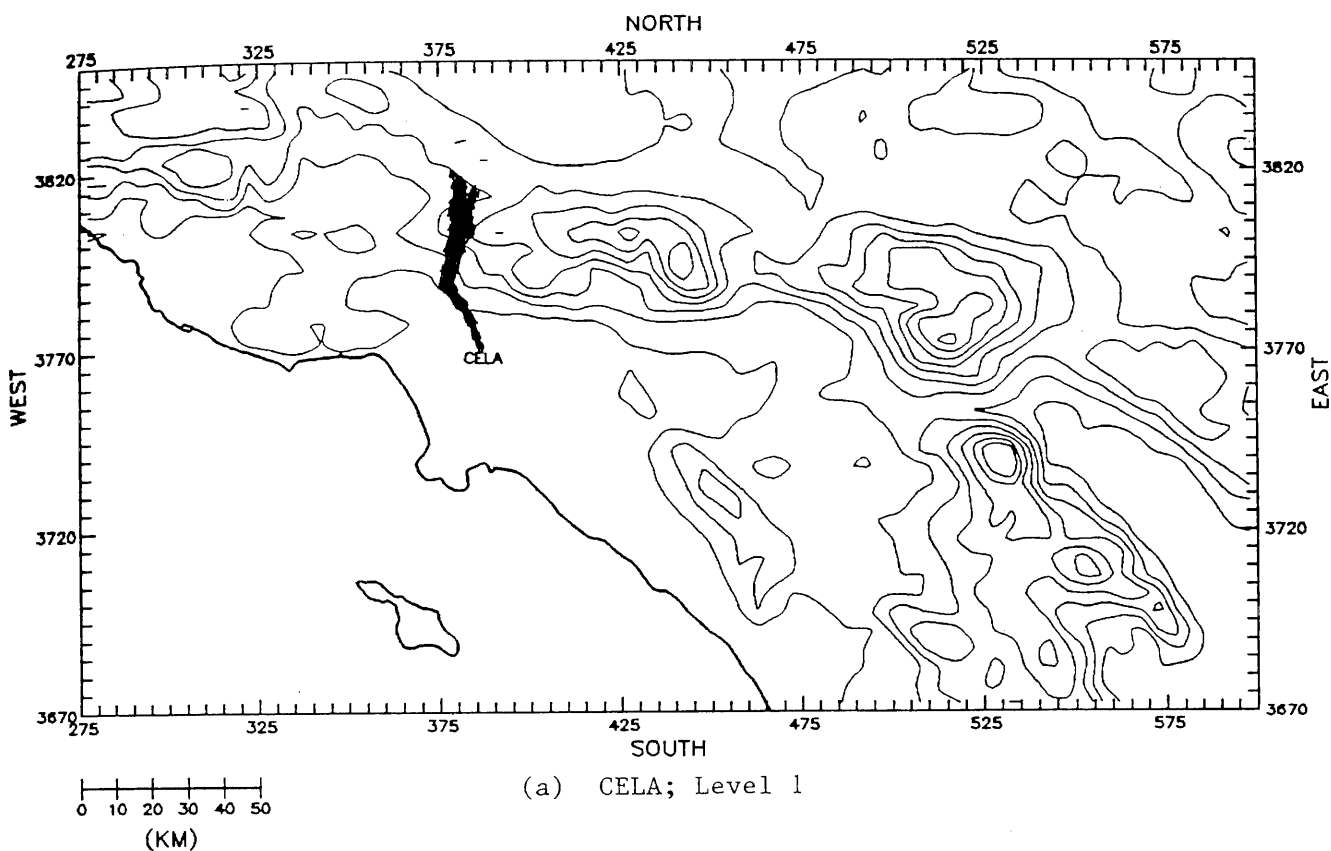
where

$$d_j = [(x_j - x_1)^2 + (y_j - y_1)^2]^{\frac{1}{2}}$$

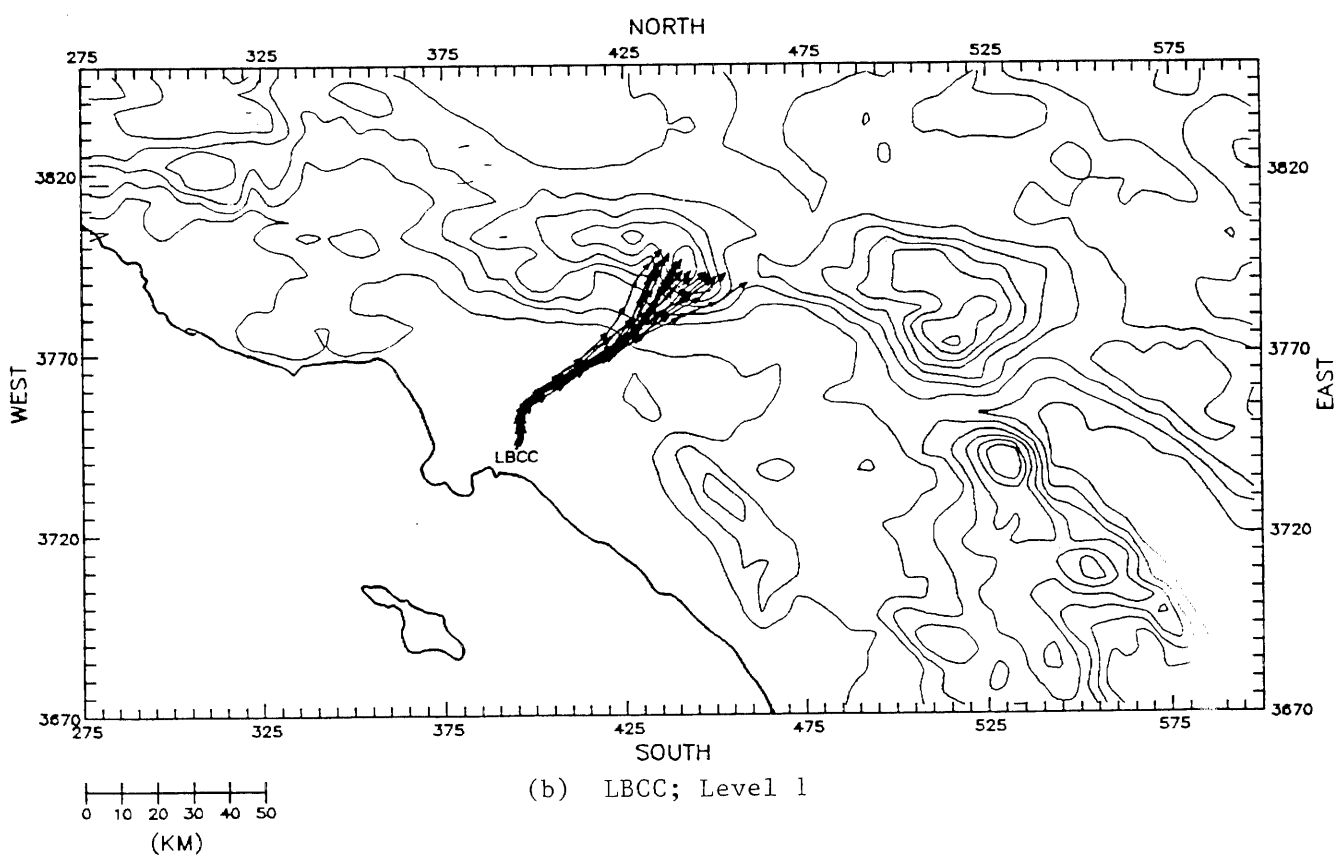
and where  $M$  is the number of particles, and  $(\cdot)_1$  represents the position of the actual particle as calculated in the previous section (i.e., the "zero" error particle path). The RMSE is used to determine the growth over time of the confidence interval about the

---

<sup>1</sup> IMSL is the registered trademark of the "Scientific Problem-Solving Software System" developed by IMSL Inc., Houston, Texas.



(a) CELA; Level 1



(b) LBCC; Level 1

FIGURE 3-1. Forward particle-path bundles initiated at 0700 PST 14 July 1987. Bundles are composed of 20 particle paths.

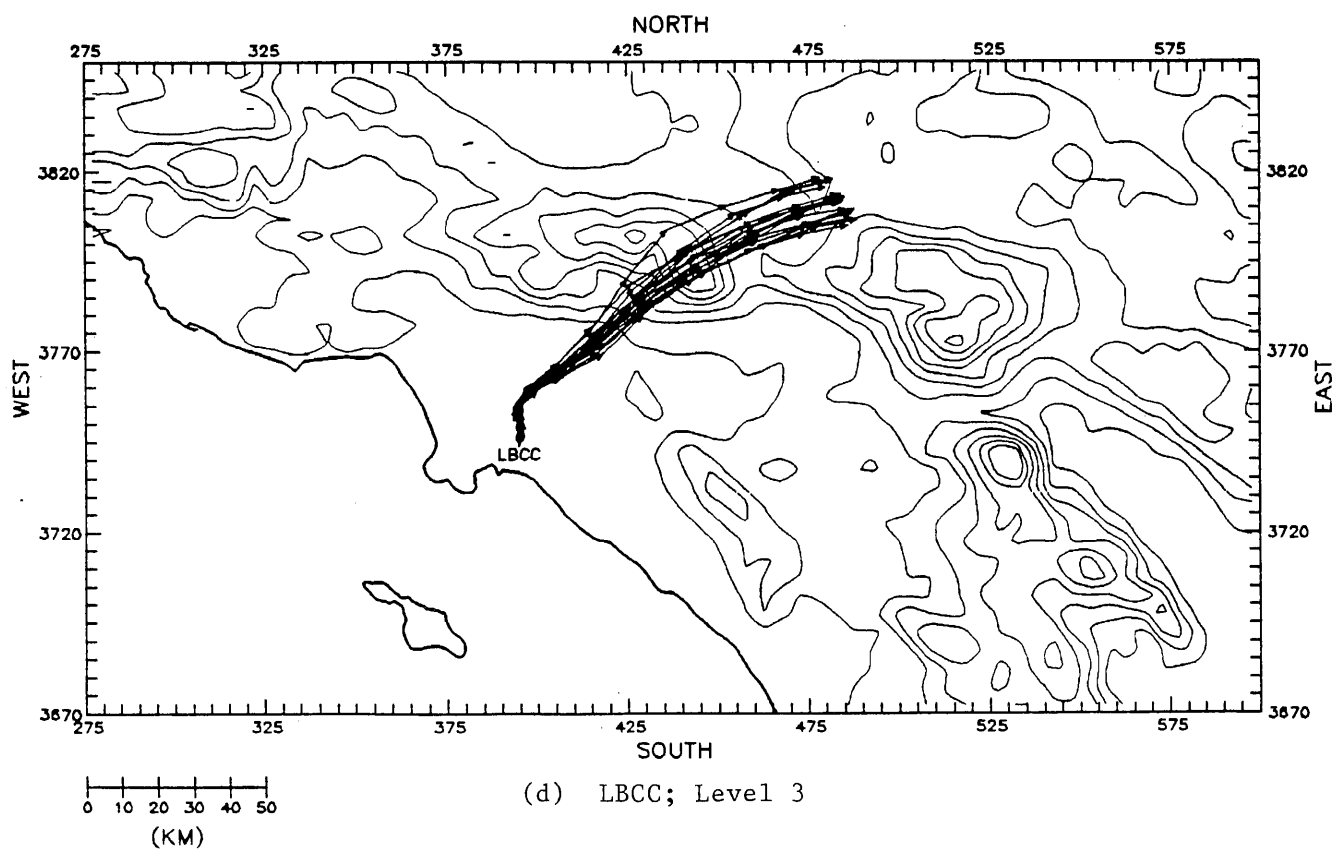
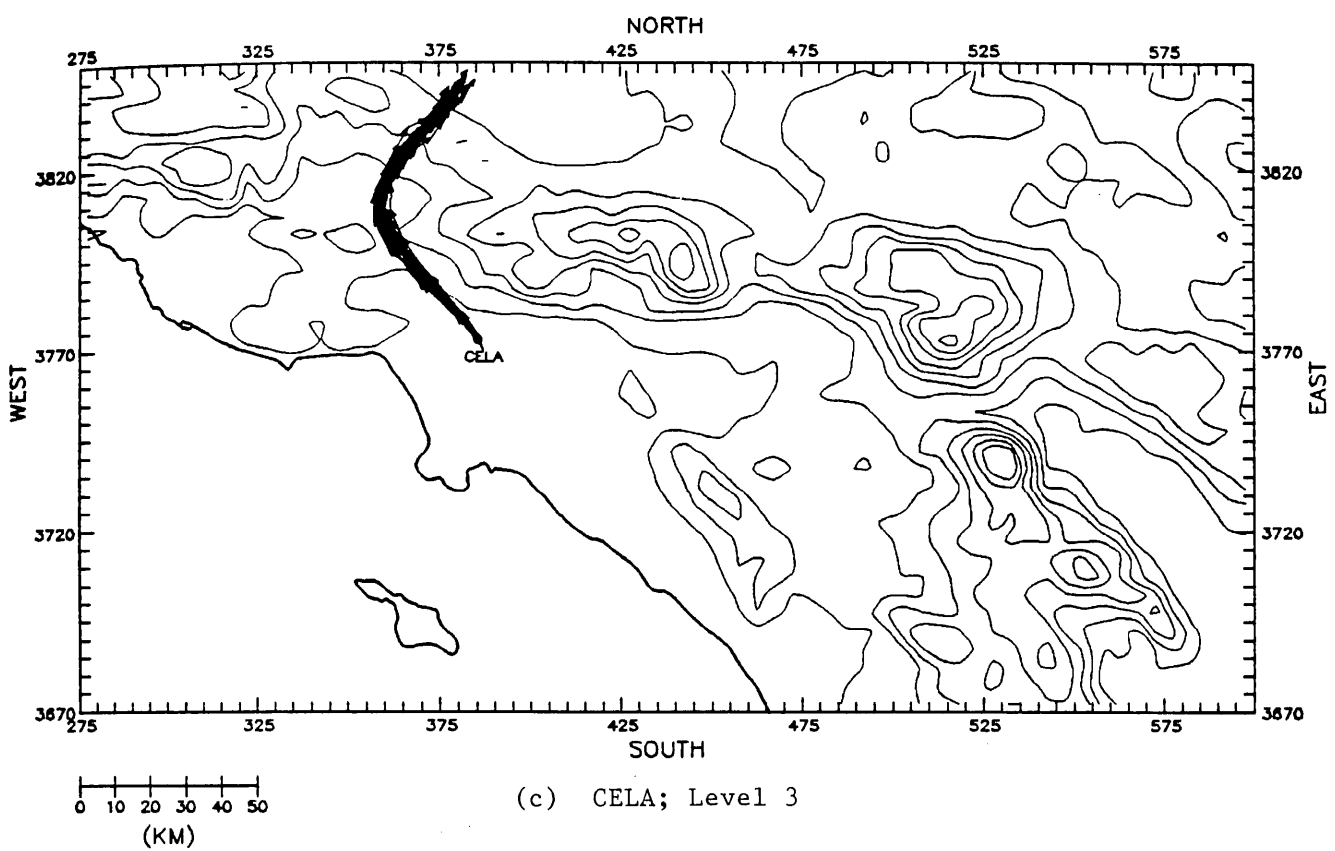


FIGURE 3-1. Concluded.

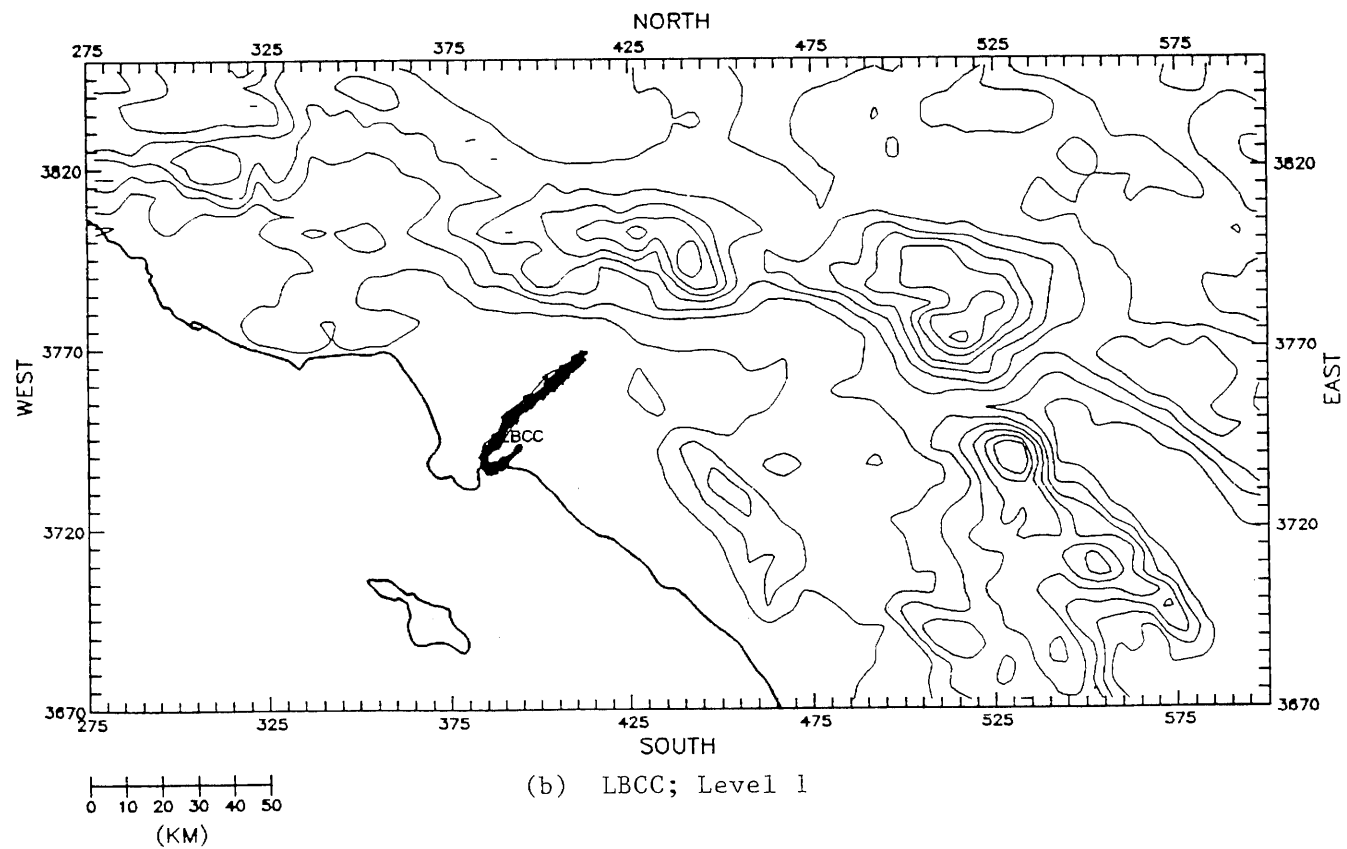
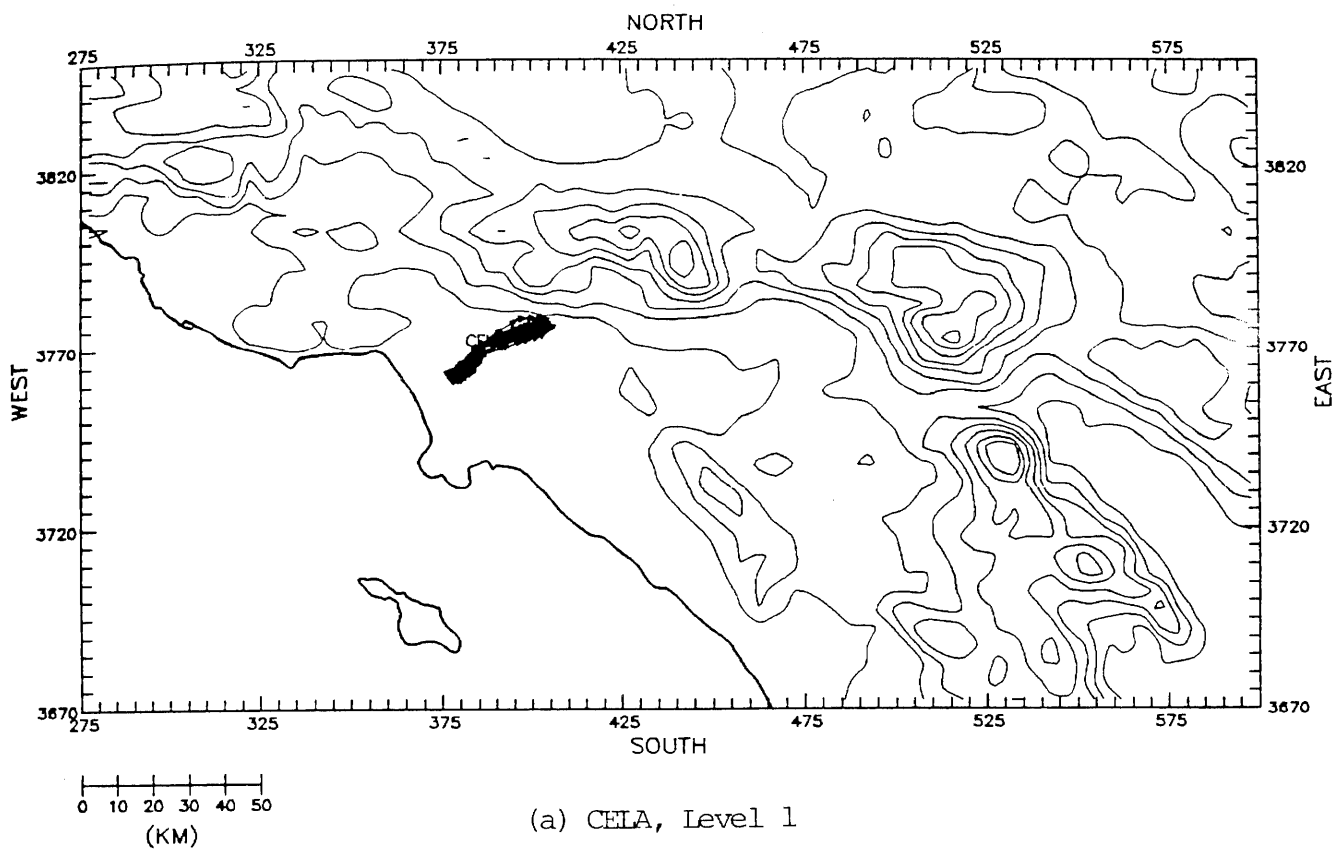
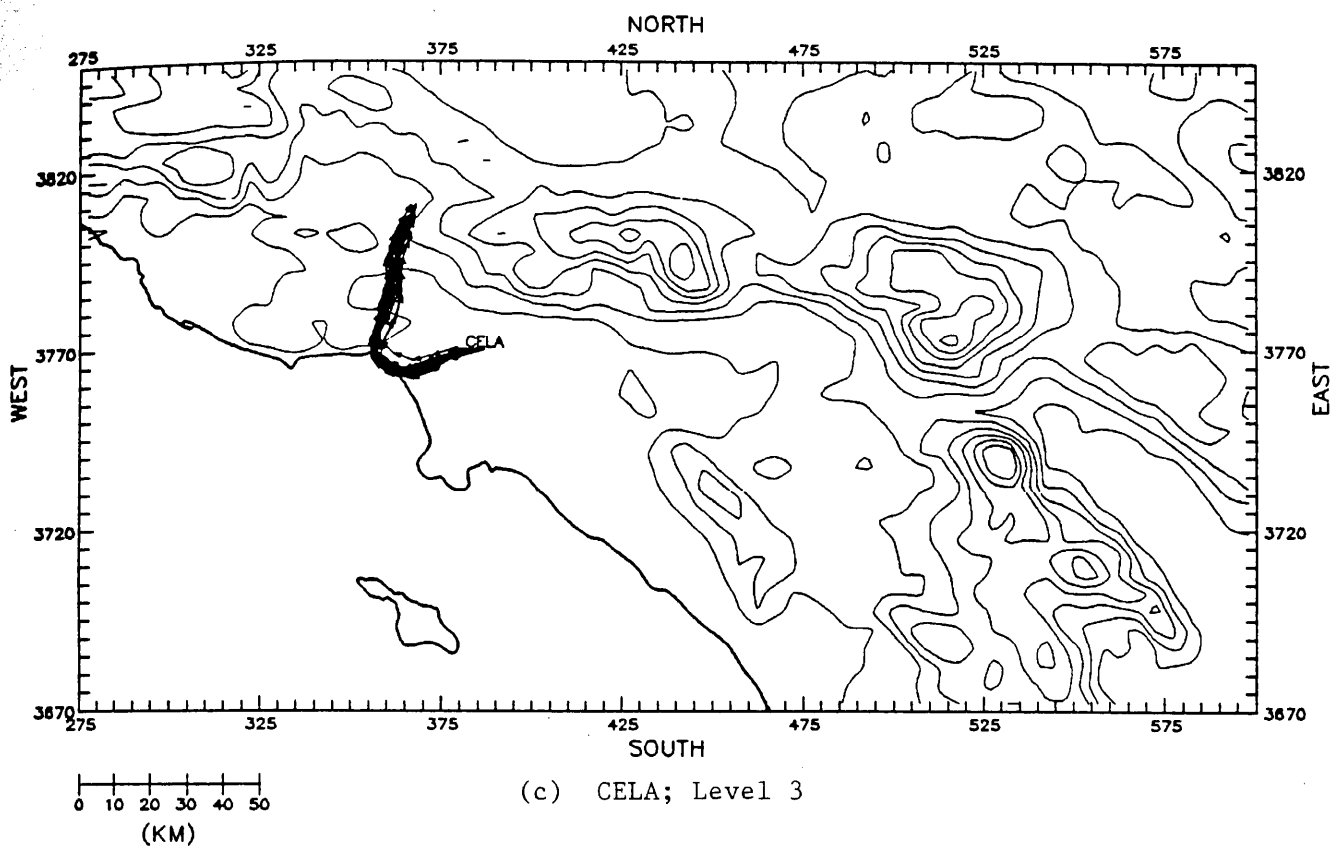
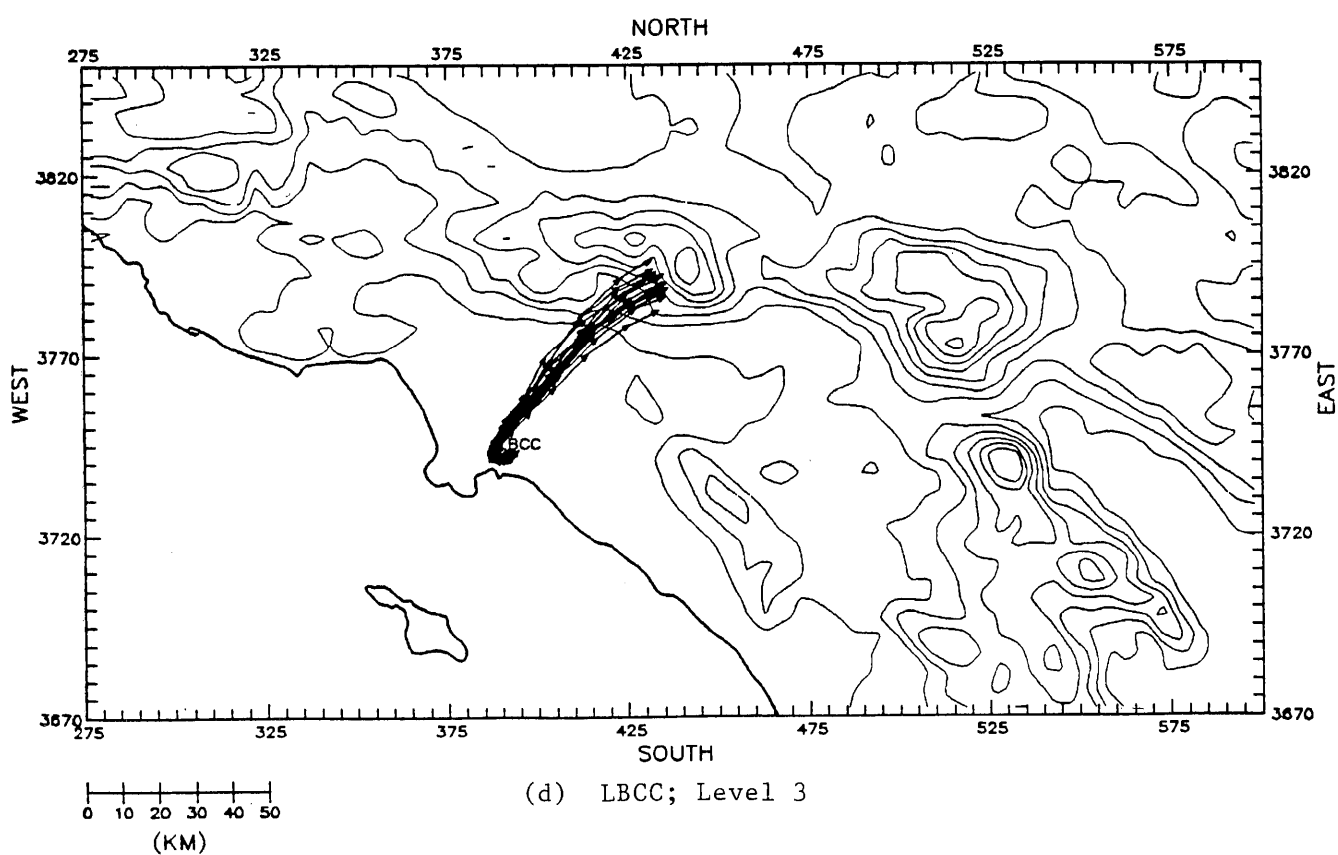


FIGURE 3-2. Forward particle-path bundles initiated at 0700 12 November 1987. Bundles are composed of 20 particle paths.



(c) CELA; Level 3



(d) LBCC; Level 3

FIGURE 3-2. Concluded.

trajectory calculated using the DWM winds. Hourly RMSE values are given for the particle paths bundles shown in Figures 3-1 and 3-2 in Tables 3-6 and 3-7, respectively. For level 1 the average RMSE after 12 hours is 5.67 km for 14 July and 1.67 km for 12 November. For level 3 the average RMSE after 12 hours is 4.16 for 14 July and 2.60 for 12 November.

**TABLE 3-6.** Hourly RMSEs for particle-path bundles initiated at 0700 PST 14 July 1987.

Time (PST)	LBCC RMSE (km)	CELA RMSE (km)
<b>Surface Level</b>		
0700	0.00	0.00
0800	0.42	0.42
0900	0.57	0.69
1000	0.63	1.00
1100	0.93	1.28
1200	0.91	1.43
1300	1.11	1.68
1400	1.36	2.17
1500	2.29	2.27
1600	2.65	2.19
1700	3.94	2.19
1800	6.20	2.65
1900	7.96	3.38
<b>Level 3</b>		
0700	0.00	0.00
0800	0.48	0.49
0900	0.64	0.90
1000	0.68	1.40
1100	0.87	1.72
1200	0.89	1.62
1300	1.23	1.80
1400	2.31	2.24
1500	3.37	2.58
1600	4.19	2.78
1700	4.27	3.06
1800	4.49	3.47
1900	4.62	3.70

TABLE 3-7. Hourly RMSEs for particle-path bundles initiated at 0700 PST 12 November 1987.

Time (PST)	LBCC RMSE (km)	CELA RMSE (km)
<b>Surface Level</b>		
0700	0.00	0.00
0800	0.47	0.49
0900	0.78	0.65
1000	0.77	0.66
1100	0.89	0.86
1200	1.09	0.94
1300	0.89	0.92
1400	1.18	1.25
1500	1.00	1.38
1600	1.29	1.50
1700	1.47	1.60
1800	1.61	1.64
1900	1.56	1.76
<b>Level 3</b>		
0700	0.00	0.00
0800	0.45	0.76
0900	0.61	1.20
1000	0.69	1.39
1100	0.92	1.71
1200	0.98	1.63
1300	0.96	1.56
1400	1.25	1.82
1500	1.50	1.75
1600	2.31	1.71
1700	2.61	1.52
1800	3.08	1.56
1900	3.45	1.75

## References

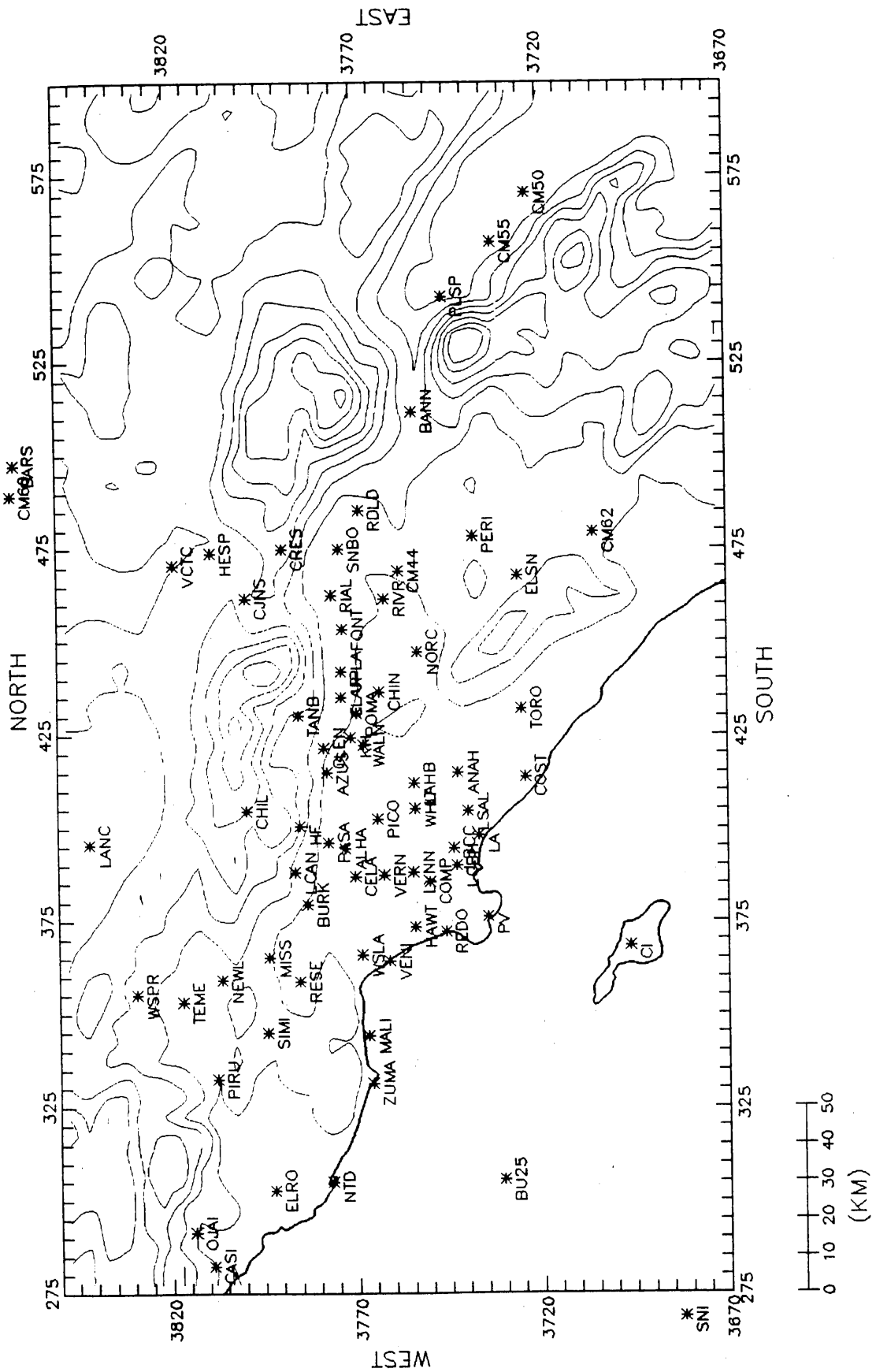
- Douglas, S. G., R. C. Kessler, and E. L. Carr. 1989. "User's Guide to the UAM Wind Preprocessor System." Systems Applications International, San Rafael, California (SYSAPP-89/079).
- England, W. G., and L. H. Teuscher. 1989. "Perfluorocarbon Tracer Experiments During the Southern California Air Quality Study." Air & Waste Management Association. For presentation at the 82nd Annual Meeting & Exhibition, Anaheim, California (June 25-30, 1989).
- Horrell, R. S., M. Deem, P. Wyckoff, F. Shair, and N. Crawford. 1989. "Ground Release SF6 Tracer Experiments Used to Characterize Transport and Dispersion of Atmospheric Pollutants During the Southern California Air Quality Study of 1987." For presentation at the 82nd Annual Meeting & Exhibition, Anaheim, California (June 25-30, 1989).
- Moore, G. E., G. Z. Whitten, J. P. Killus, and R. D. Stevens. 1989. "Analysis of 1985 Air Quality and Air Chemistry Data Collected Under the South Central Coast Cooperative Aerometric Monitoring Program." Systems Applications International, San Rafael, California (SYSAPP-89/058).
- Ross, D. G., and I. Smith. 1986. "Diagnostic Wind Field Modelling for Complex Terrain—Testing and Evaluation." Centre for Applied Mathematical Modelling (CAMM Report No. 5/86).



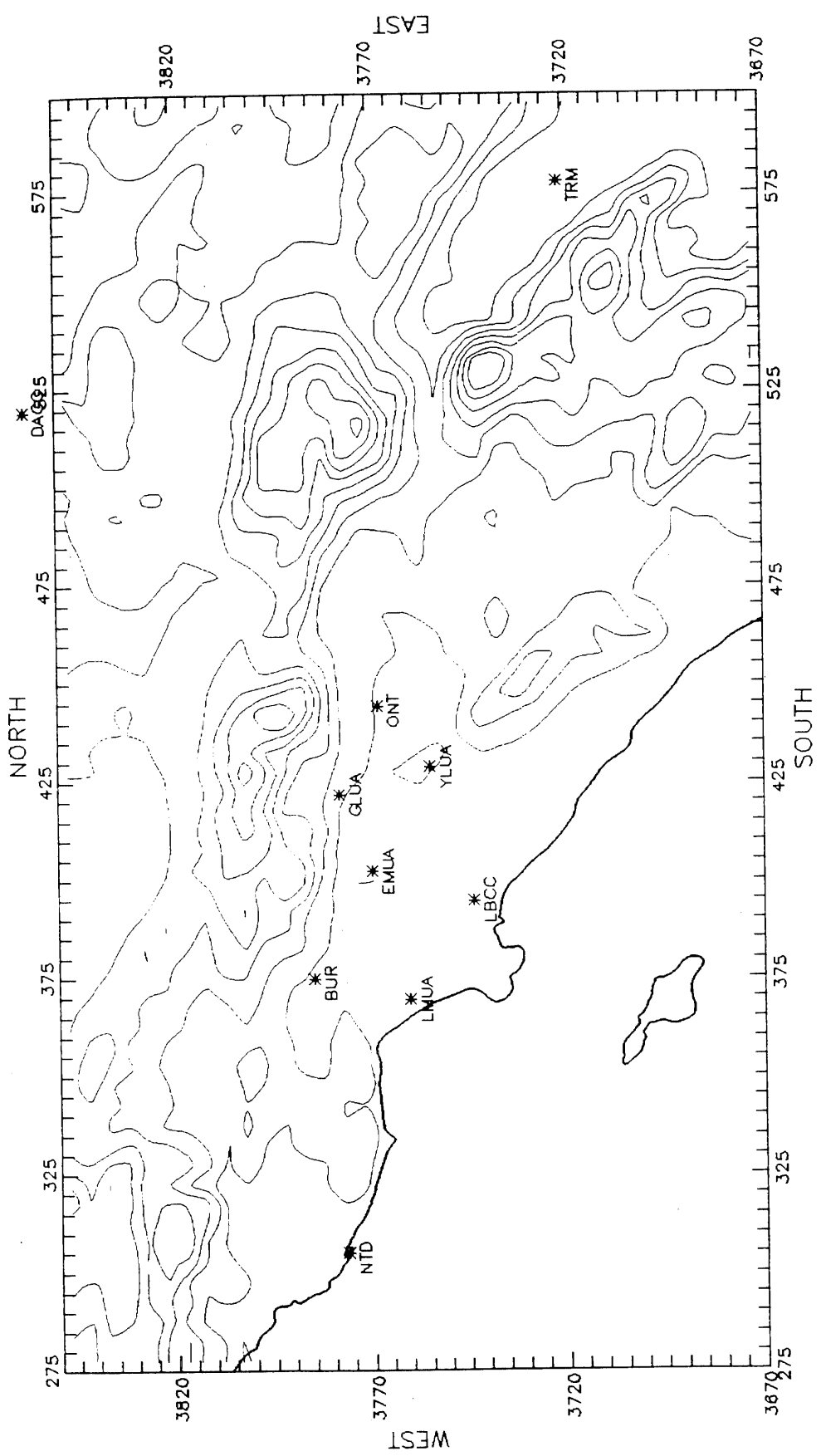
**Appendix A**

**SCAQS WIND MONITORING SITES**

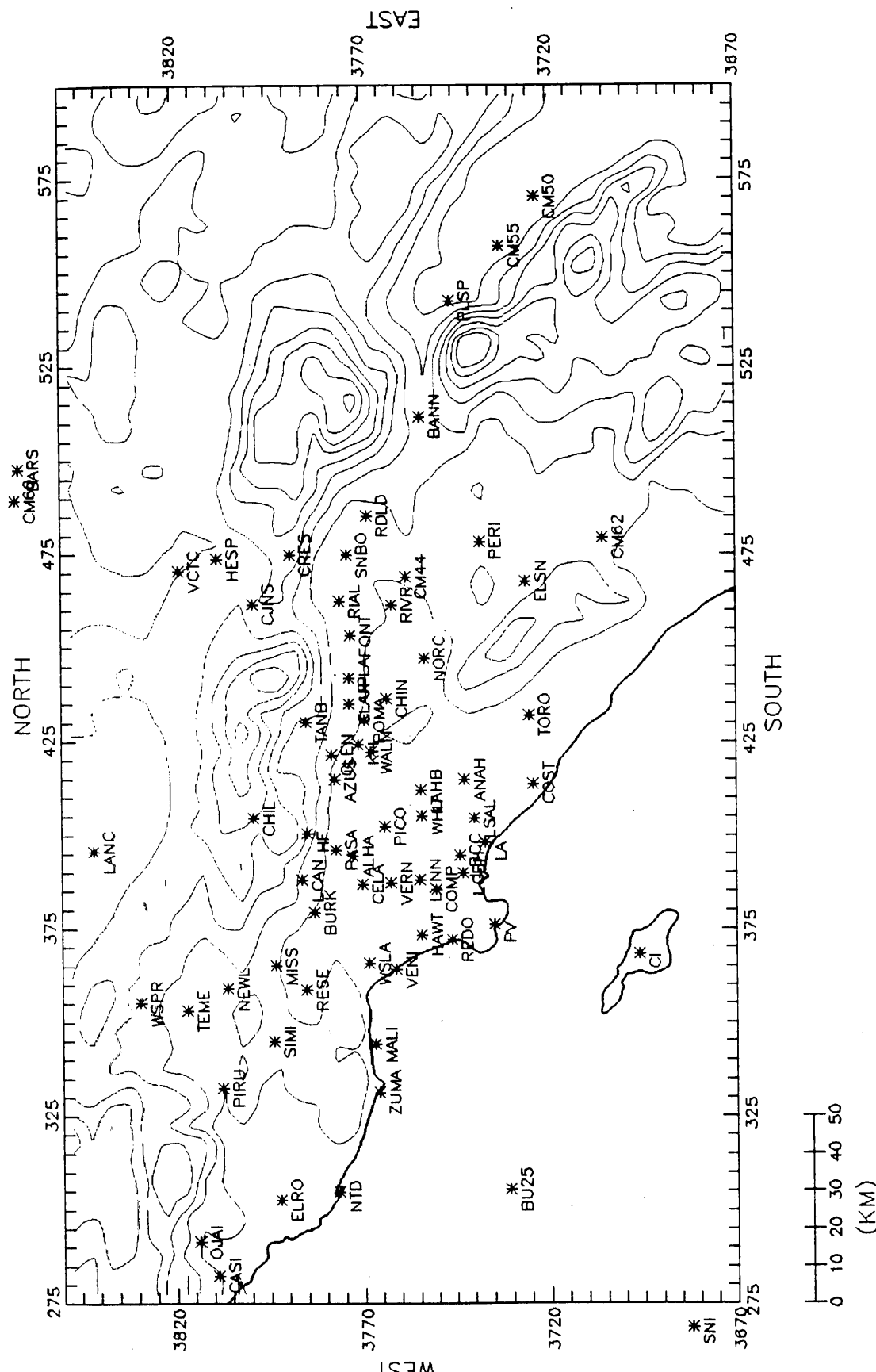




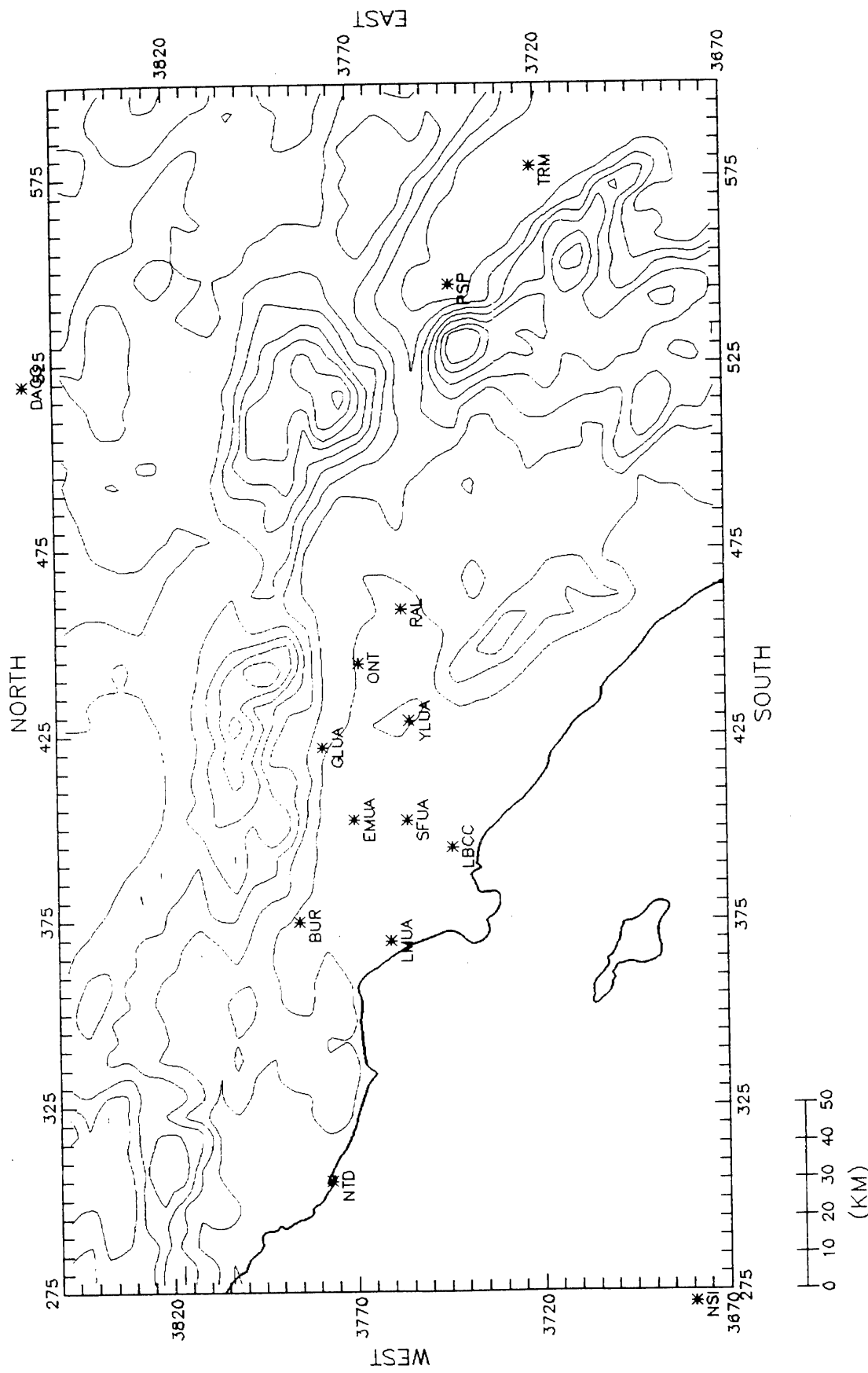
SCAQS SURFACE WIND MONITORING SITES  
19 JUNE 1987



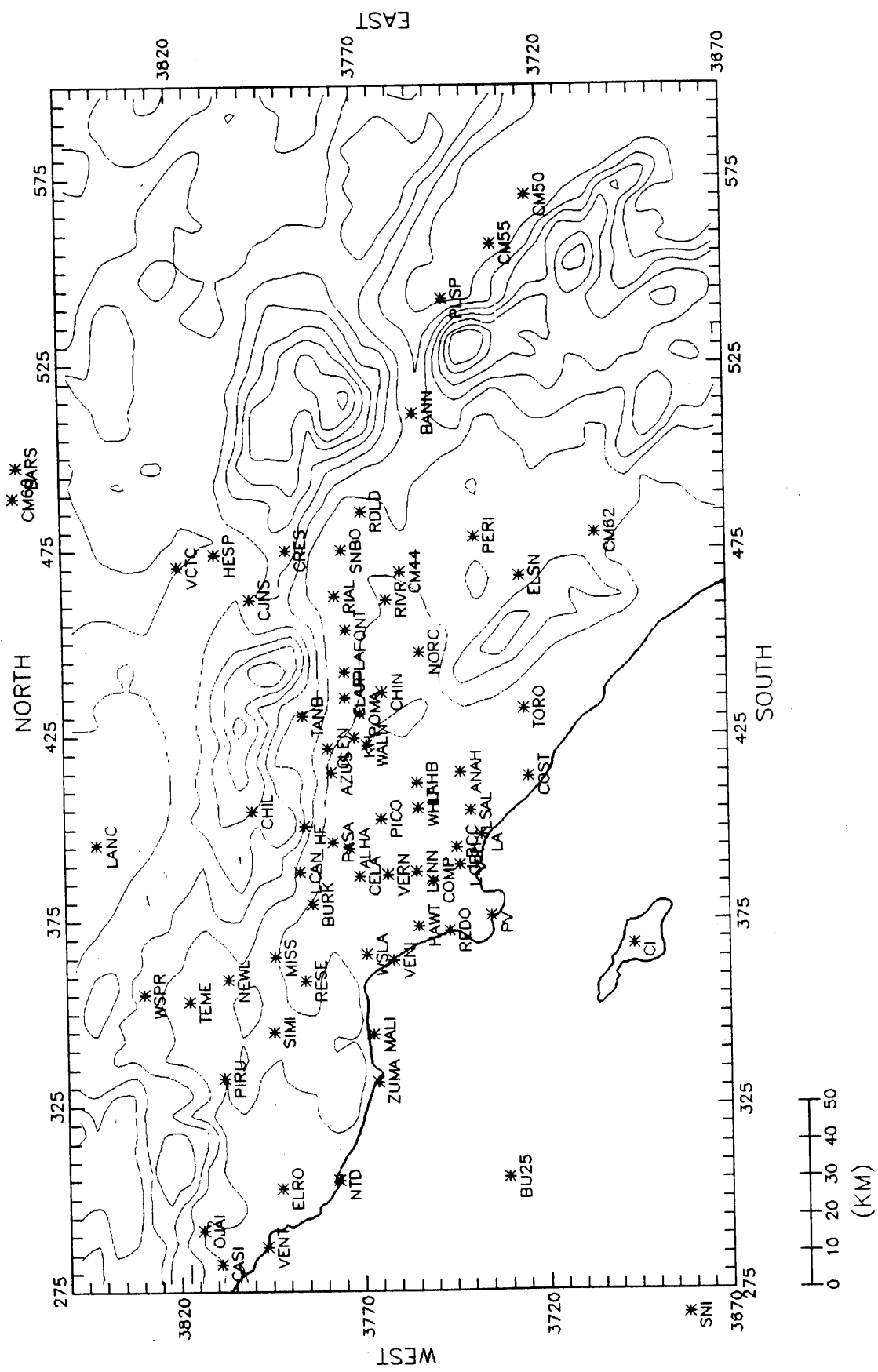
SCAQS UPPER-AIR WIND MONITORING SITES  
 19 JUNE 1987



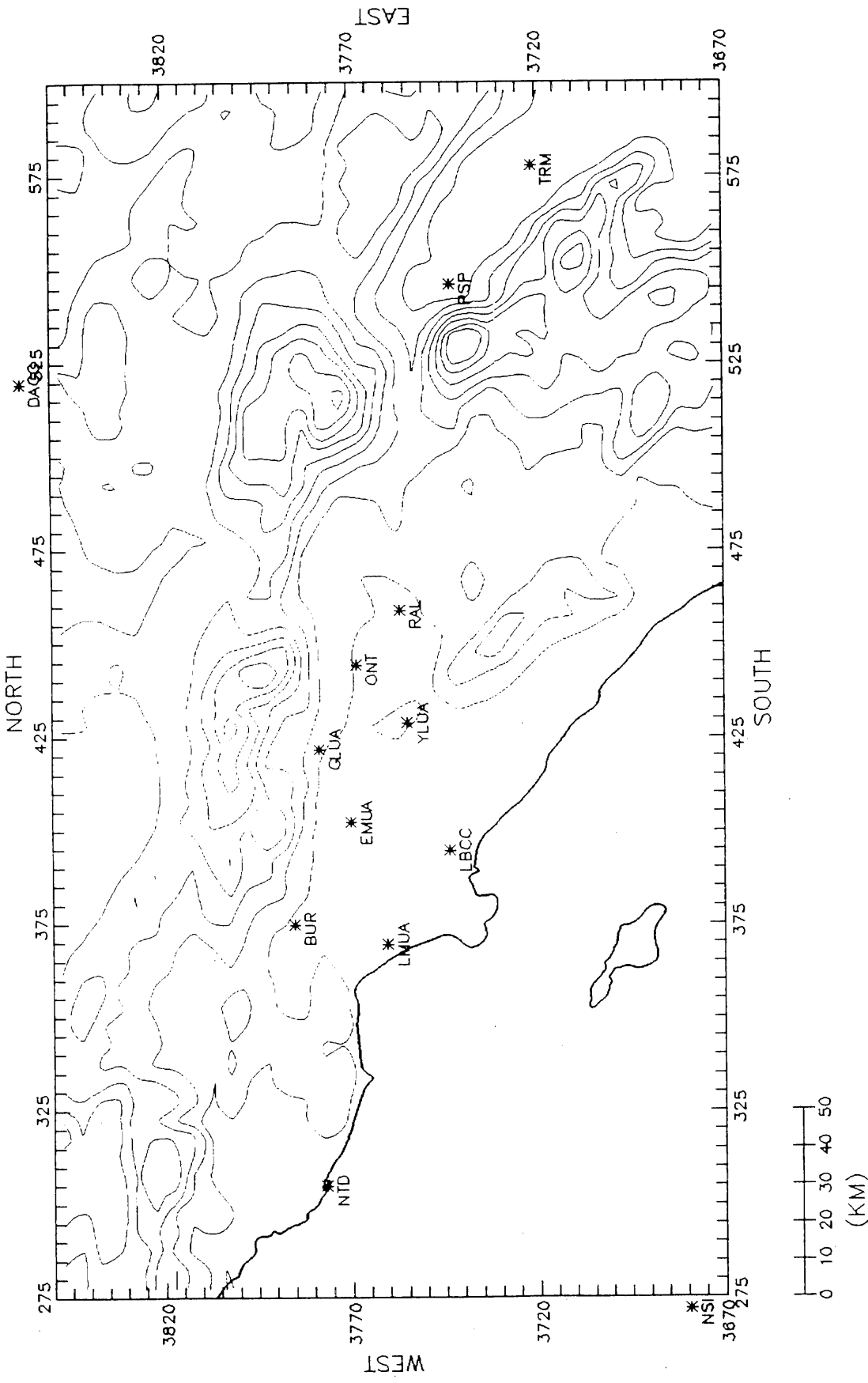
SCAQCS SURFACE WIND MONITORING SITES  
24-25 JUNE 1987



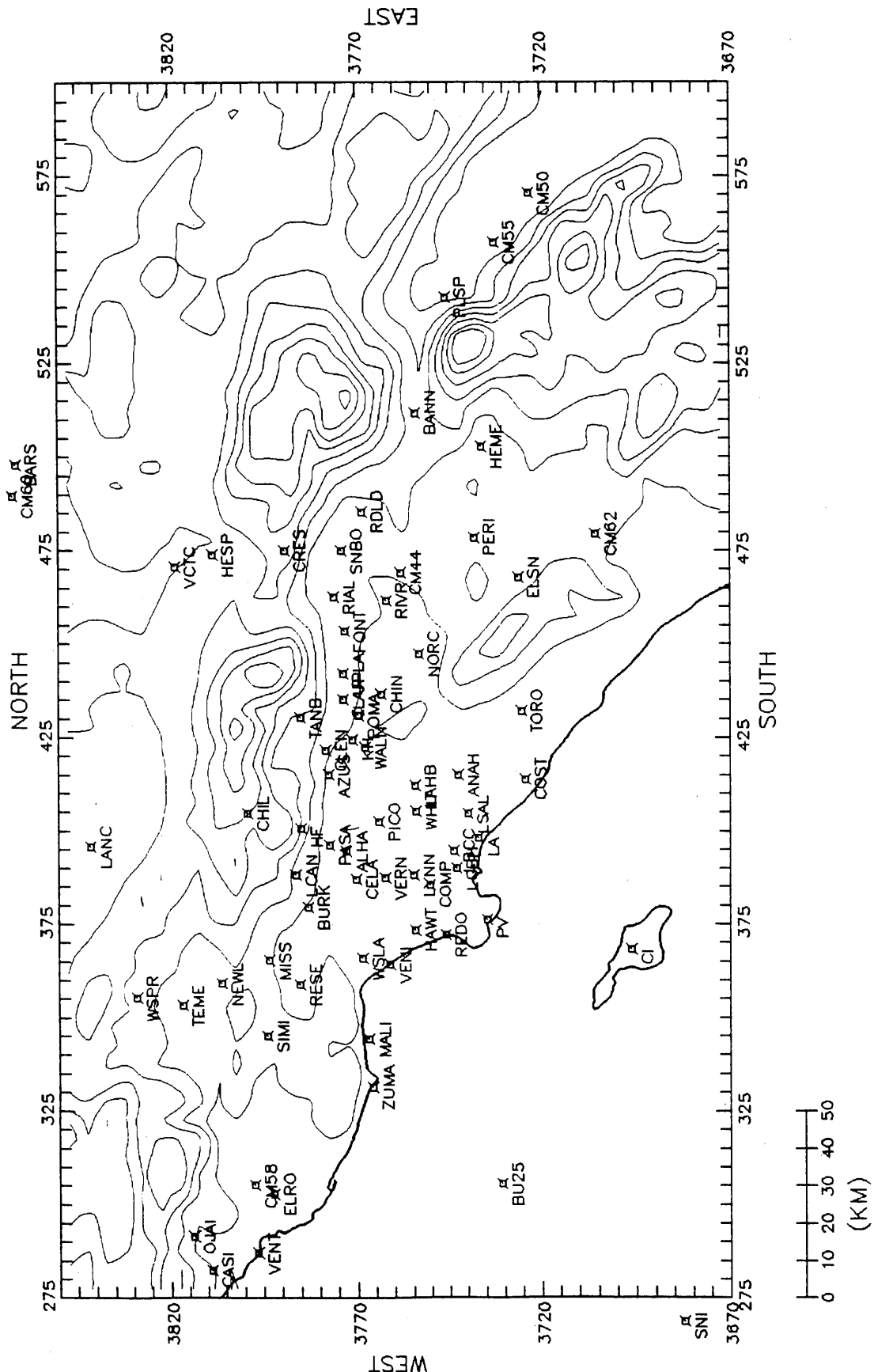
SCAQS UPPER-AIR WIND MONITORING SITES  
24-25 JUNE 1987



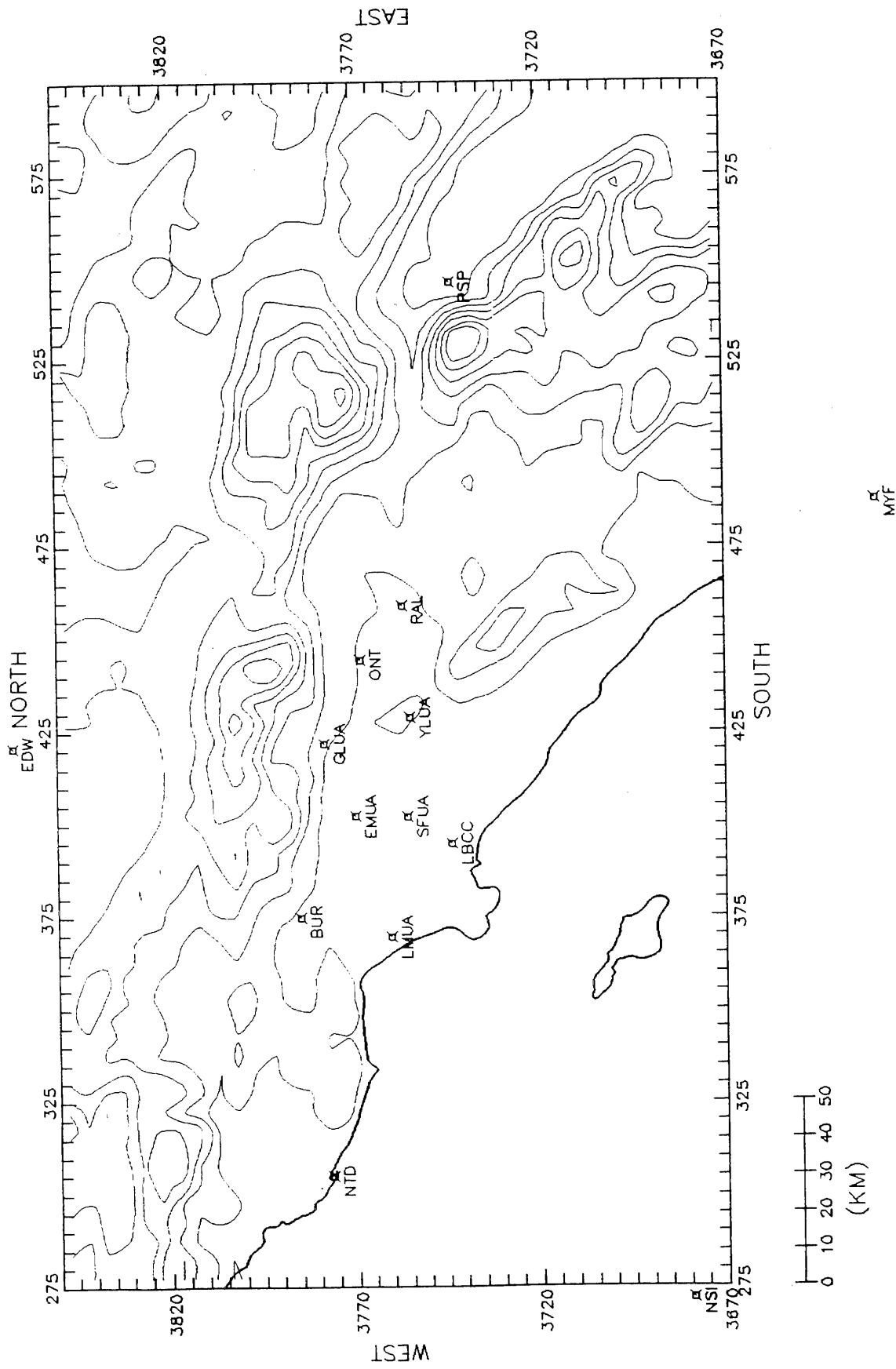
SCAQCS SURFACE WIND MONITORING SITES  
13-15 JULY 1987



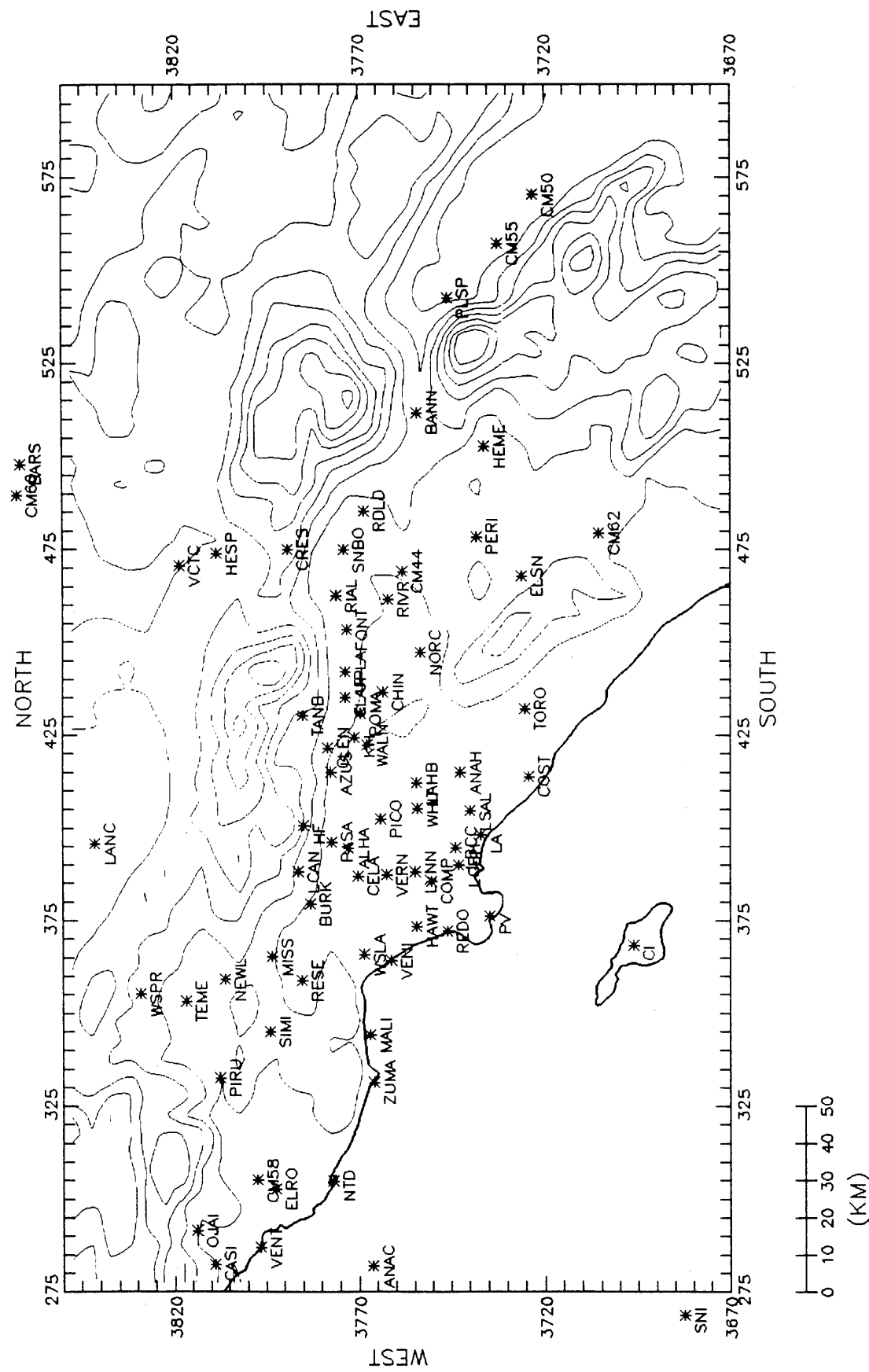
SCAQS UPPER-AIR WIND MONITORING SITES  
13-15 JULY 1987



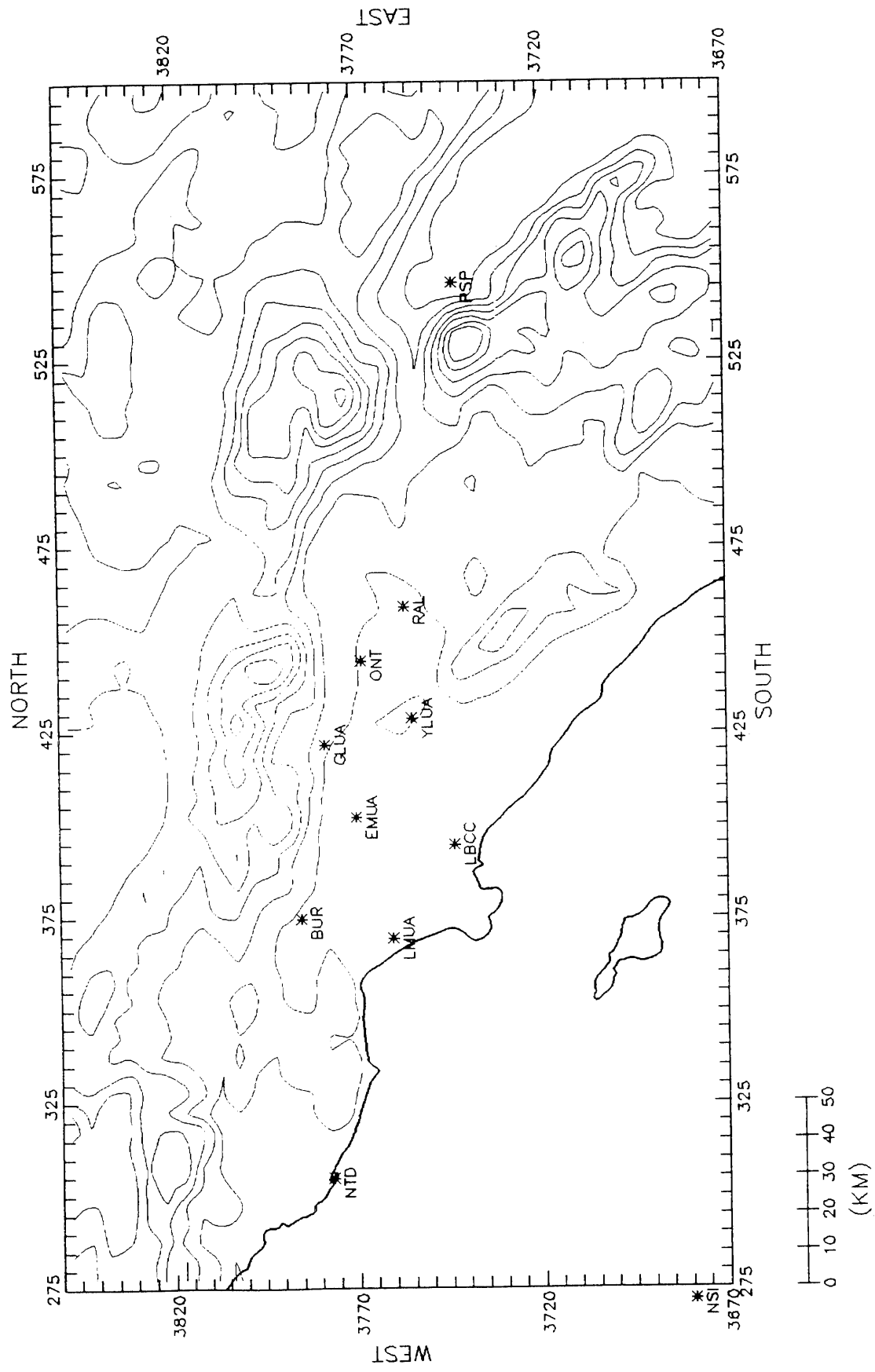
**SCAQS SURFACE WIND MONITORING SITES  
27-29 AUGUST 1987**



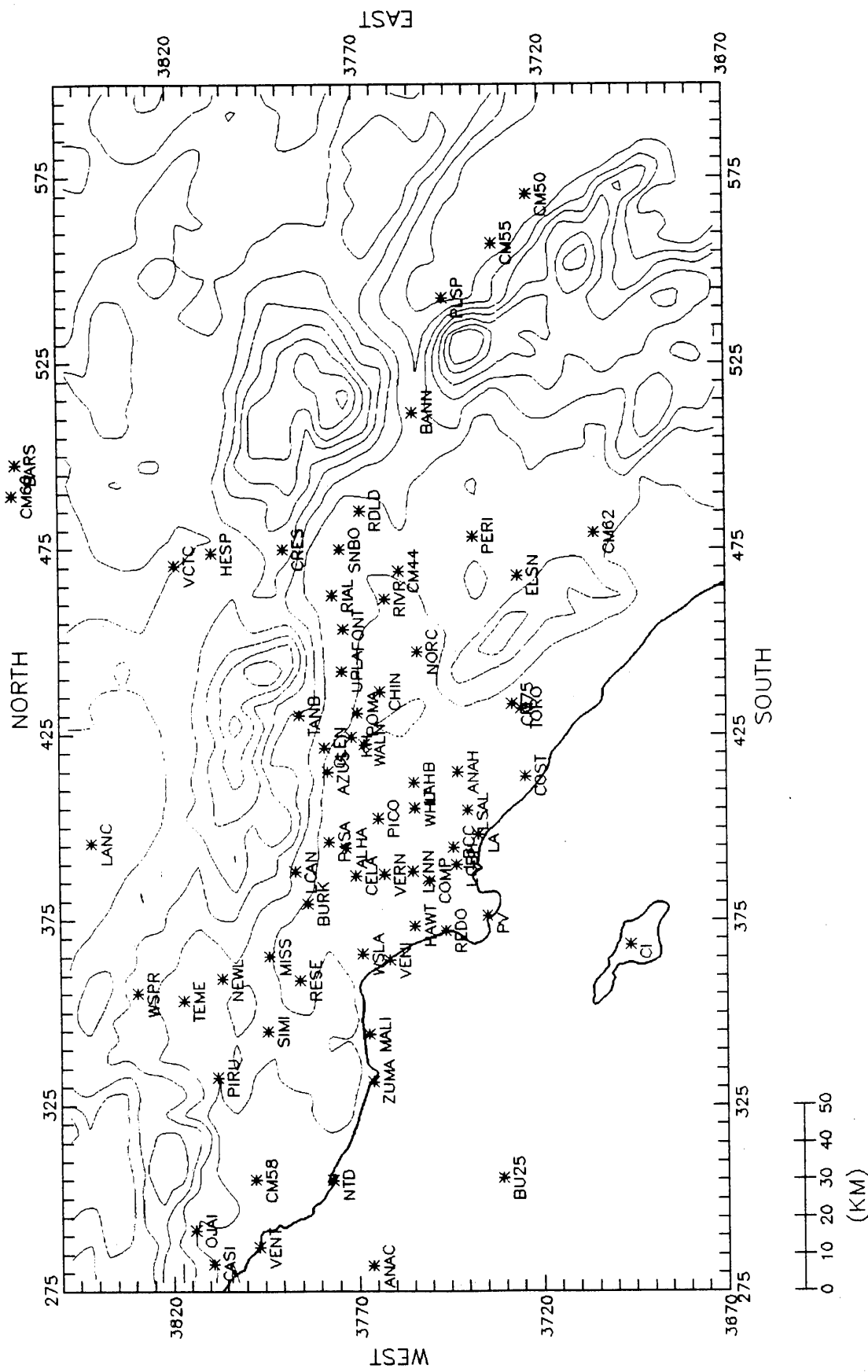
SCAQS UPPER-AIR WIND MONITORING SITES  
27-29 AUGUST 1987



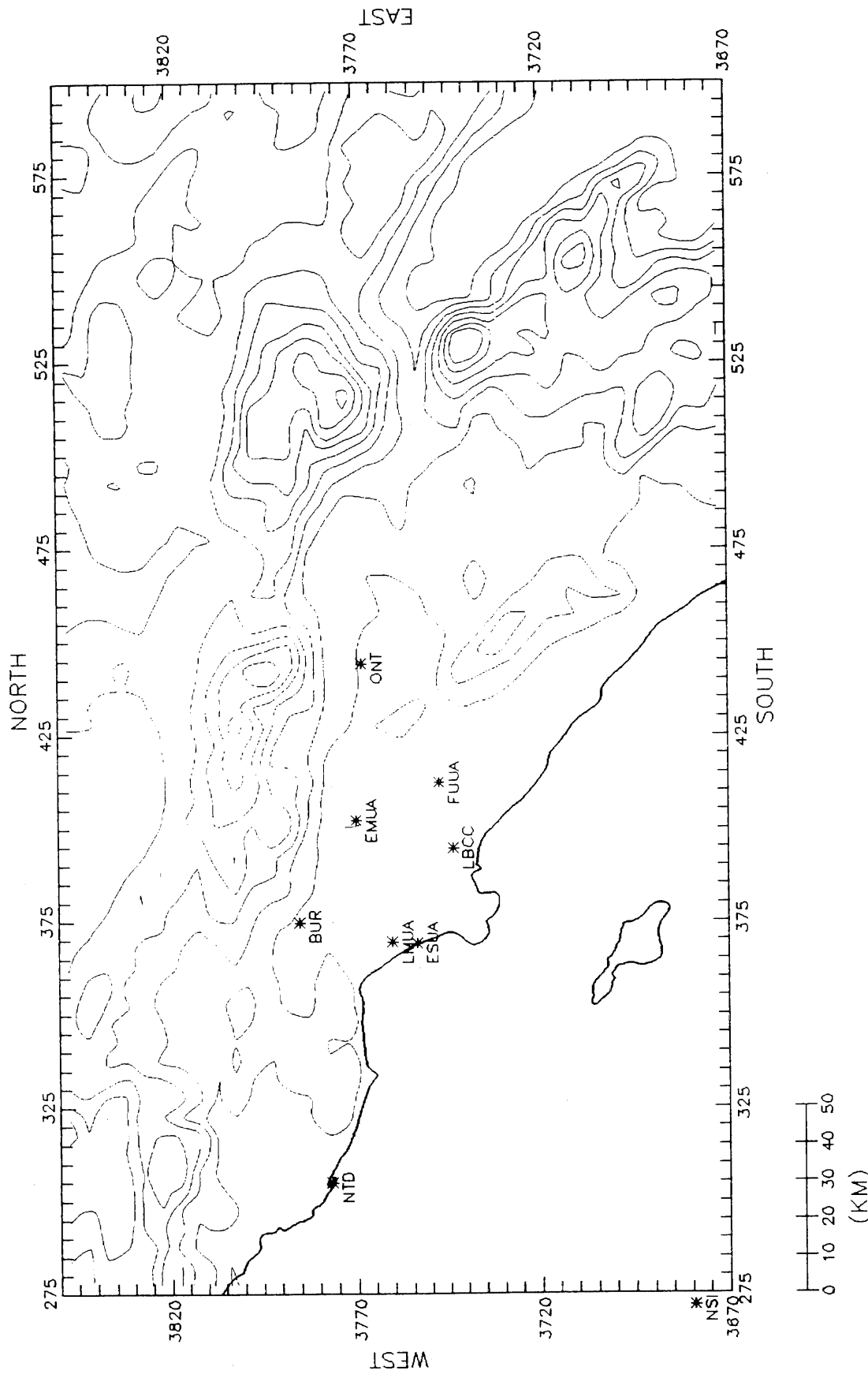
SCAQs SURFACE WIND MONITORING SITES  
02-03 SEPTEMBER 1987



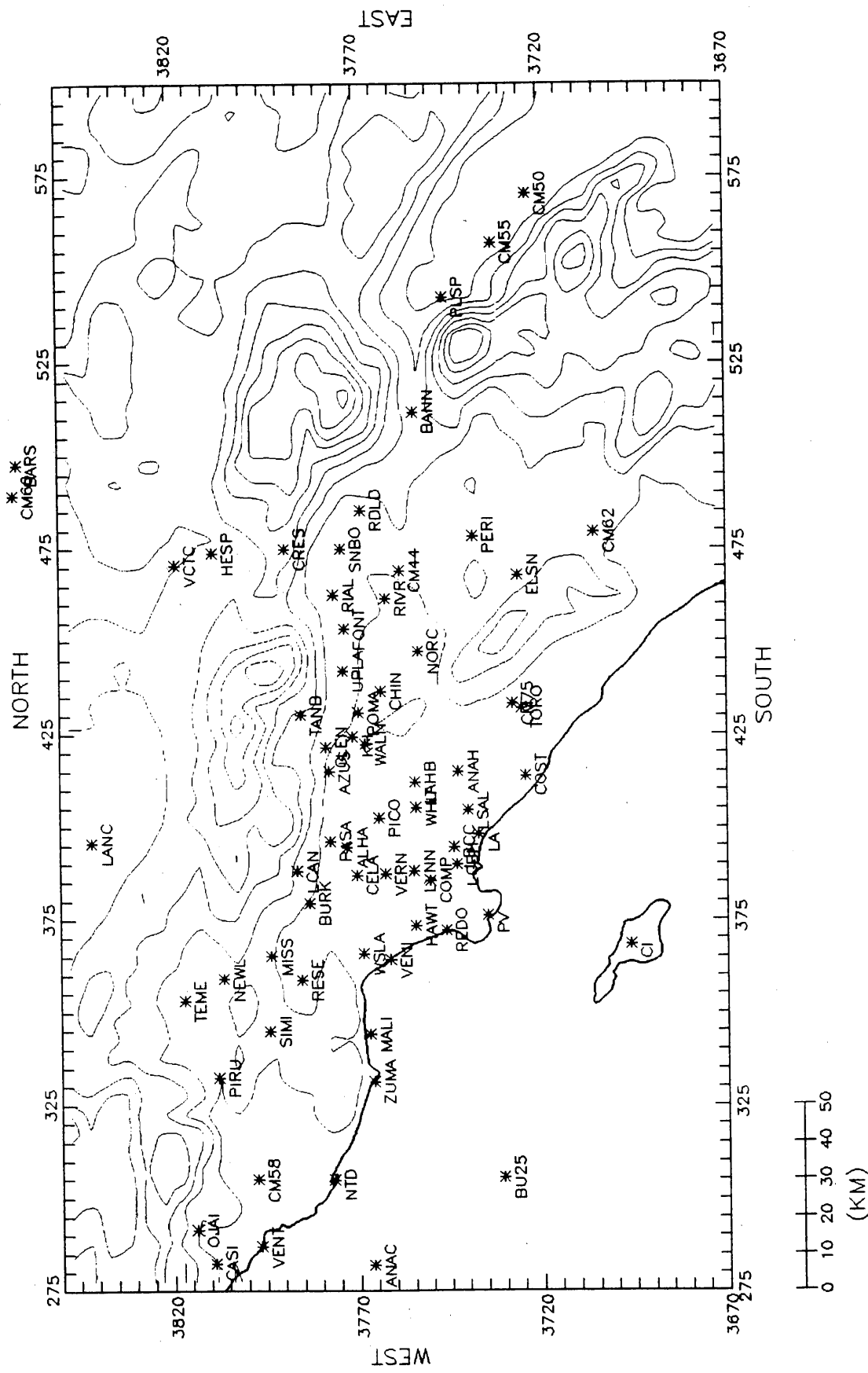
SCAQS UPPER-AIR WIND MONITORING SITES  
02-03 SEPTEMBER 1987



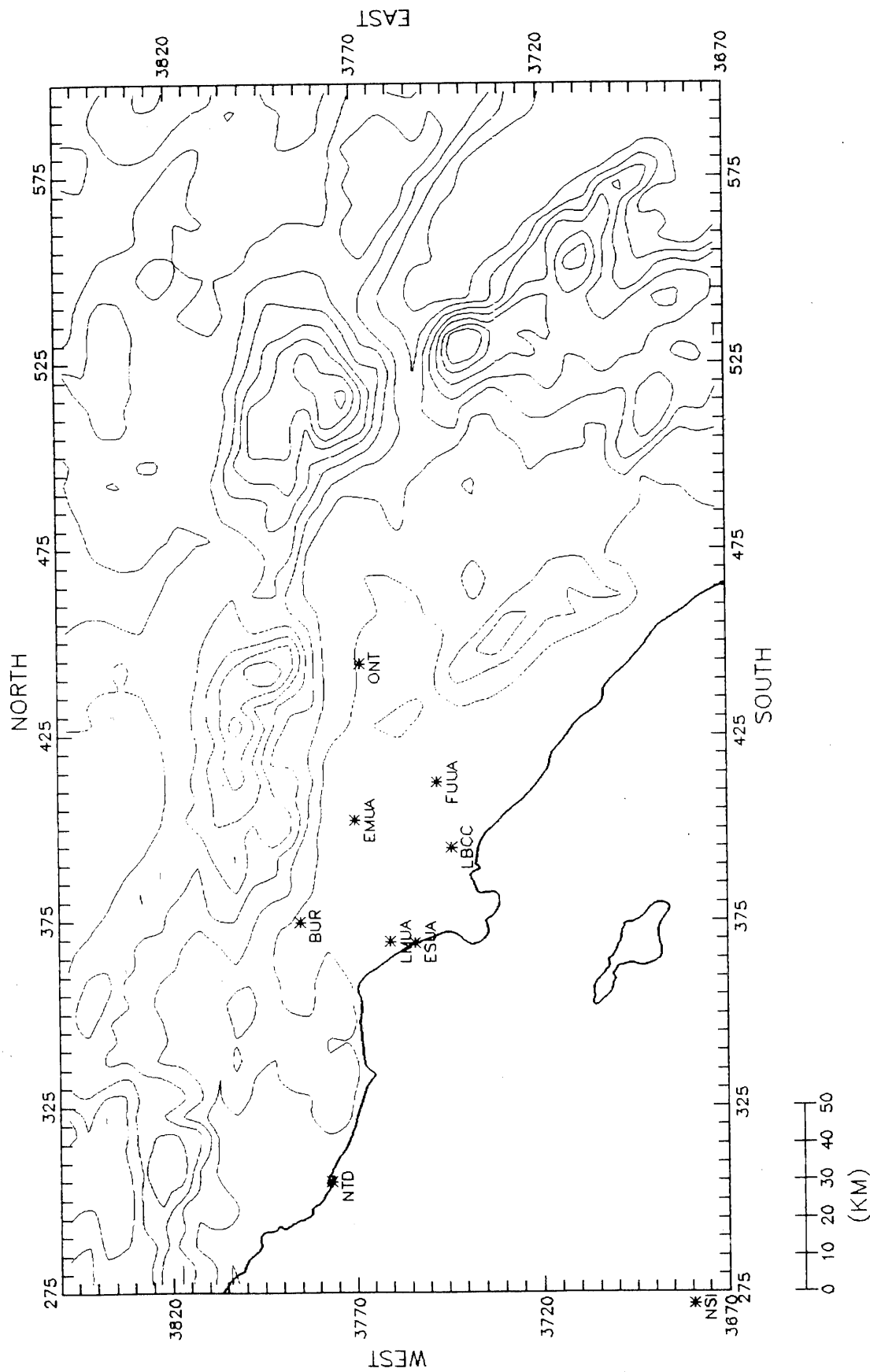
SCAQS SURFACE WIND MONITORING SITES  
11–13 NOVEMBER 1987



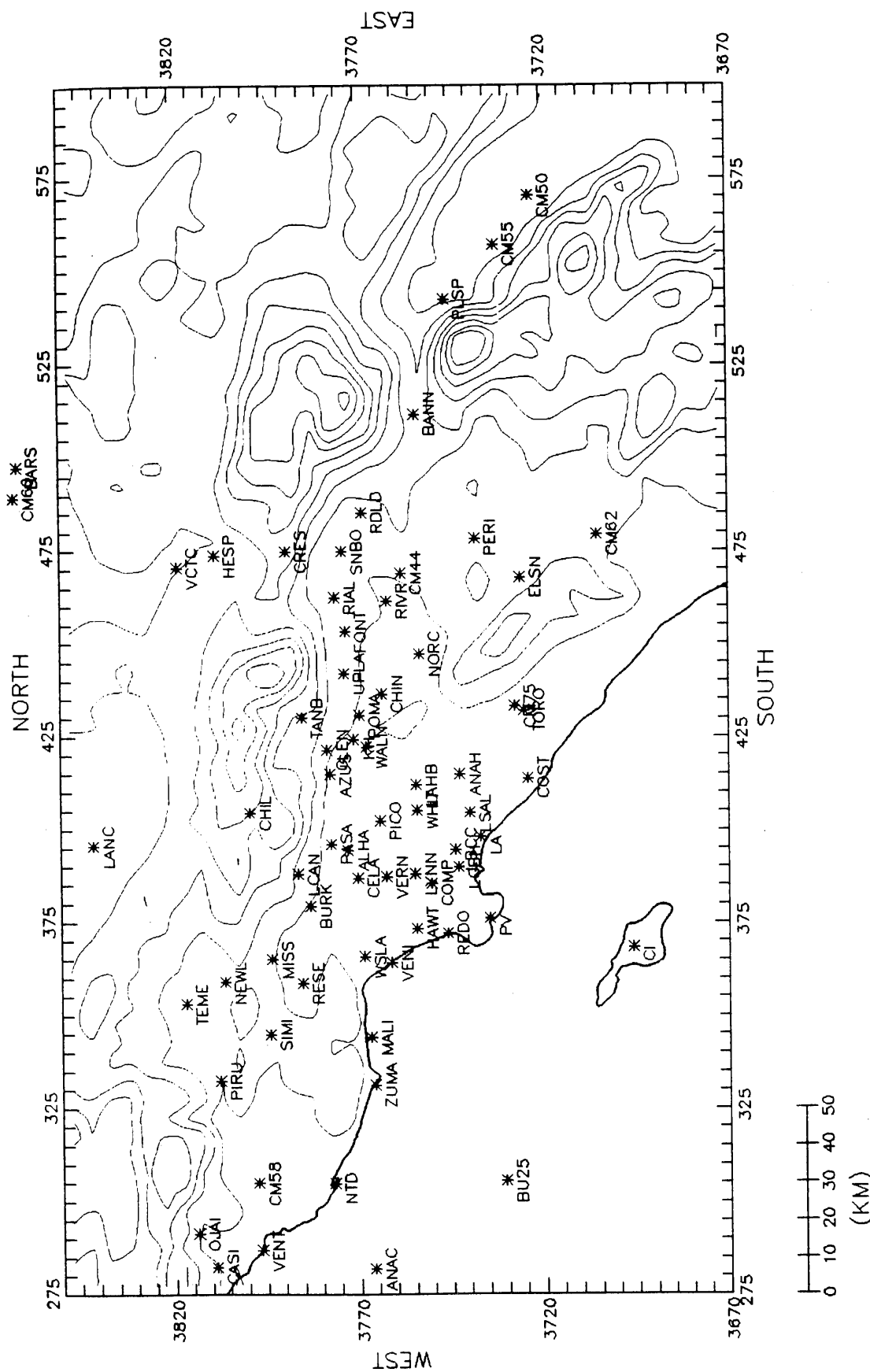
SCAQs UPPER-AIR WIND MONITORING SITES  
11-13 NOVEMBER 1987



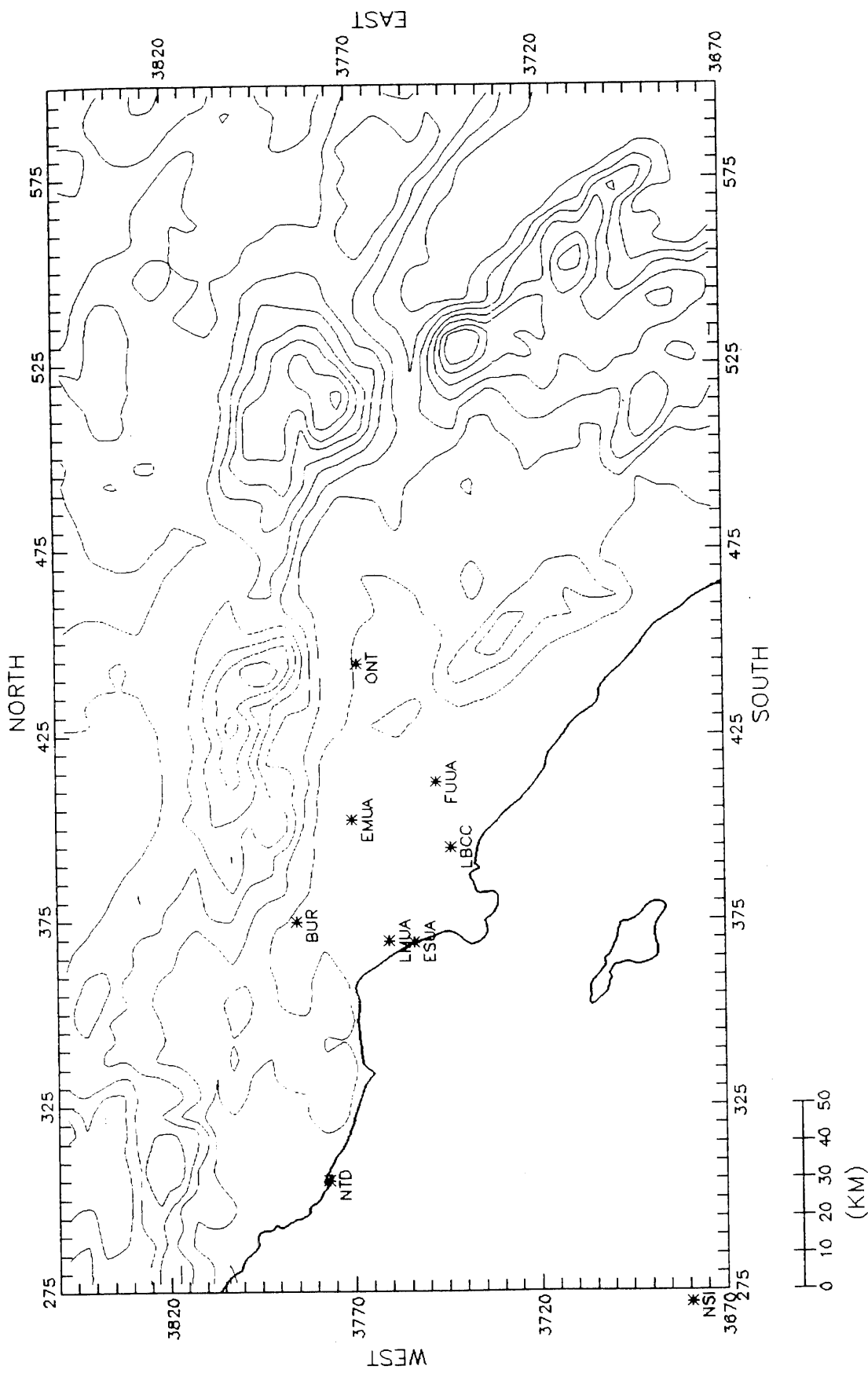
SCAQ SURFACE WIND MONITORING SITES  
03 DECEMBER 1987



SCAQS UPPER-AIR WIND MONITORING SITES  
03 DECEMBER 1987



SCAQs SURFACE WIND MONITORING SITES  
10-11 DECEMBER 1987



SCAQs UPPER-AIR WIND MONITORING SITES  
10-11 DECEMBER 1987

## **Appendix B**

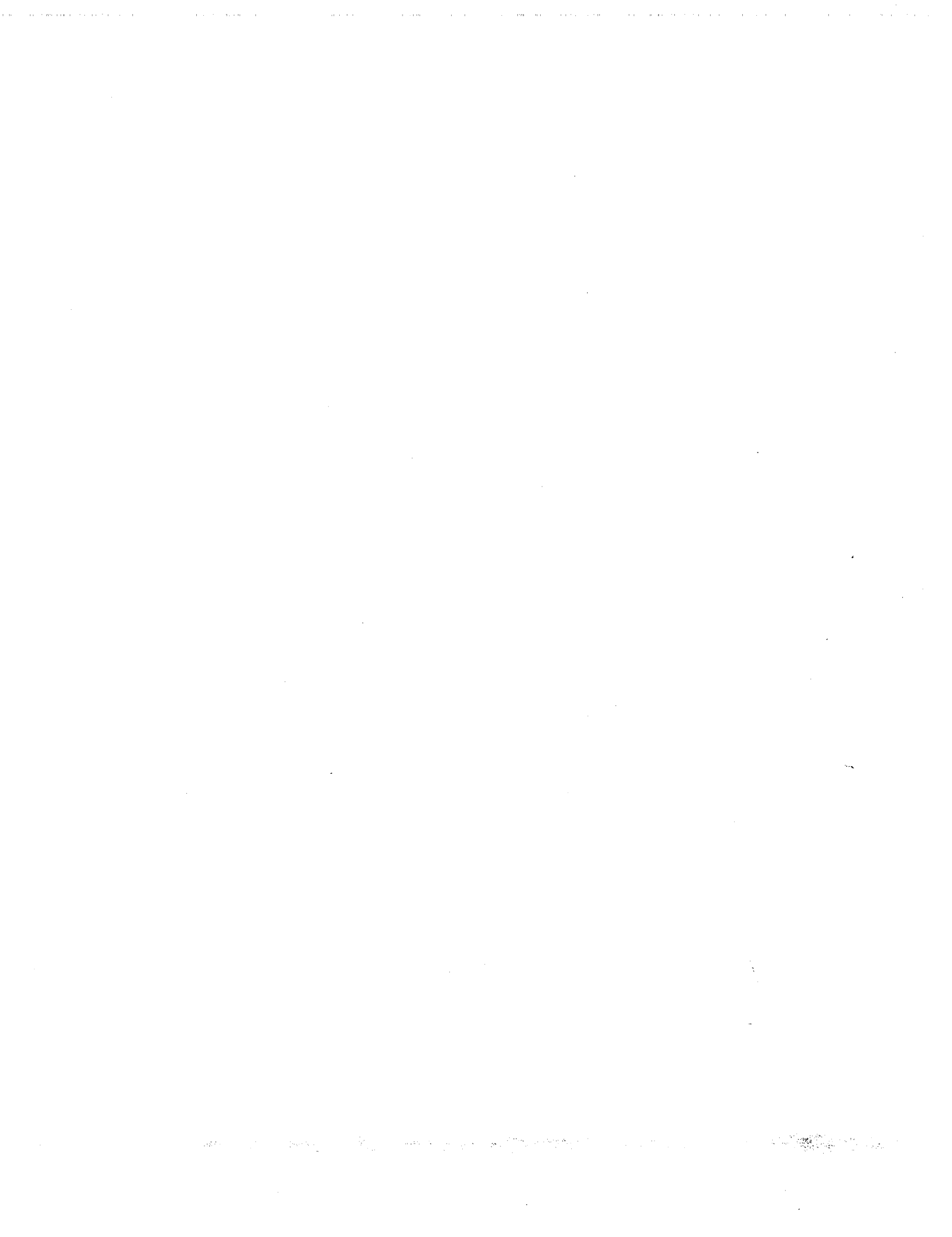
### **SCAQS DIAGNOSTIC WIND ANALYSES (Six-hourly plots; Levels 1, 3, and 5)**

#### **Summer Intensive Monitoring Periods                    Page**

19 June 1987	B-1
24-25 June 1987	B-13
13-15 July 1987	B-37
27-29 August 1987	B-73
2-3 September 1987	B-109

#### **Autumn Intensive Monitoring Periods**

11-13 November 1987	B-133
3 December 1987	B-169
10-11 December 1987	B-181

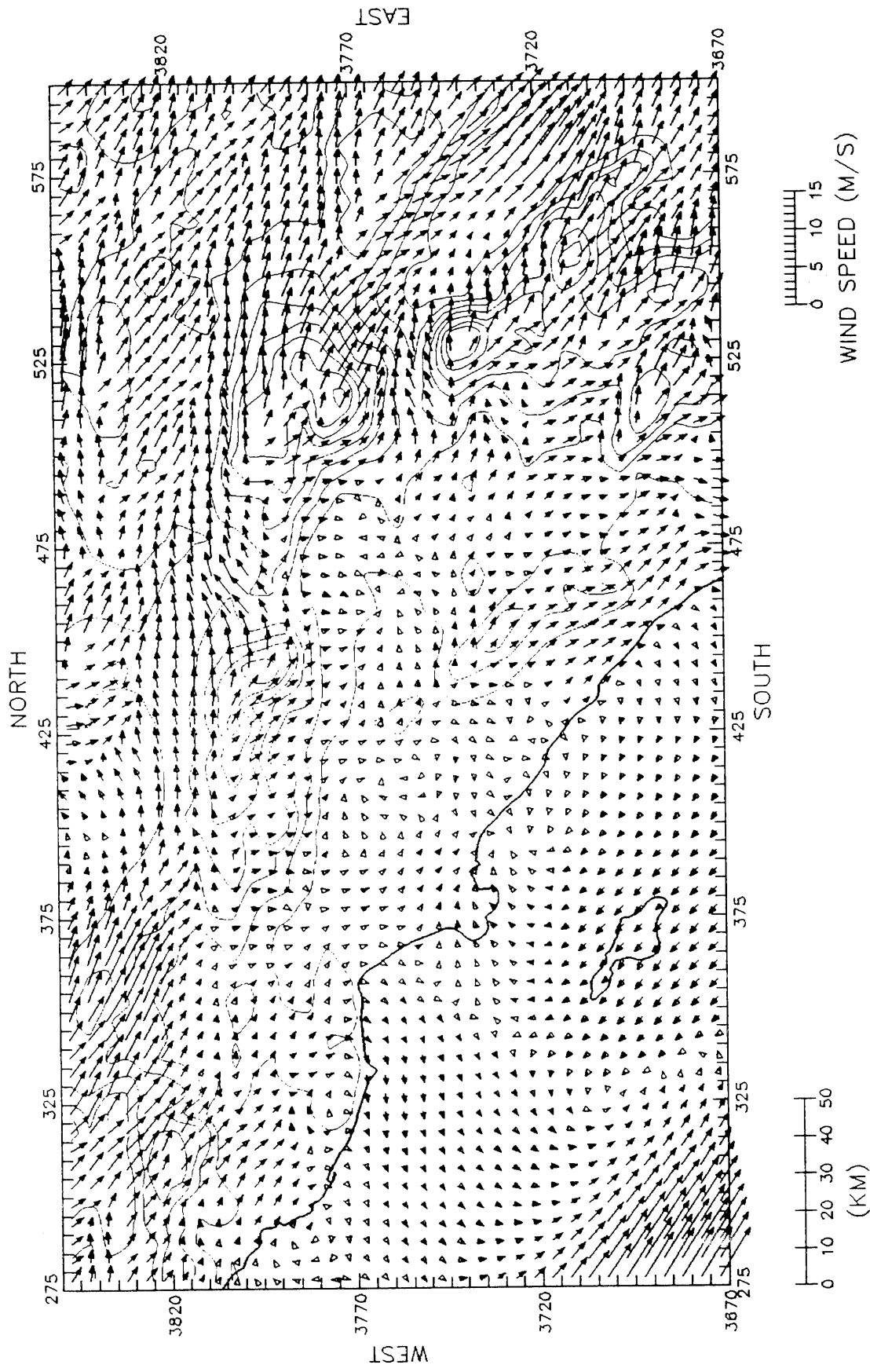


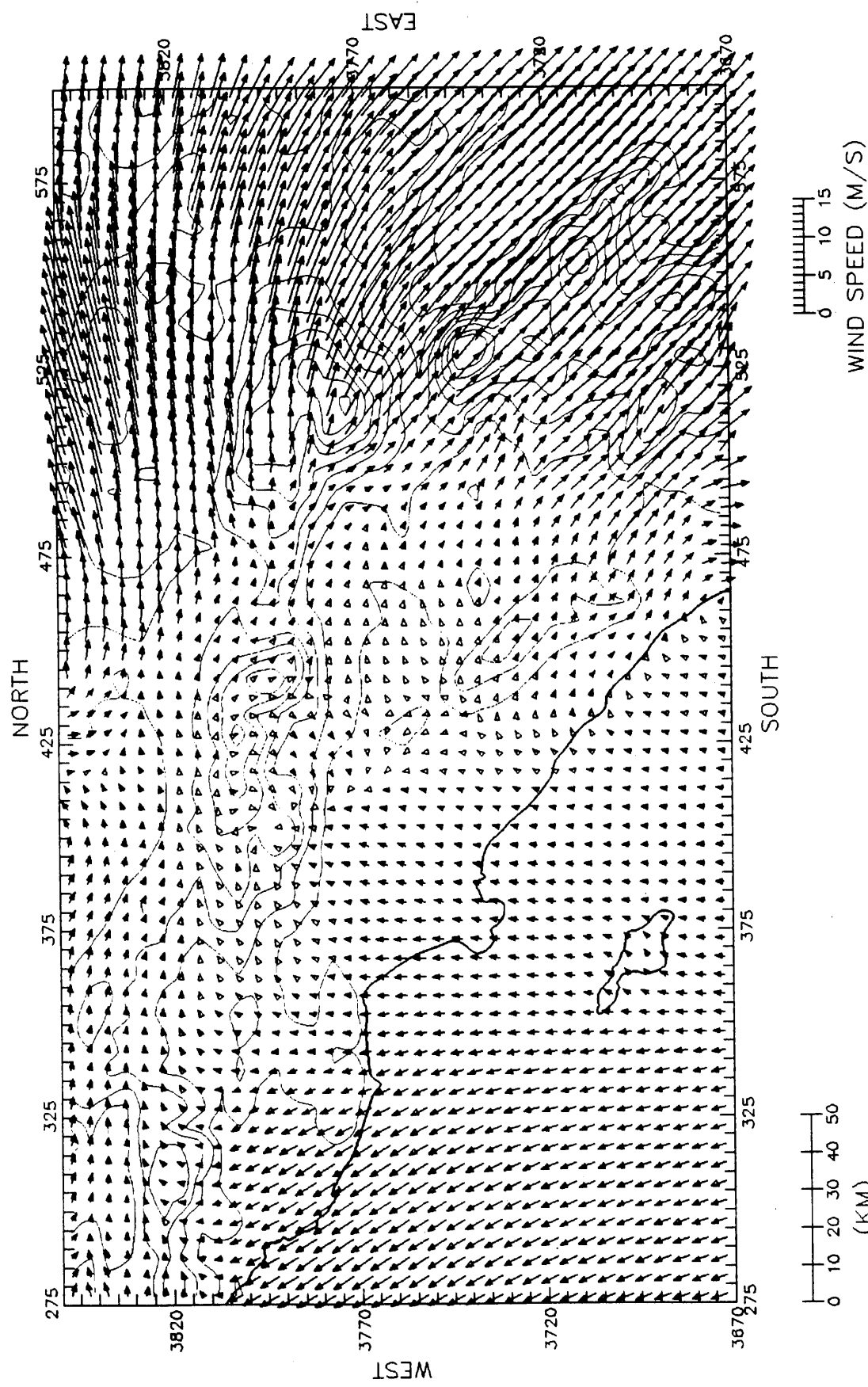
## **Summer Intensive Monitoring Periods**



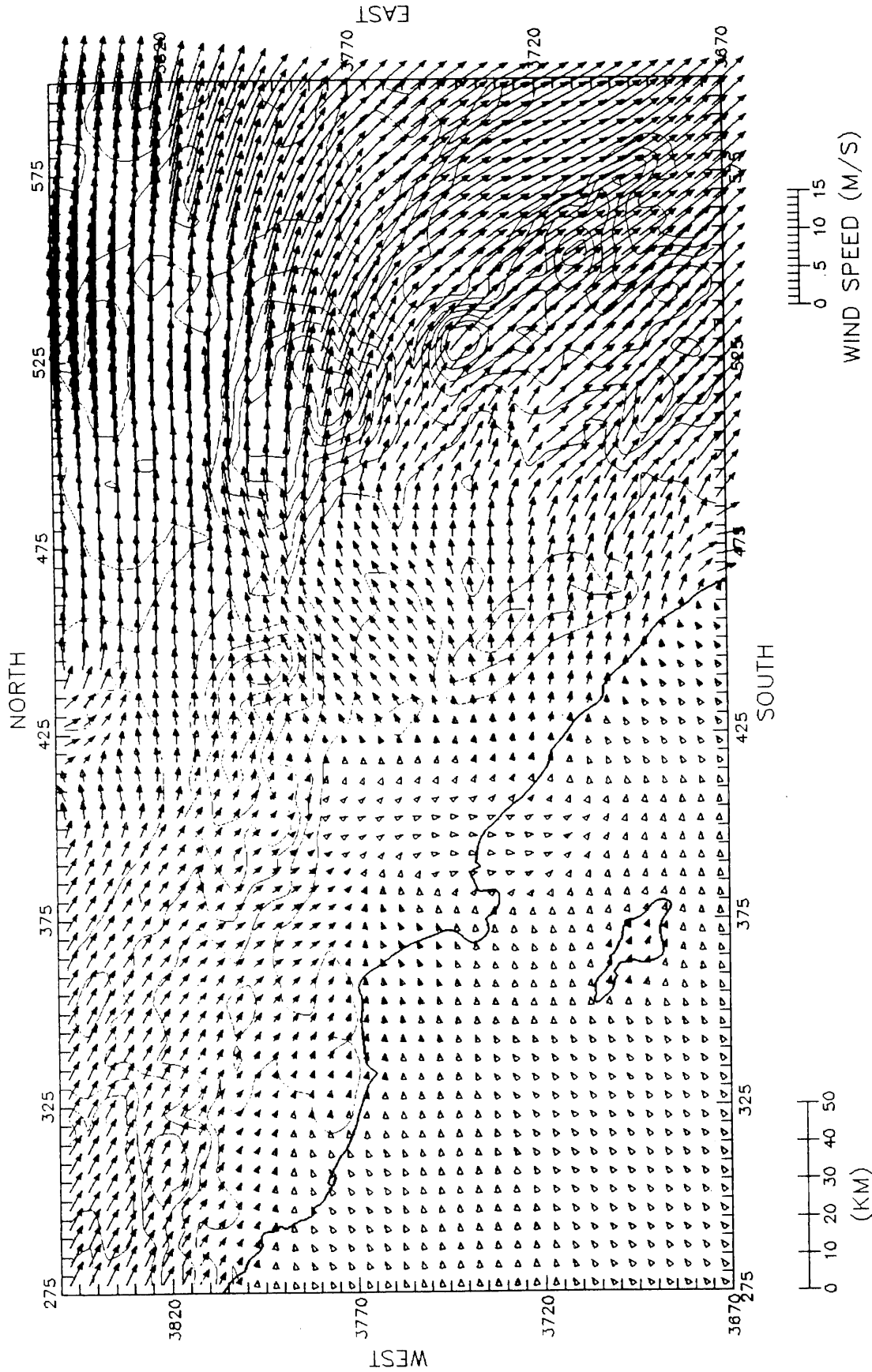
**19 June 1987**

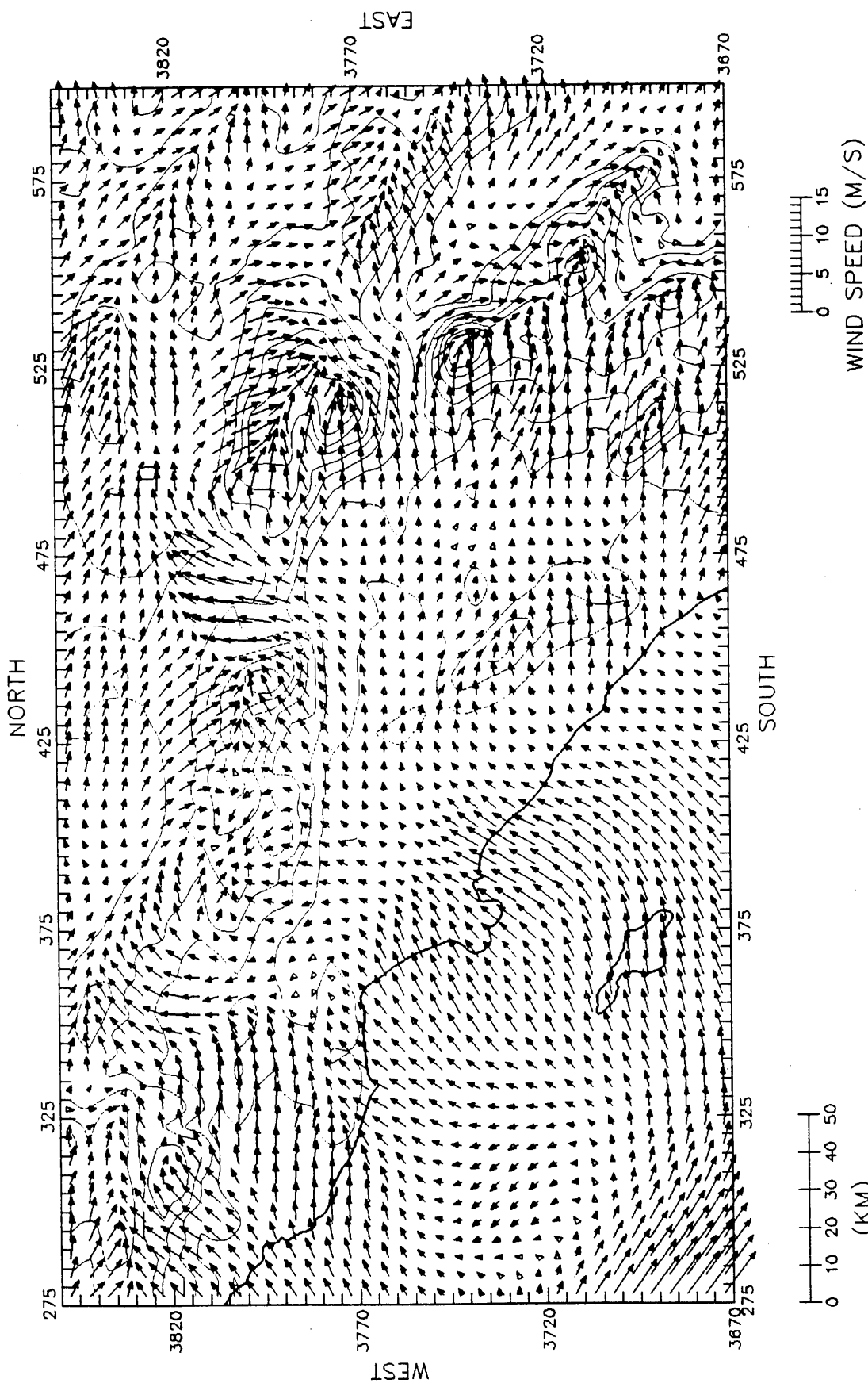
**91061.03**



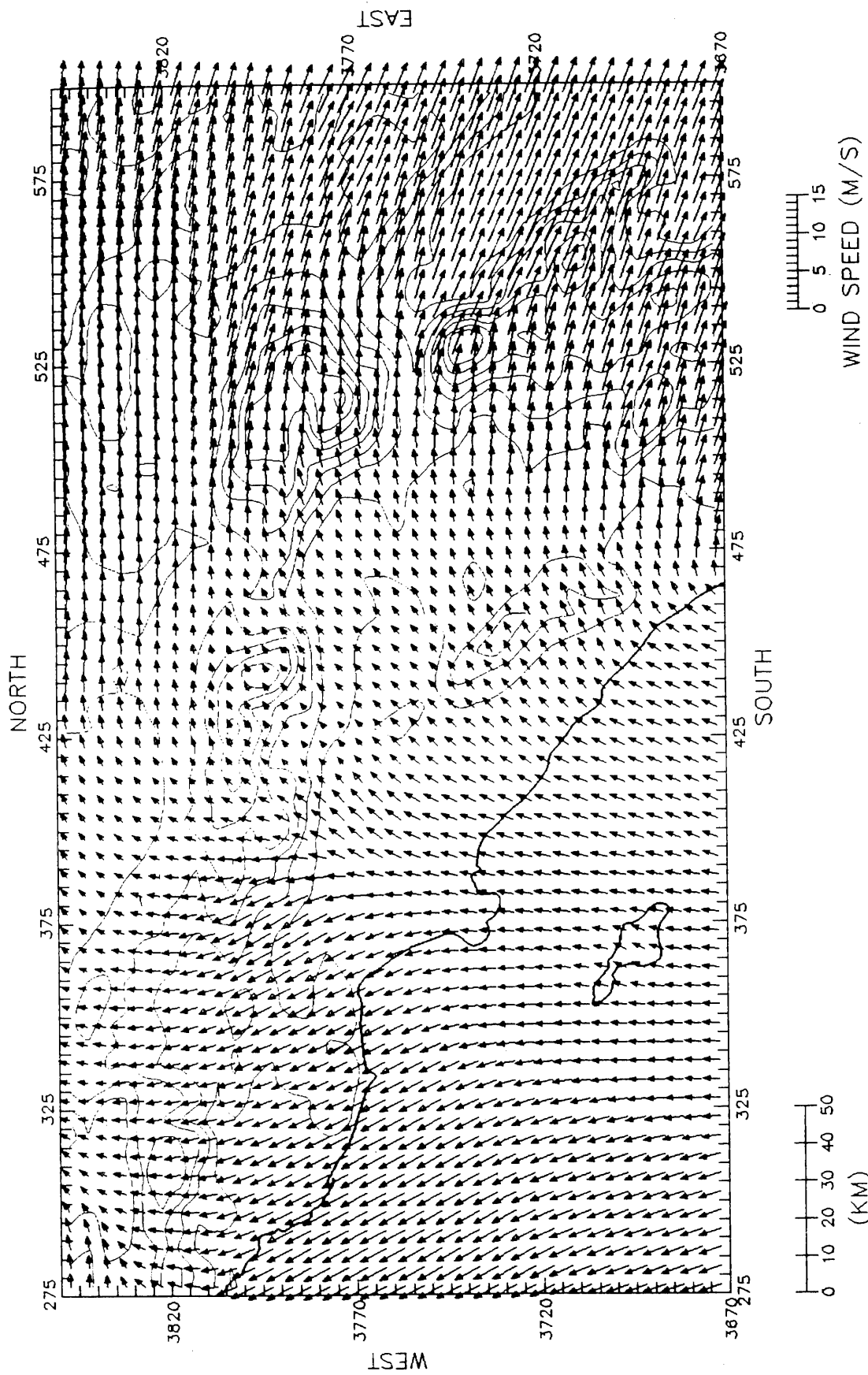


DWM WINDS AT LEVEL 3 (300M)  
 400 PST 19JUN87

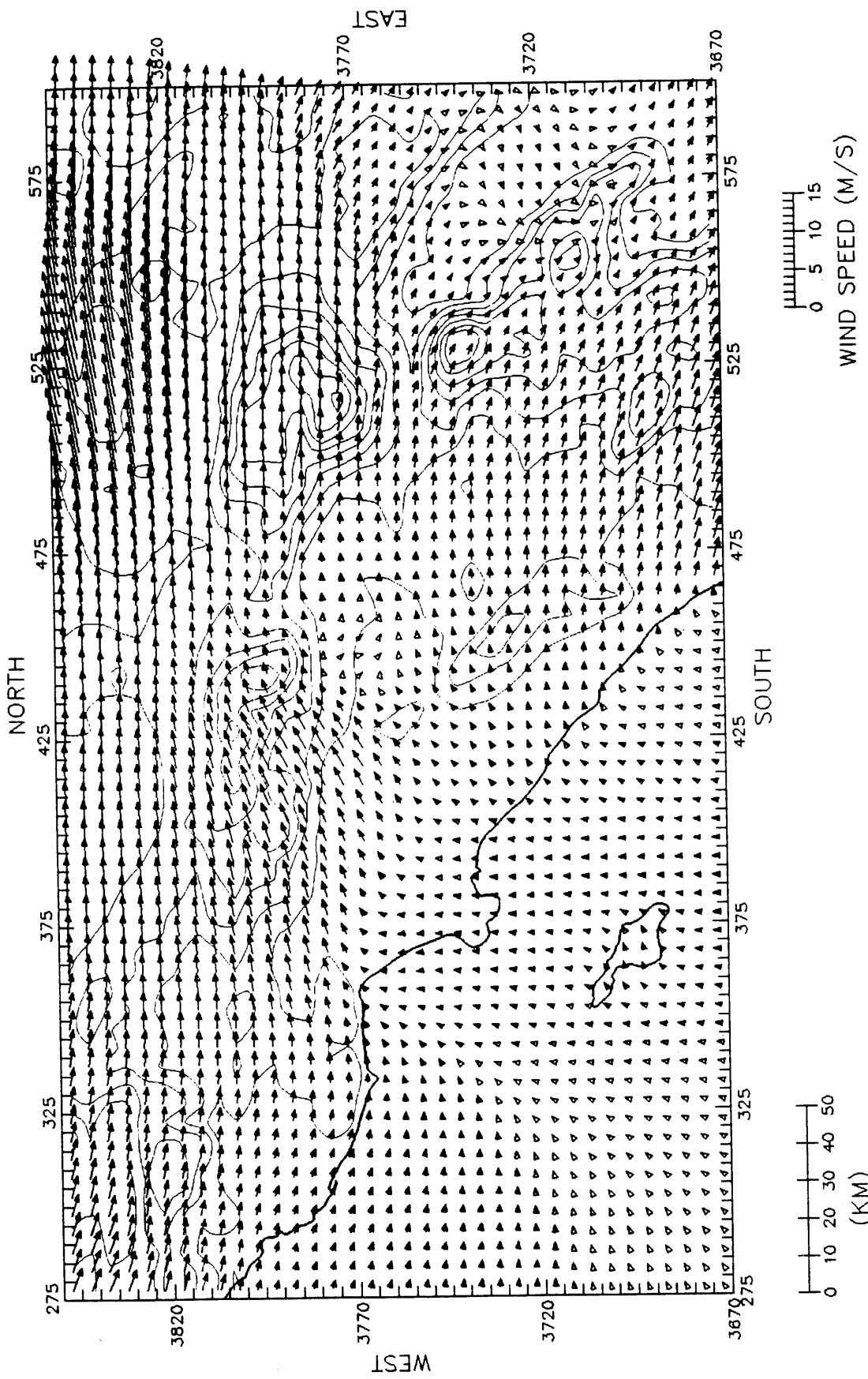


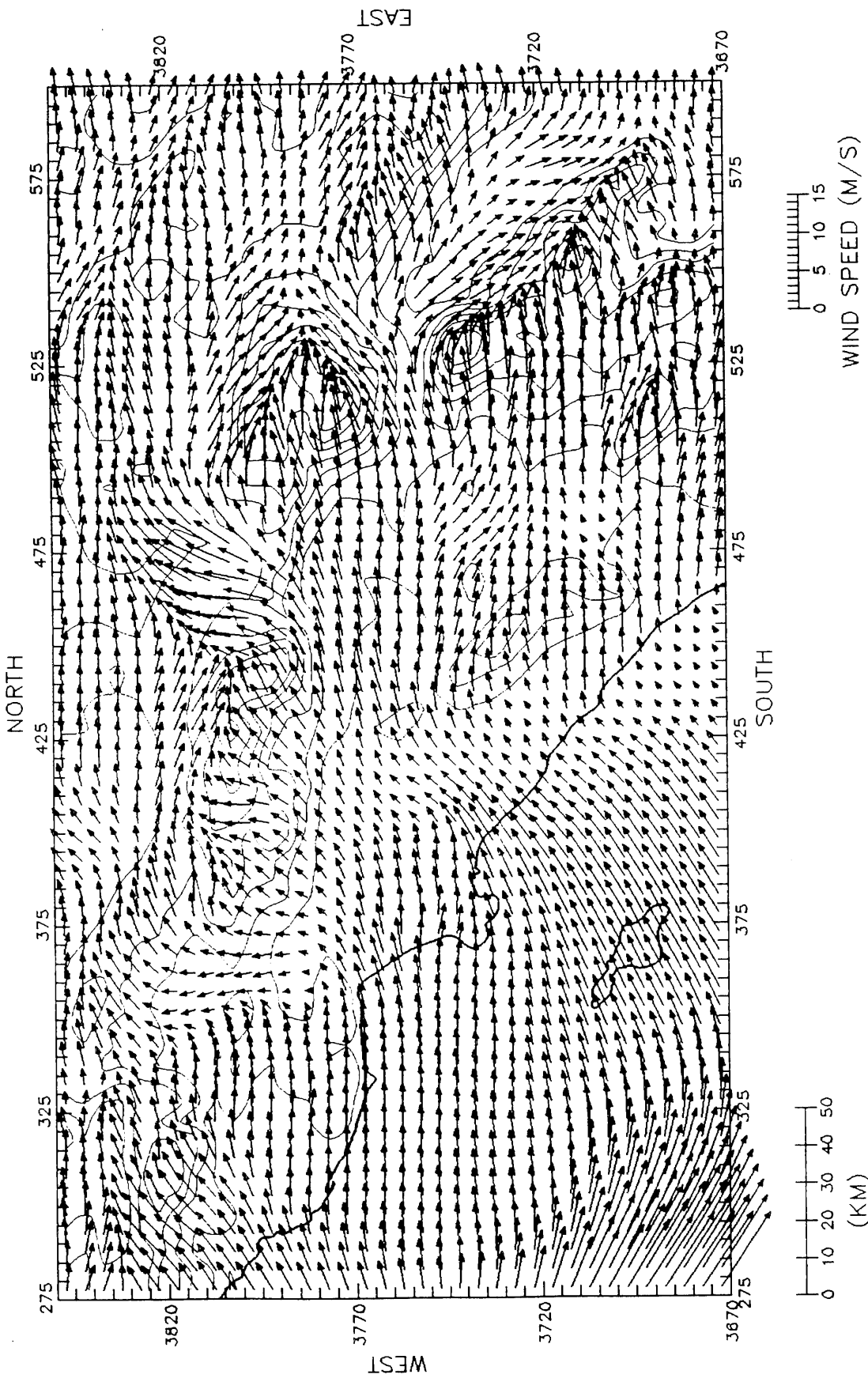


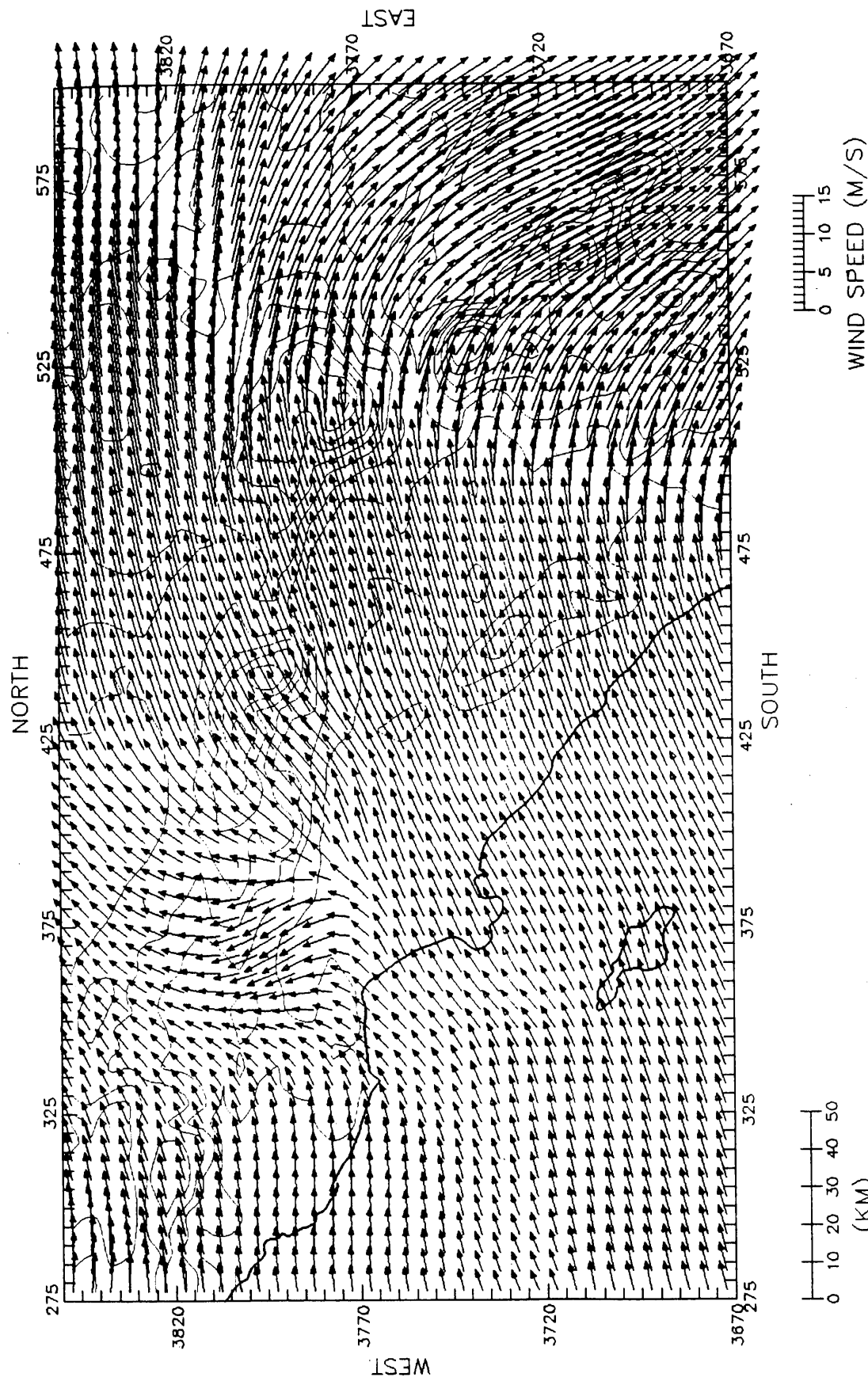
DWM WINDS AT LEVEL 1 (10M)  
1000 PST 19JUN87

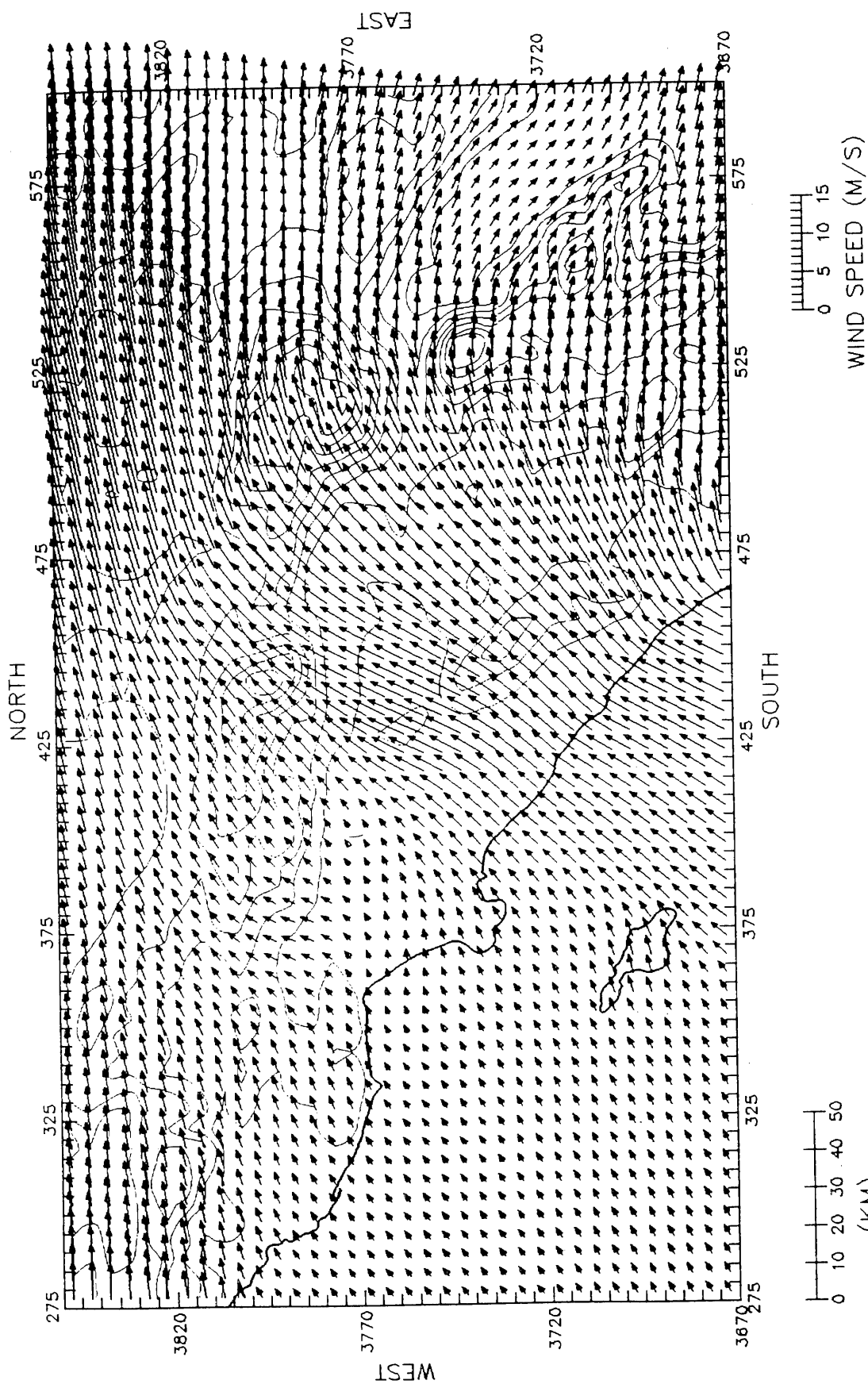


DWM WINDS AT LEVEL 3 (300M)  
1000 PST 19JUN87

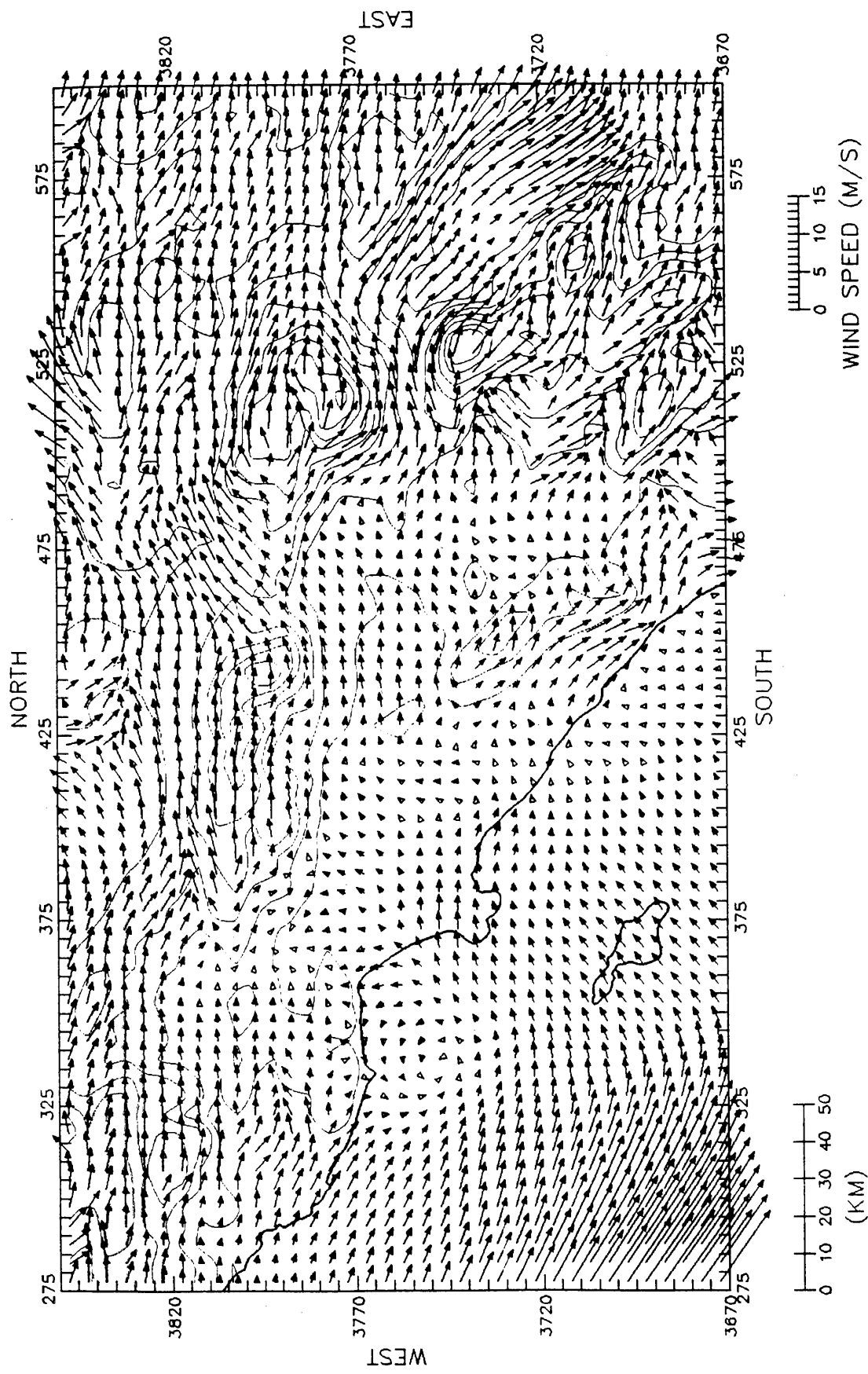


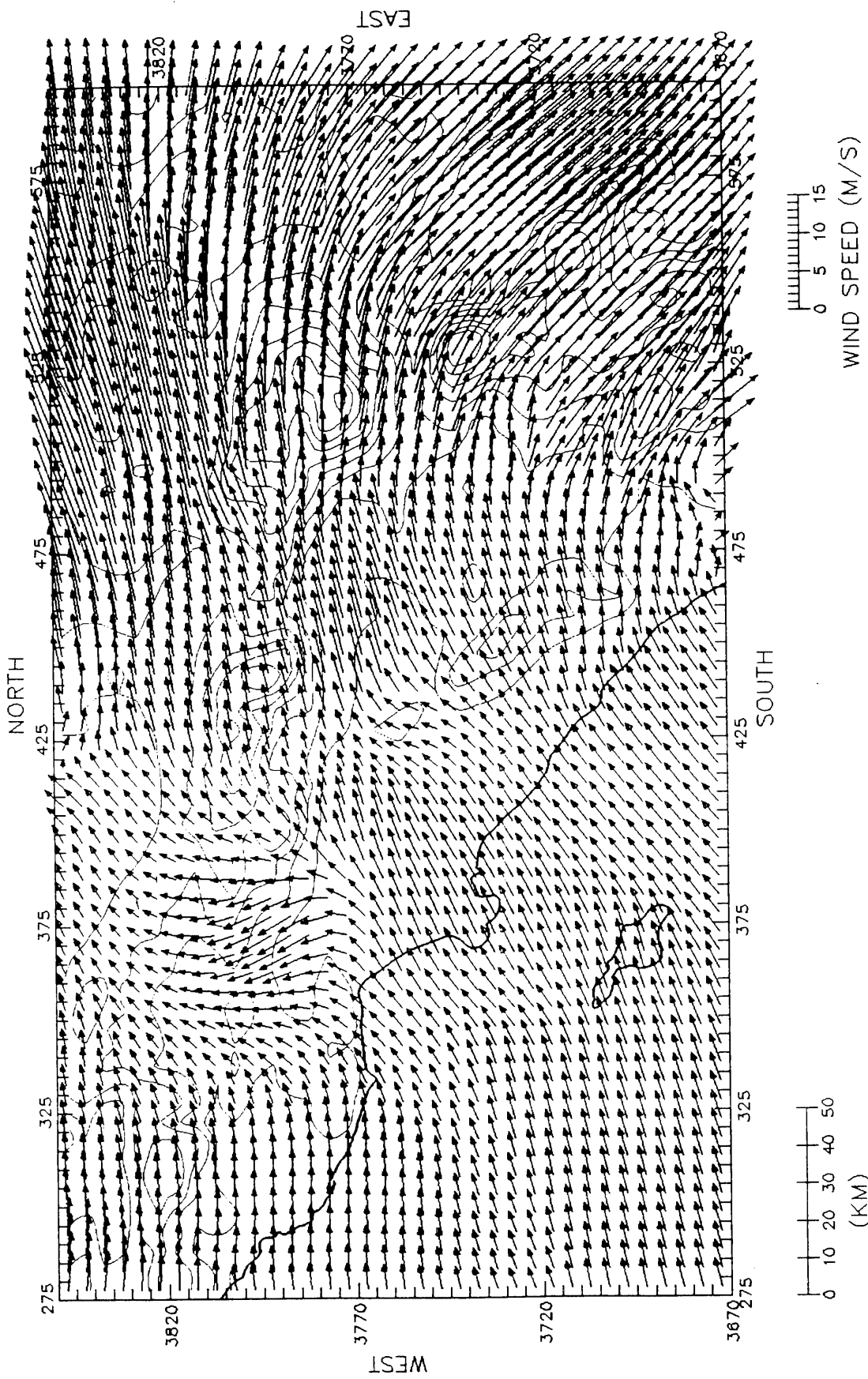




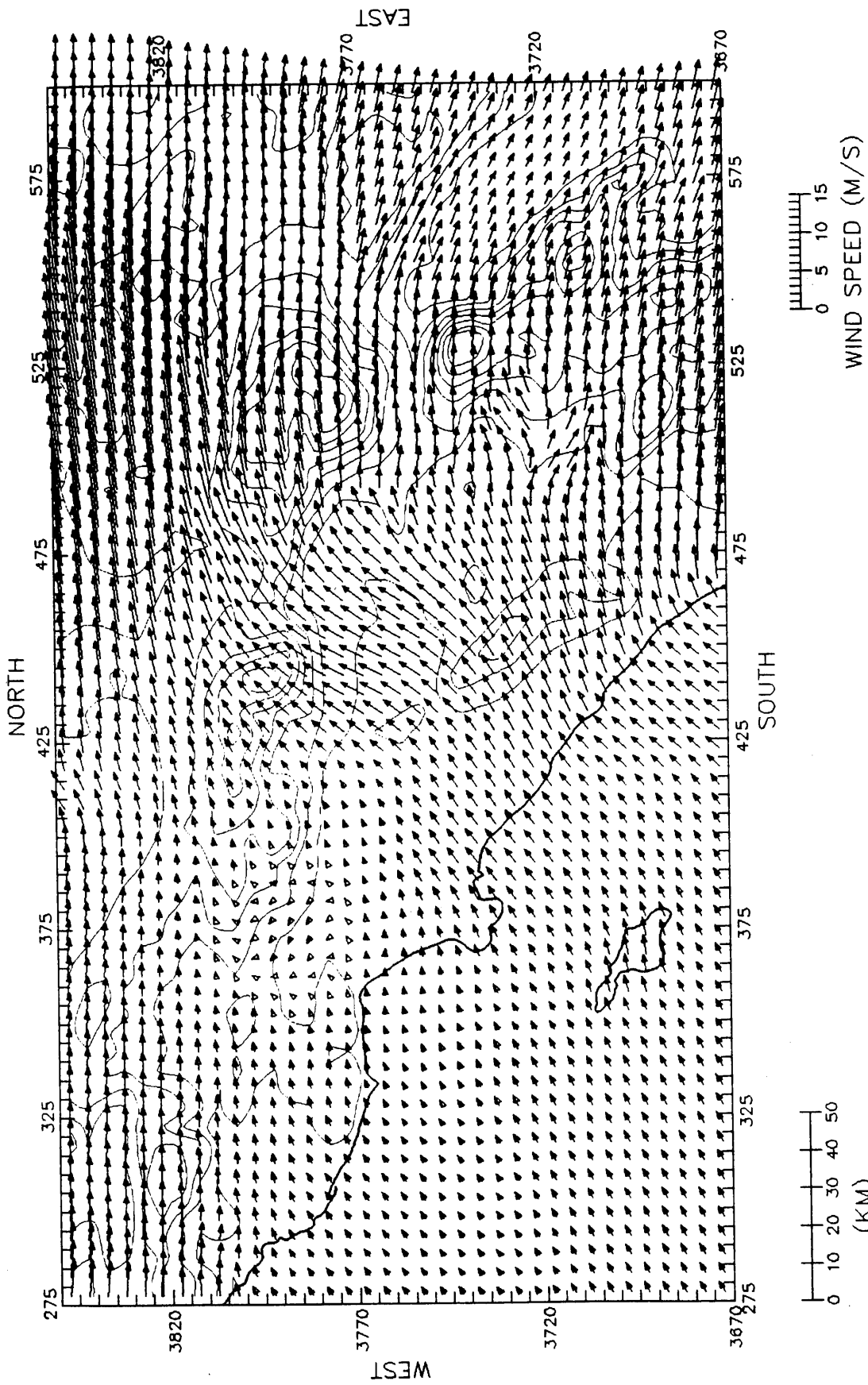


DWM WINDS AT LEVEL 5 (1000M)  
 1600 PST 19JUN87





DWM WINDS AT LEVEL 3 (300M)  
 2200 PST 19JUN87

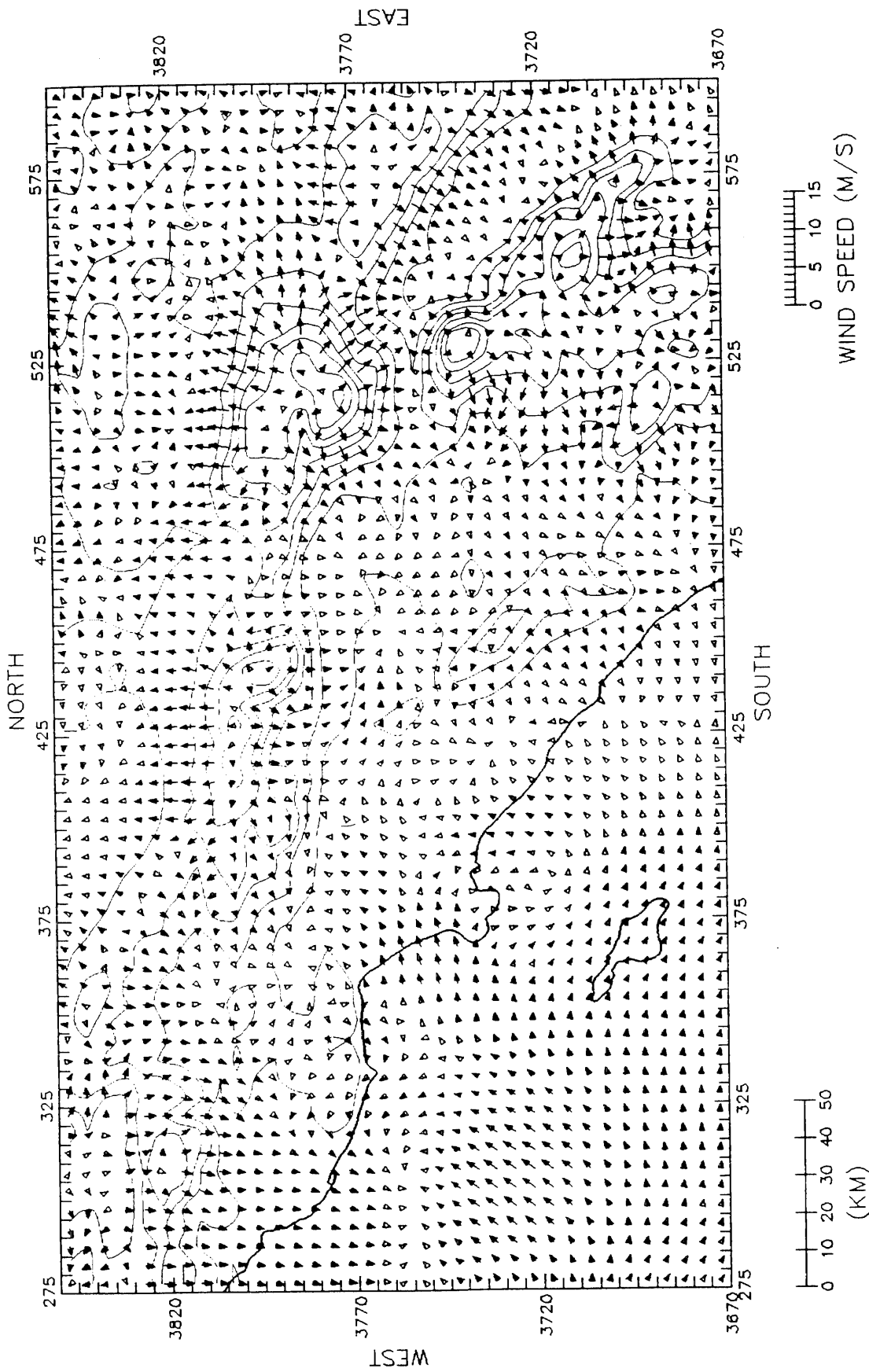


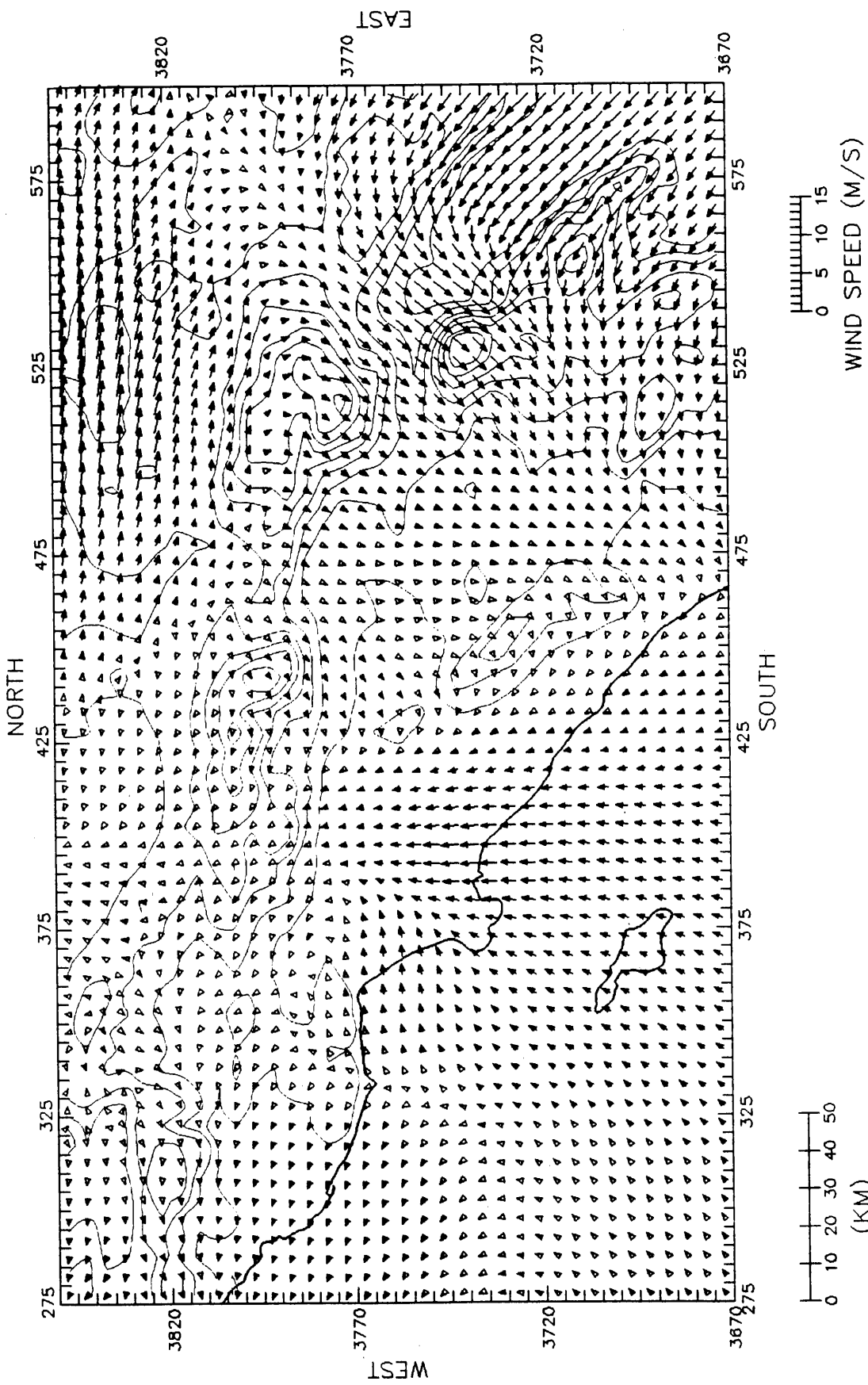
DWM WINDS AT LEVEL 5 (1000M)  
2200 PST 19JUN87

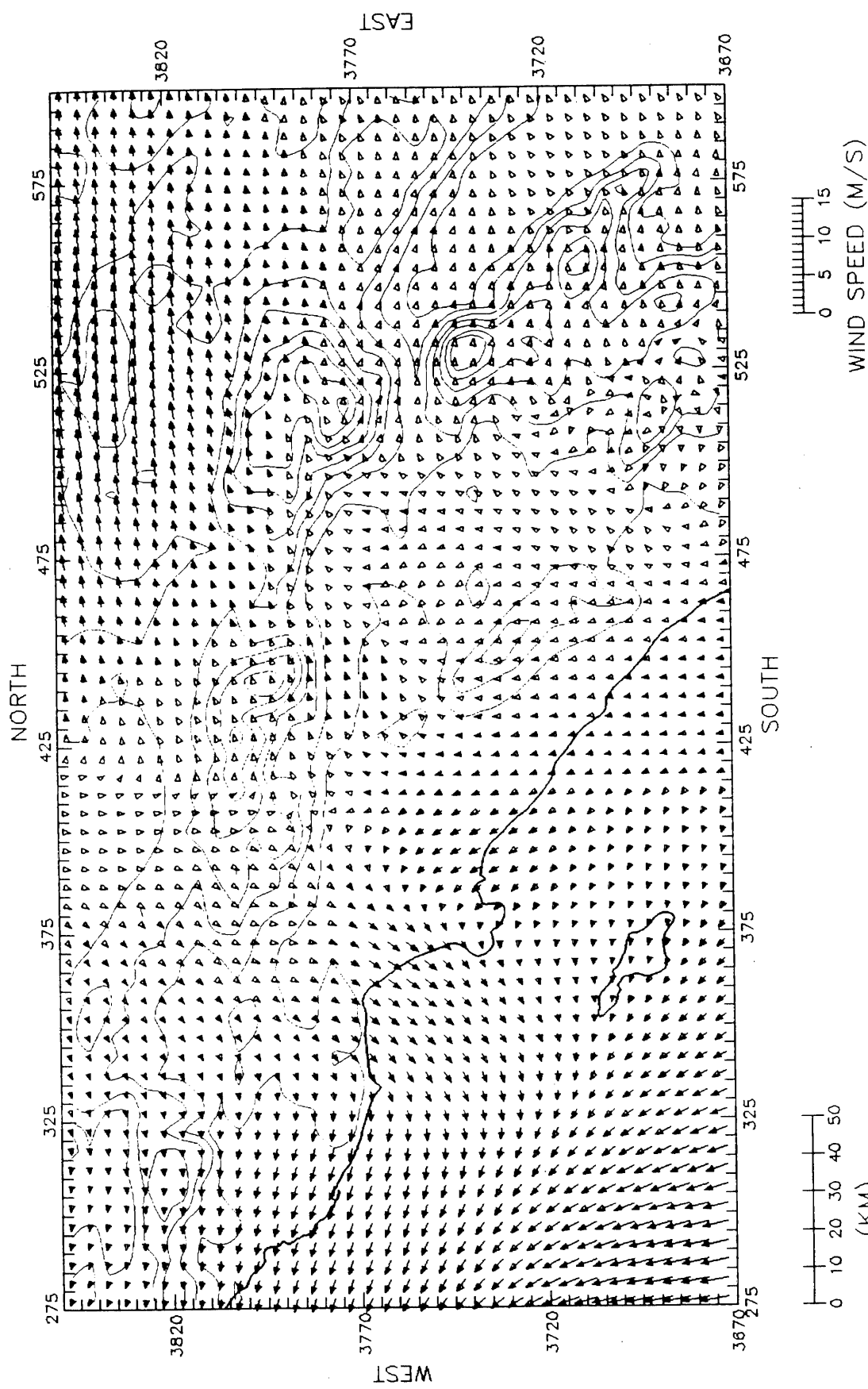


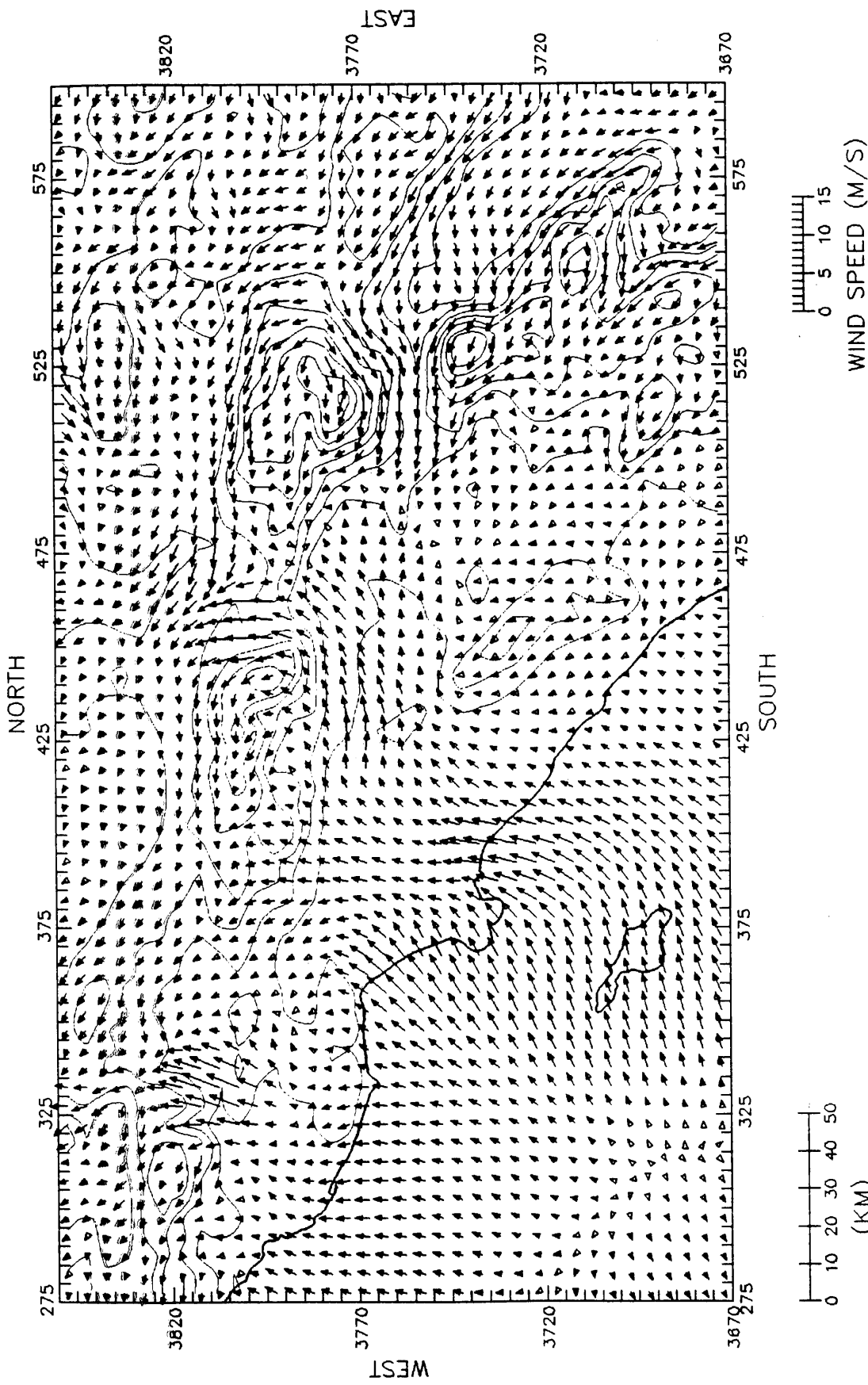
**24-25 June 1987**

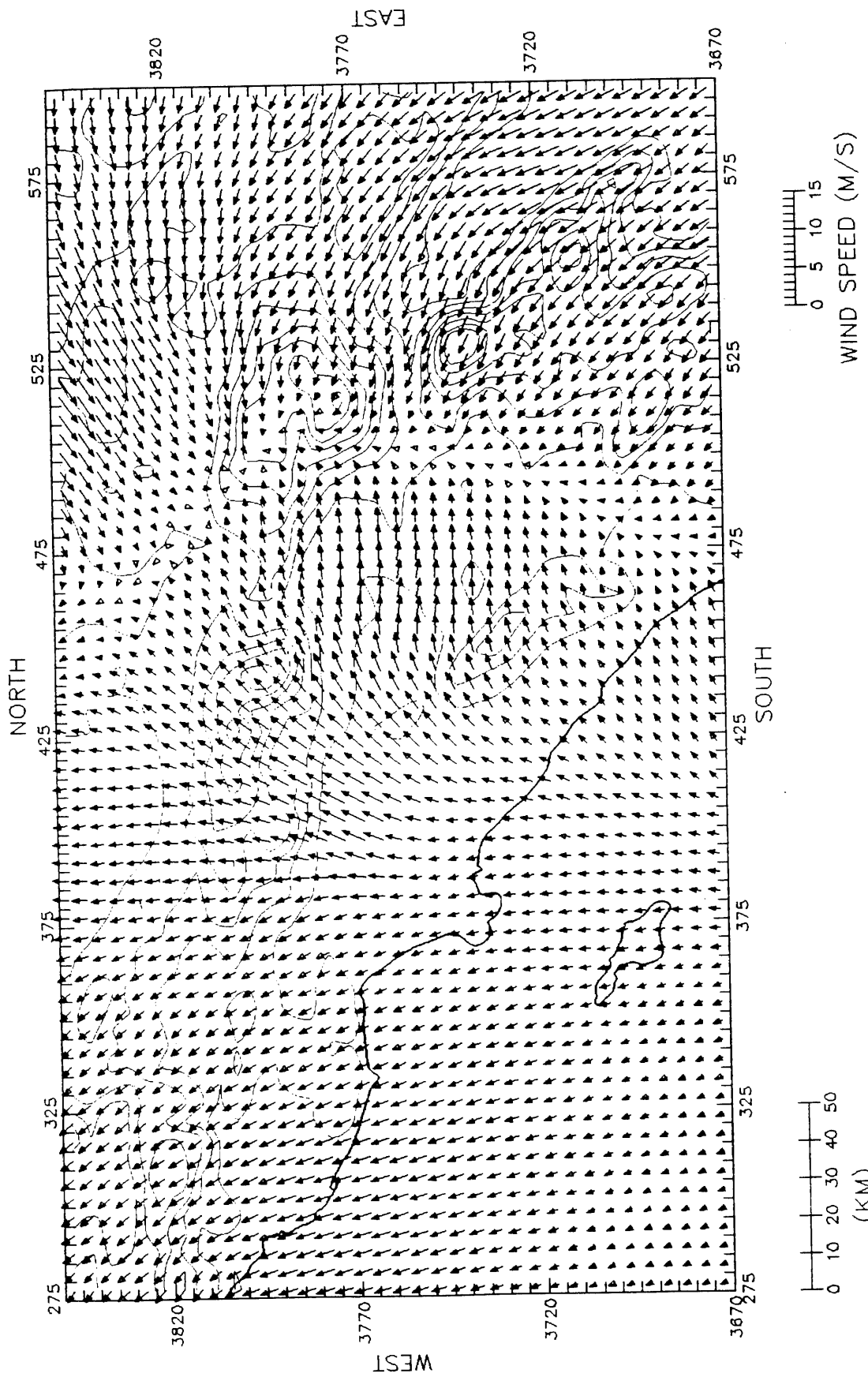
91061.03



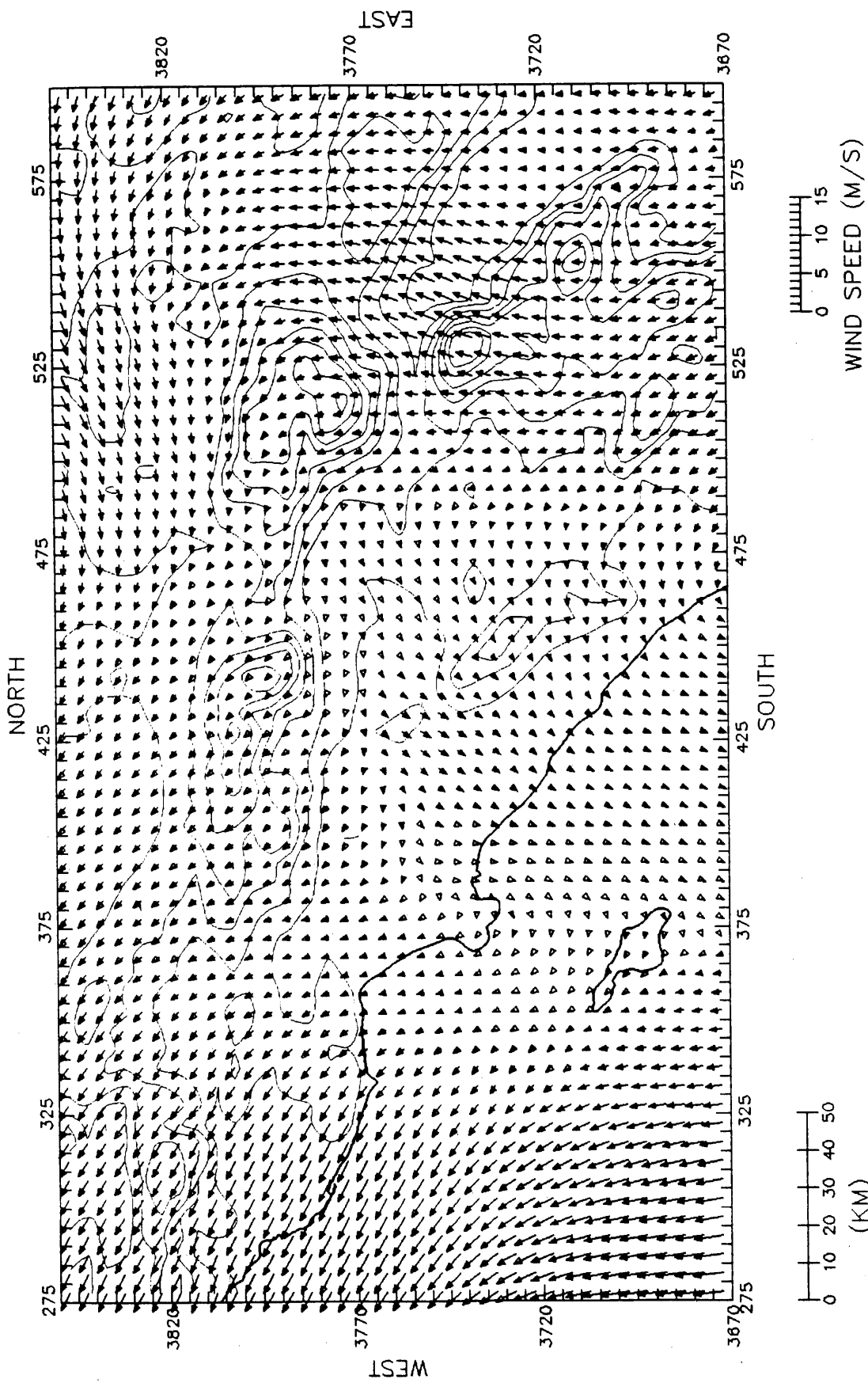




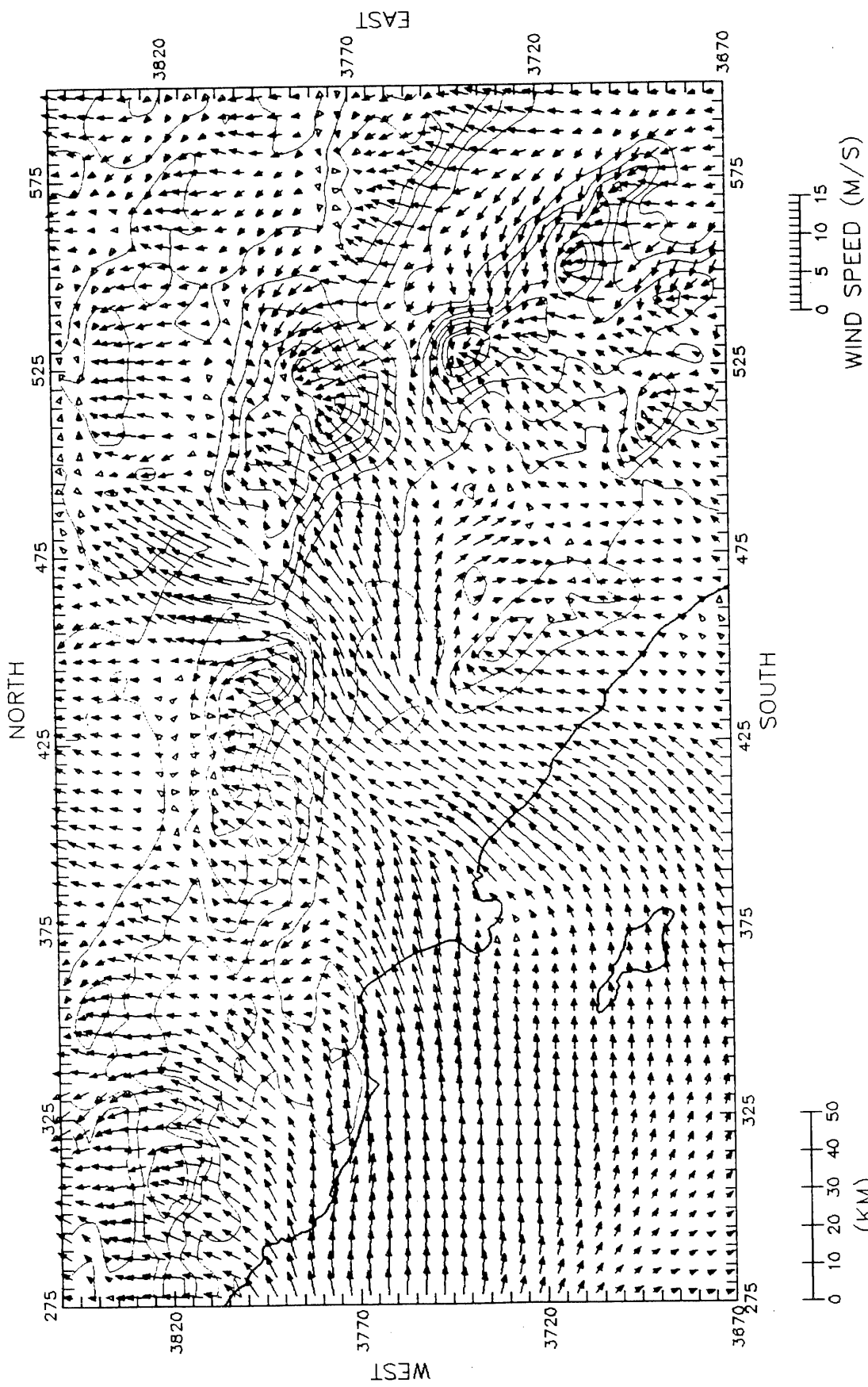




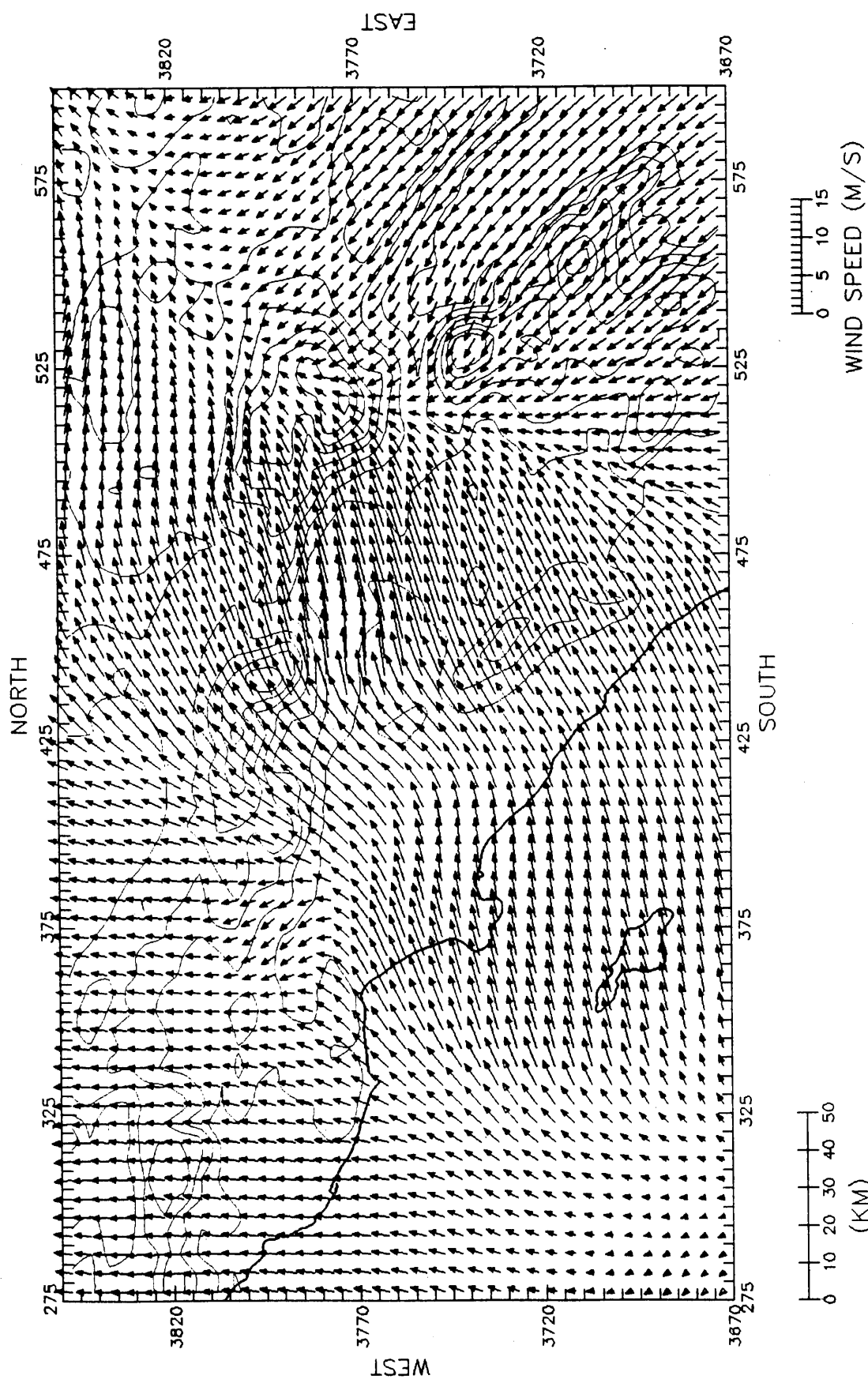
DWM WINDS AT LEVEL 3 (300M)  
 1000 PST 24JUN87



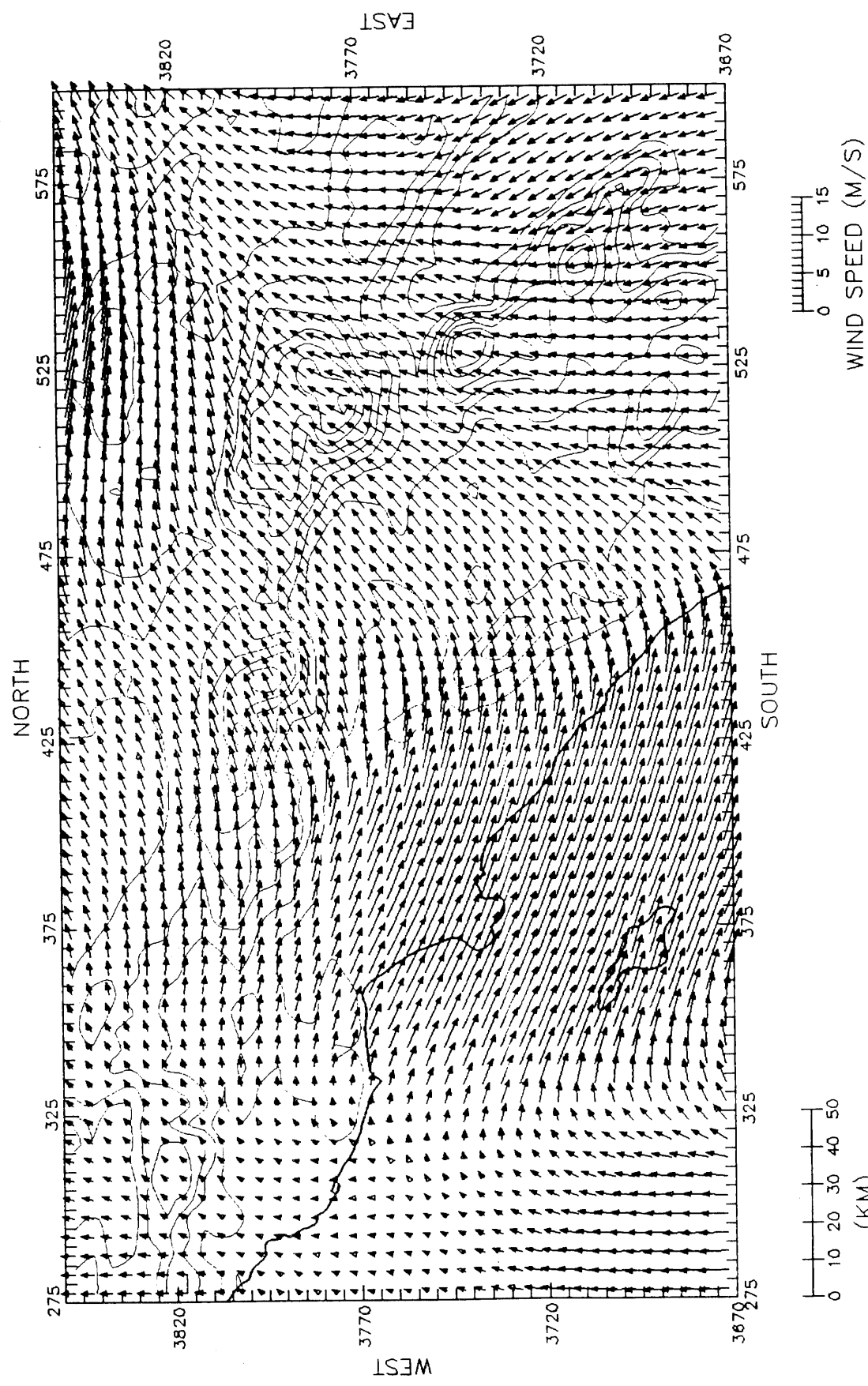
DWM WINDS AT LEVEL 5 (1000M)  
 1000 PST 24JUN87



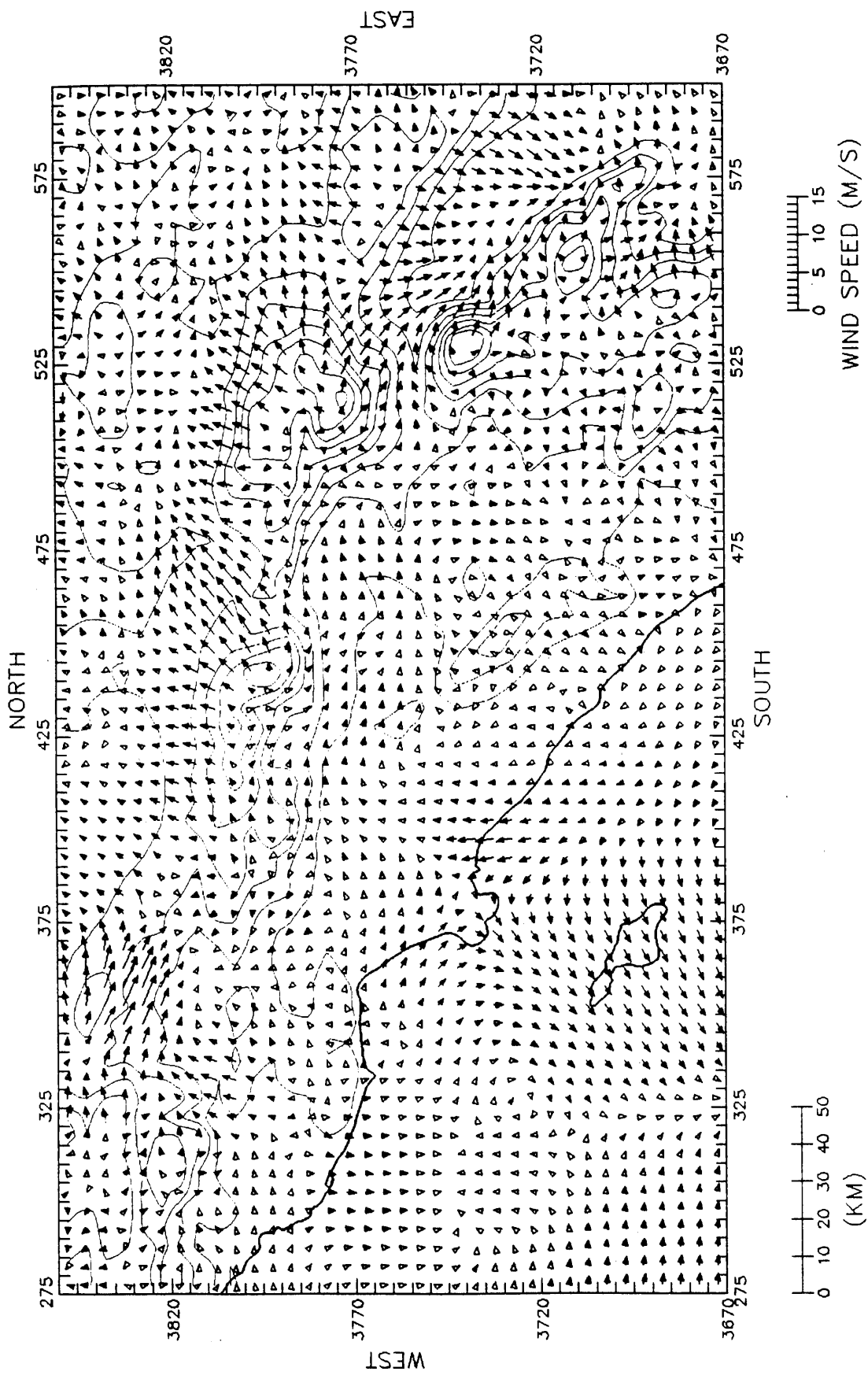
DWM WINDS AT LEVEL 1 (10M)  
 1600 PST 24JUN87

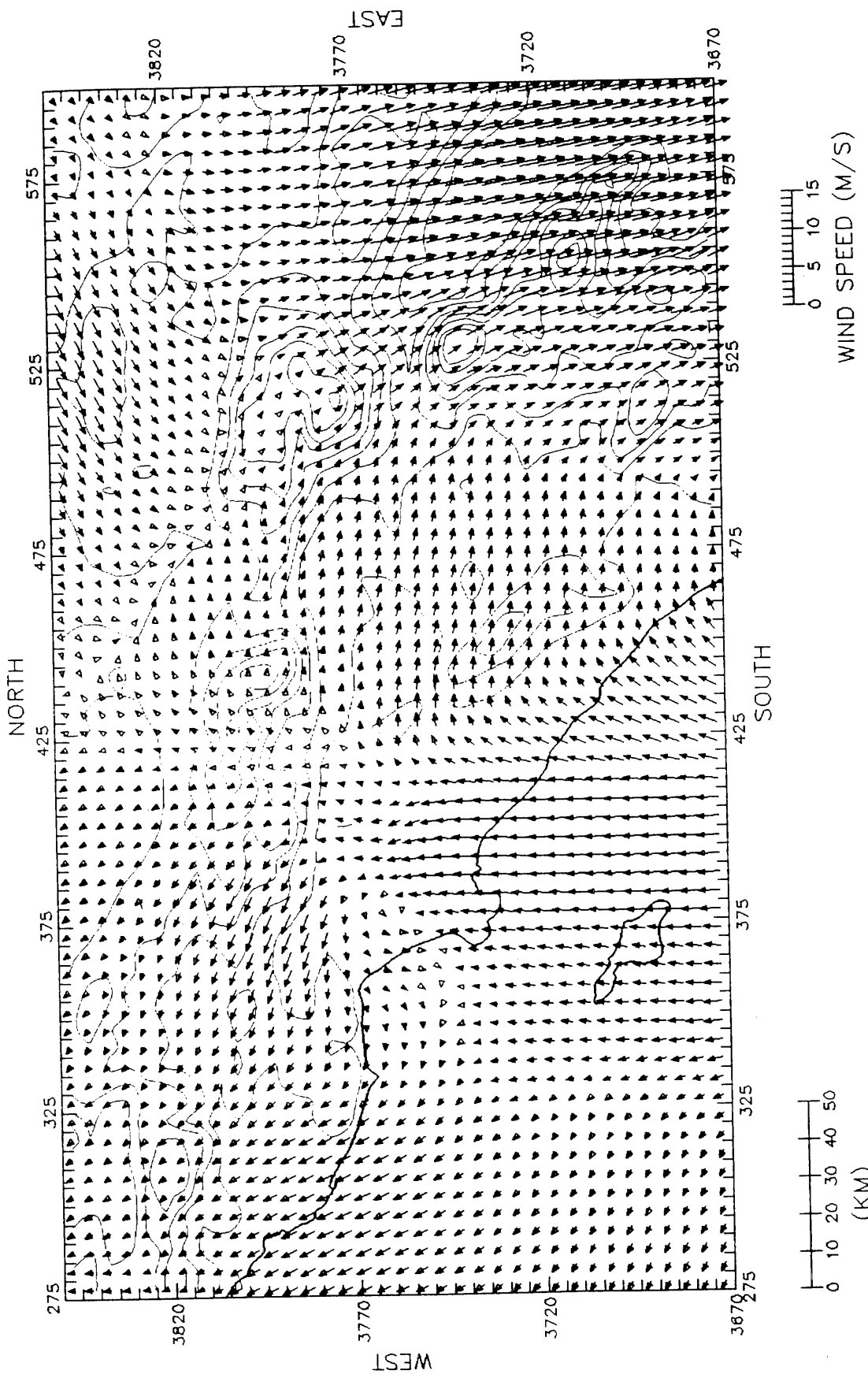


DWM WINDS AT LEVEL 3 (300M)  
 1600 PST 24JUN87

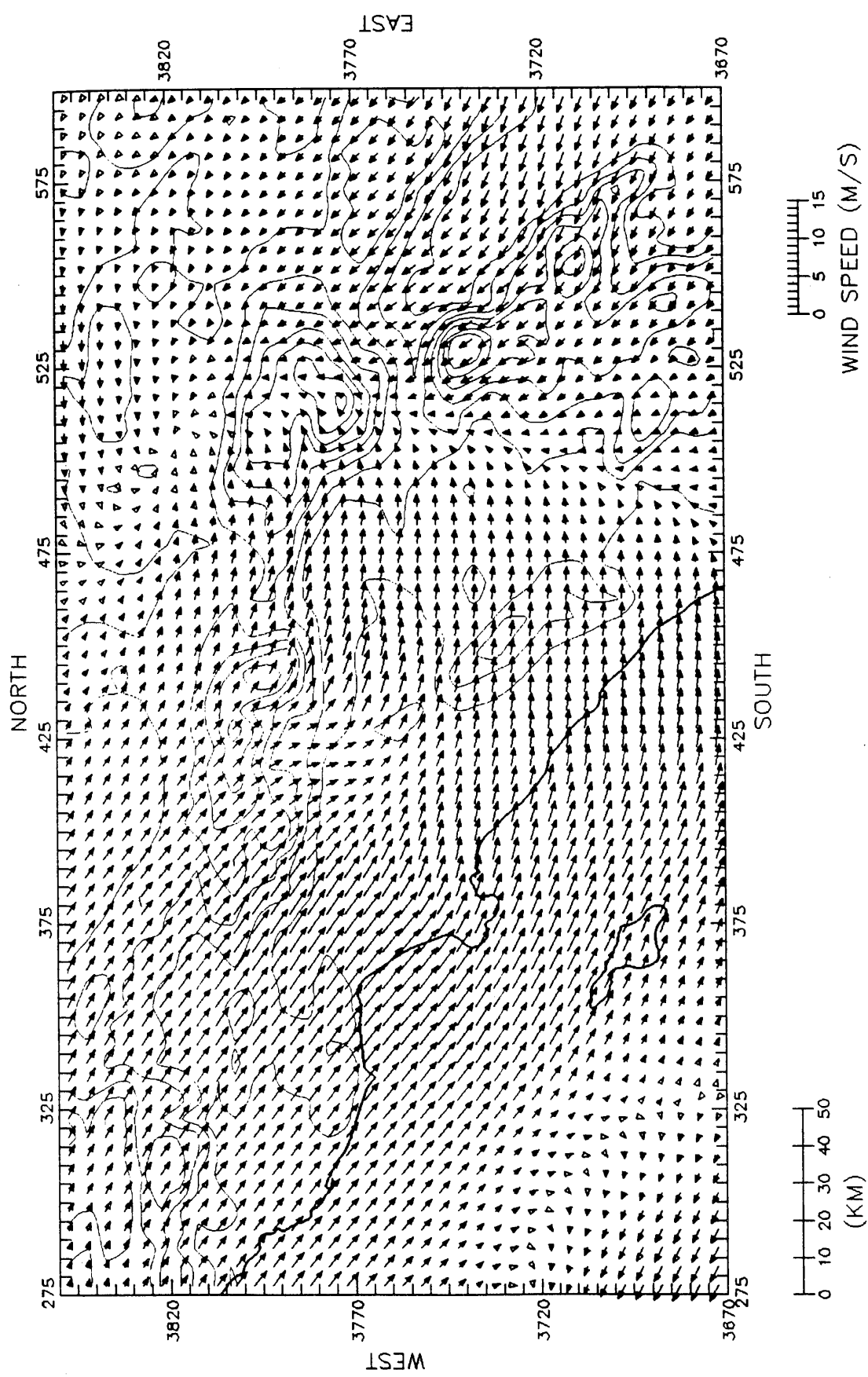


DWM WINDS AT LEVEL 5 (1000M)  
1600 PST 24JUN87

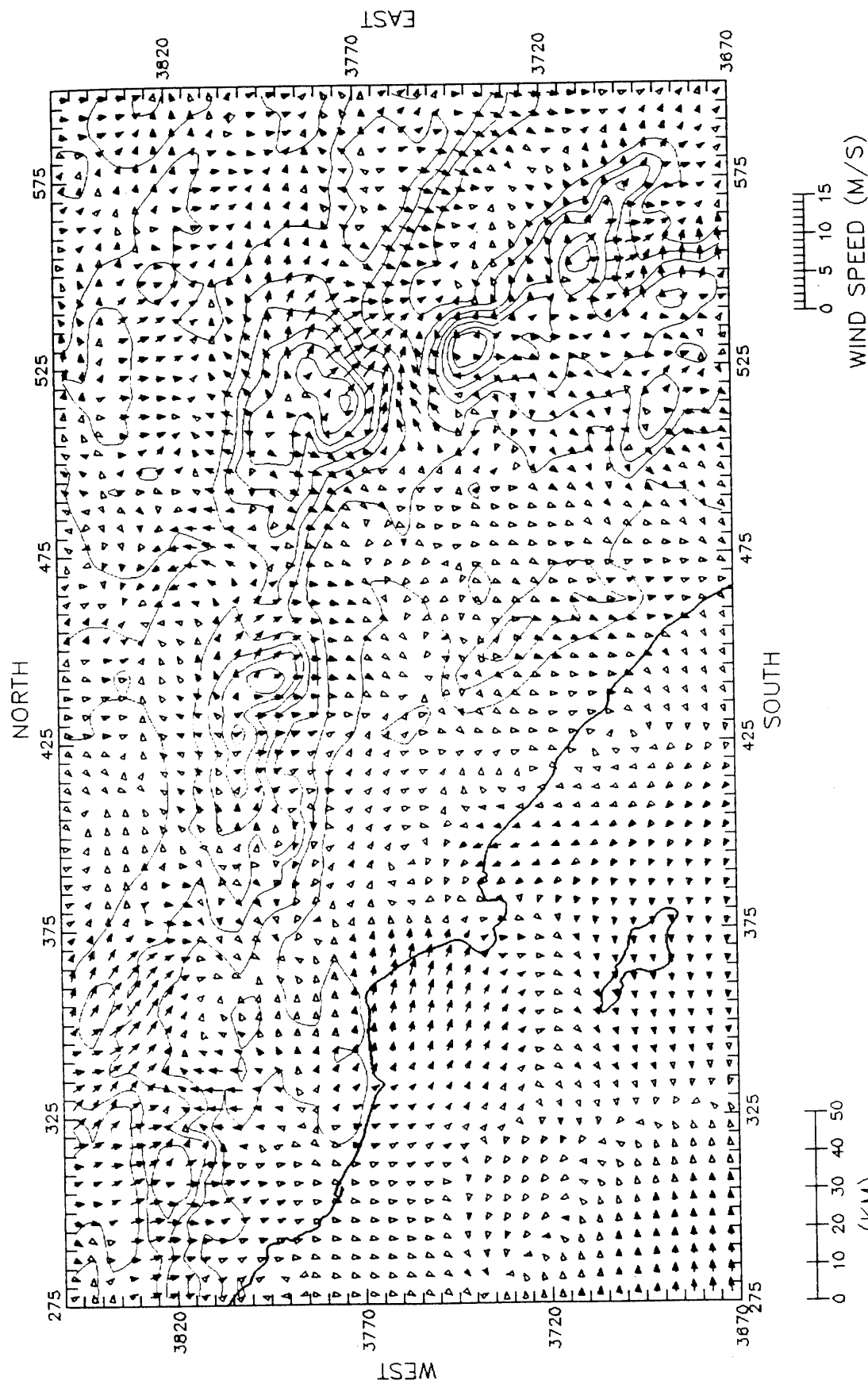


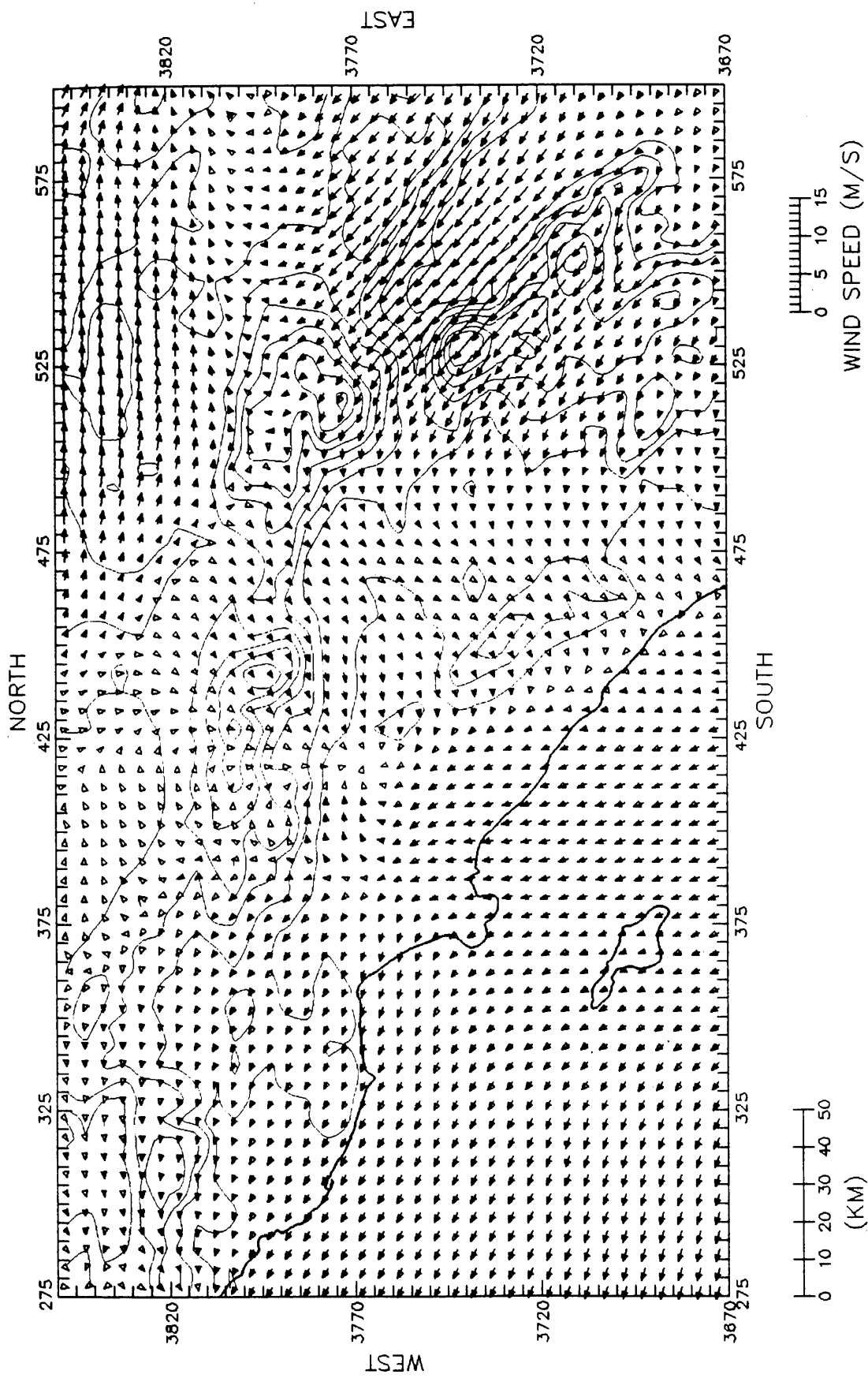


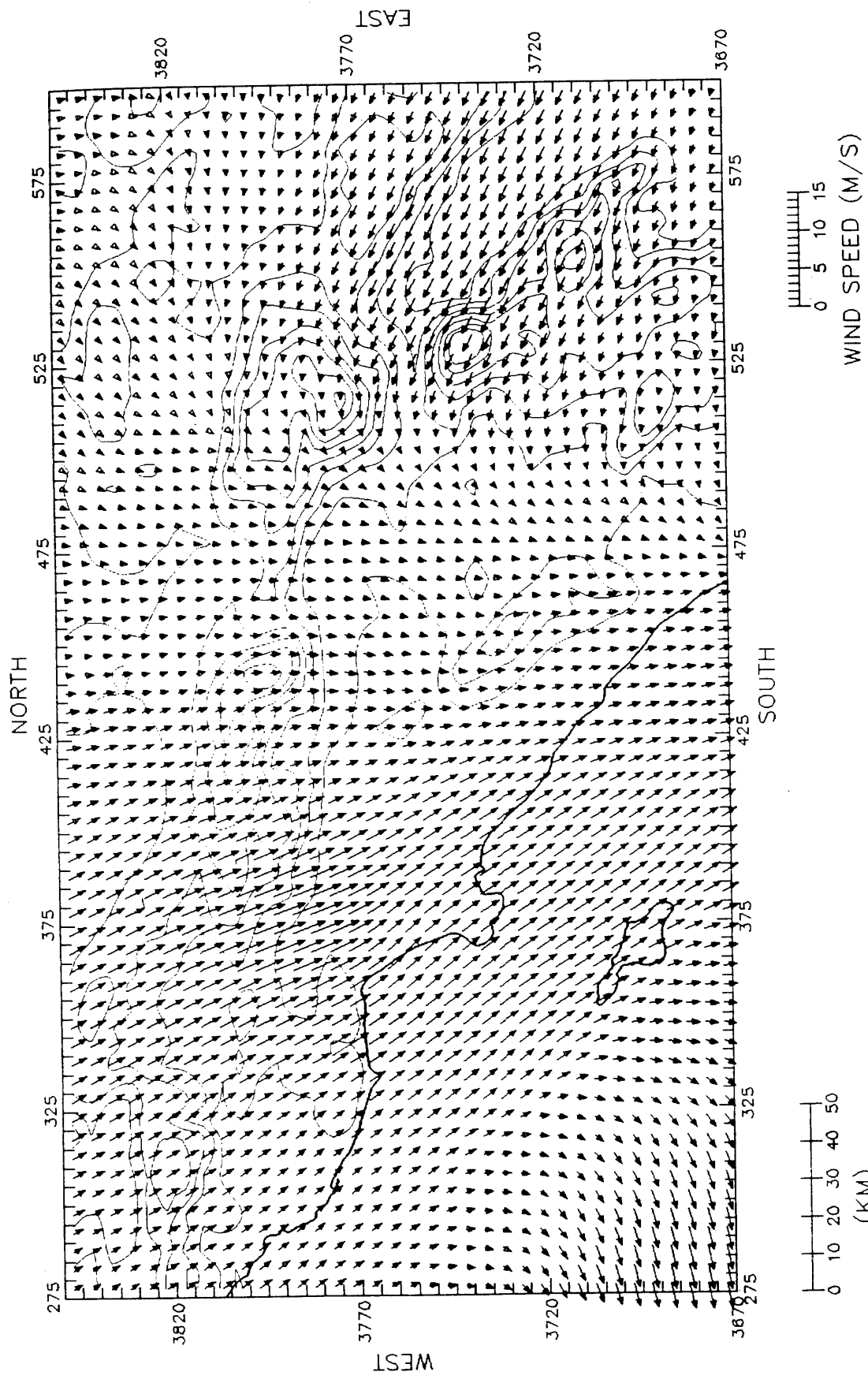
DWM WINDS AT LEVEL 3 (300M)  
2200 PST 24JUN87



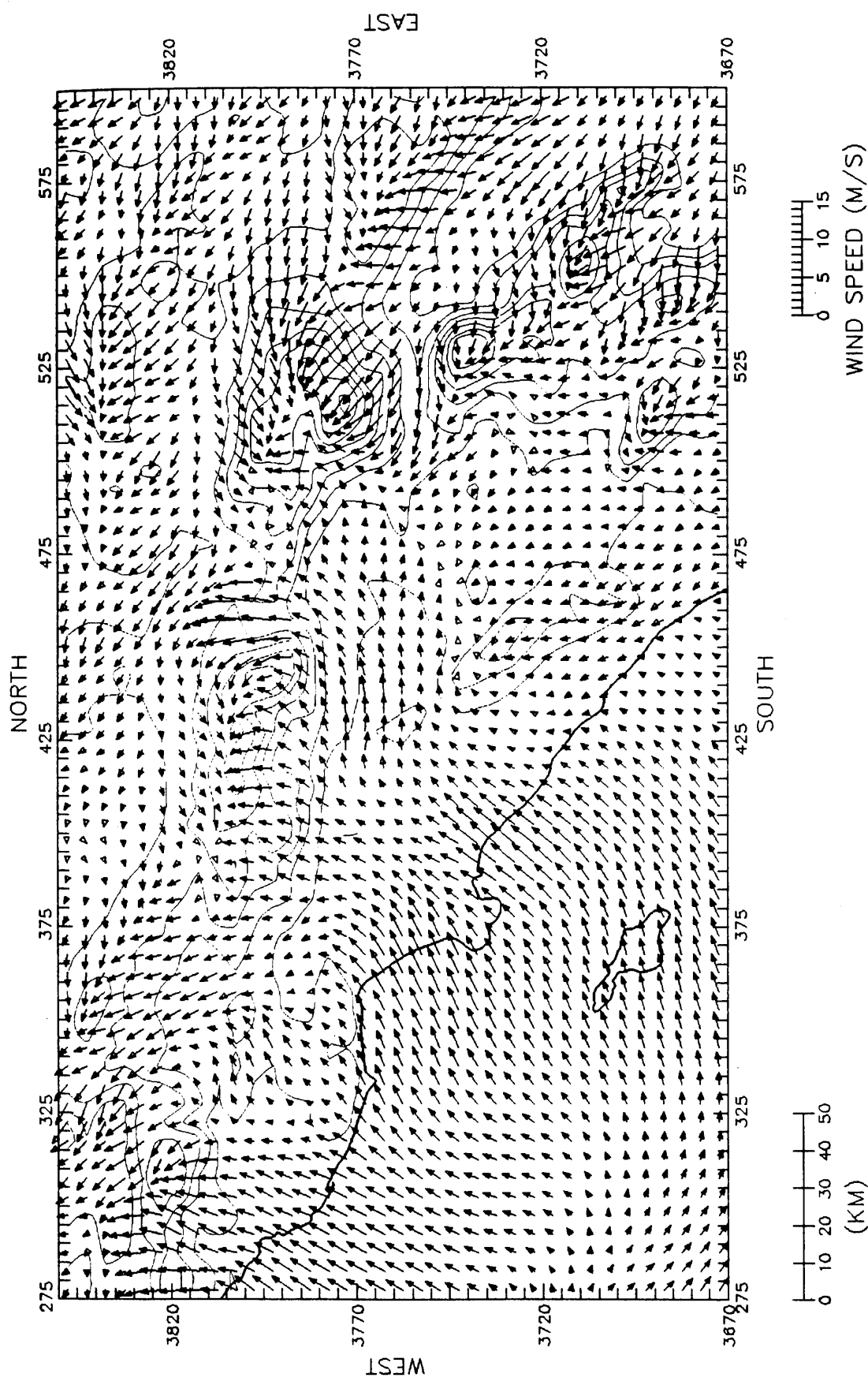
DWM WINDS AT LEVEL 5 (1000M)  
 2200 PST 24JUN87



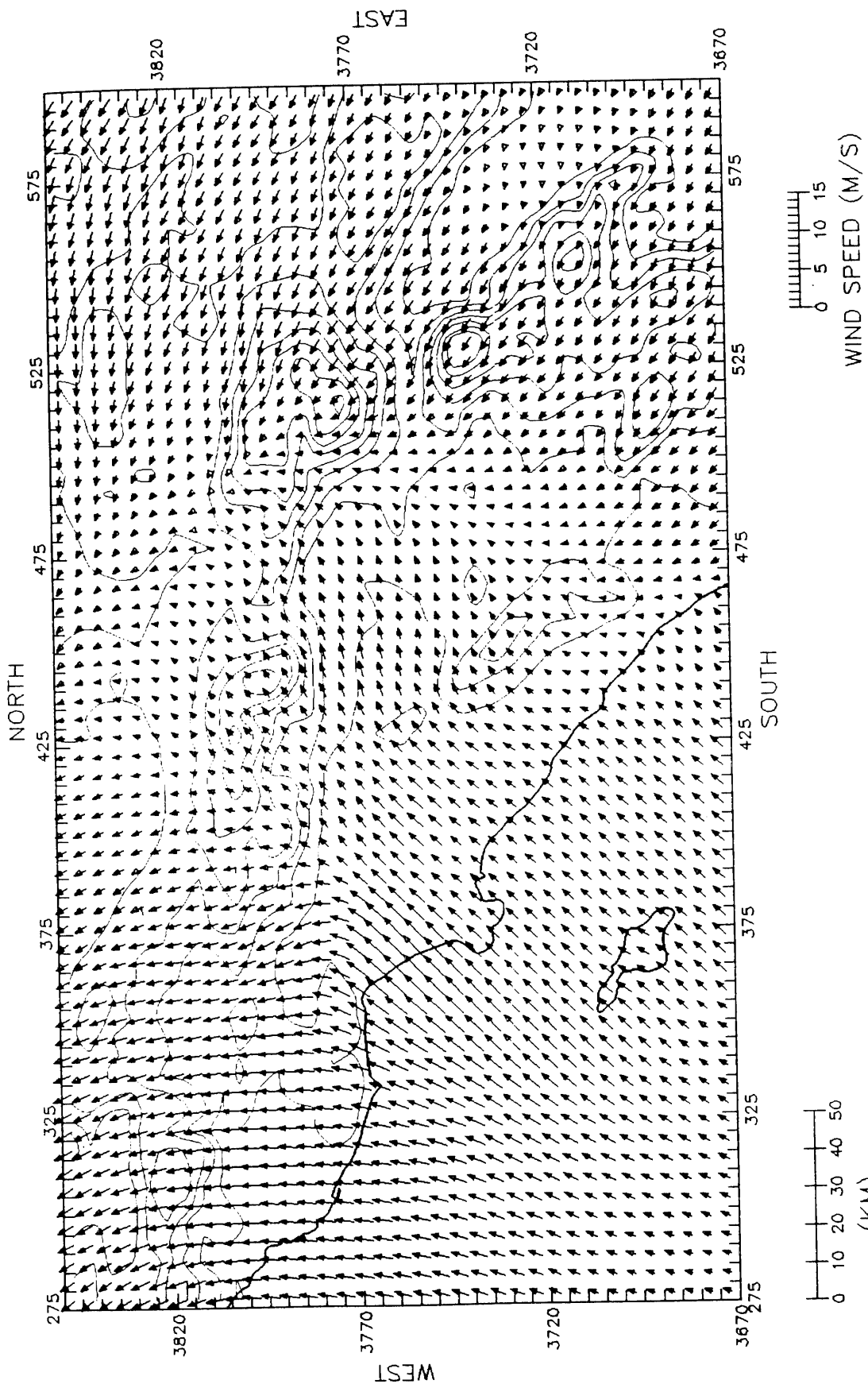




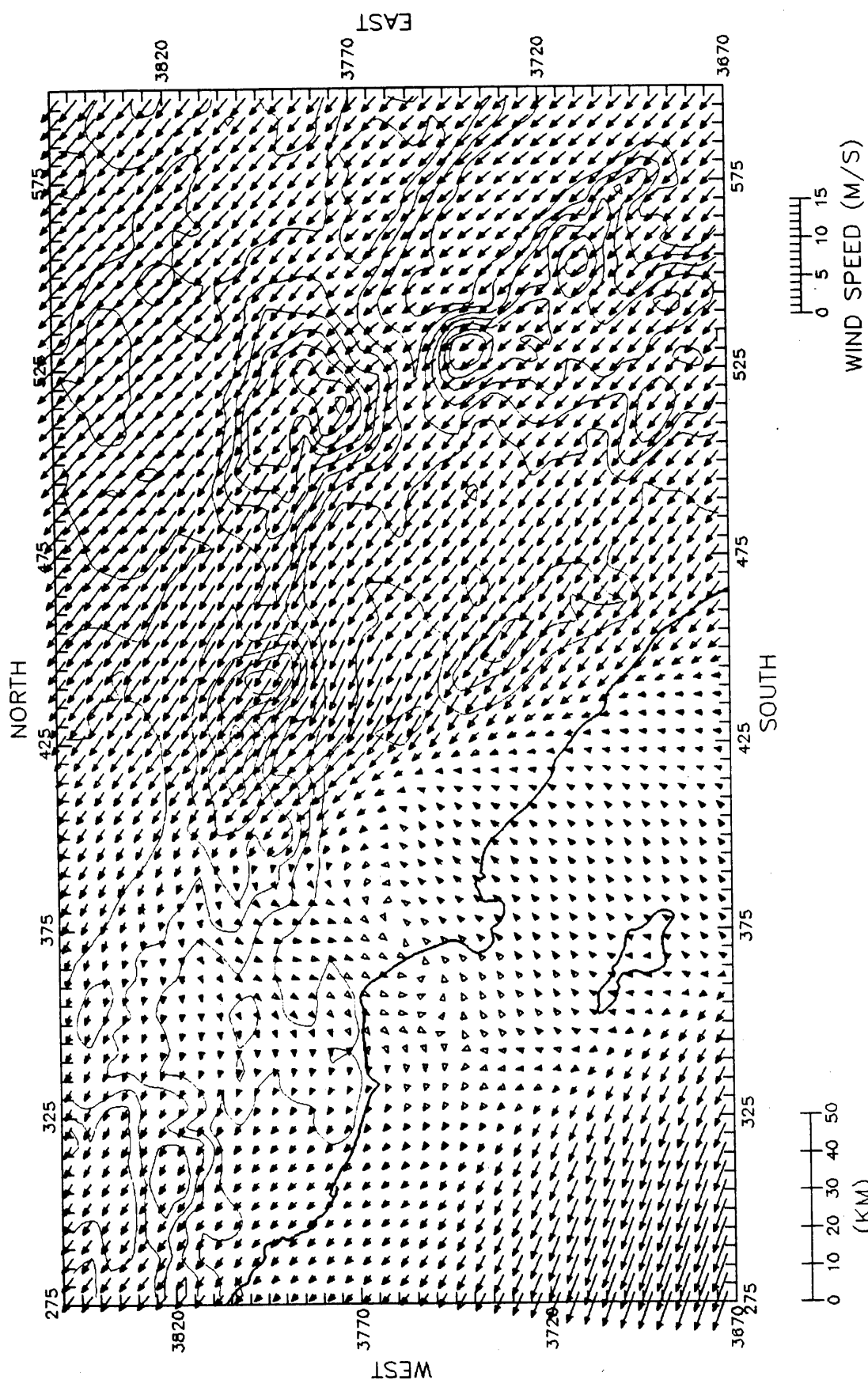
DWM WINDS AT LEVEL 5 (1000M)  
400 PST 25JUN87



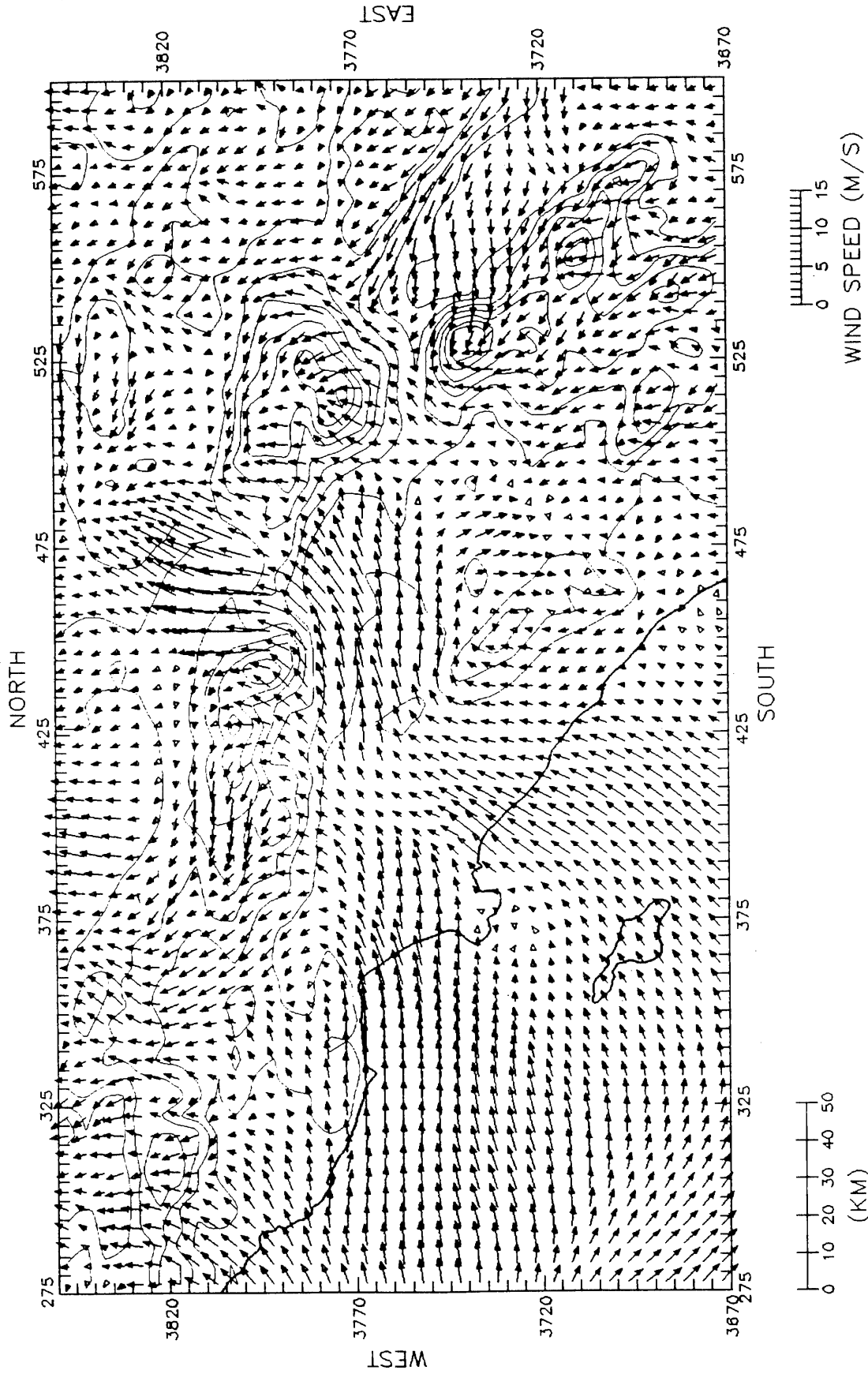
DWM WINDS AT LEVEL 1 (10M)  
 1000 PST 25JUN87

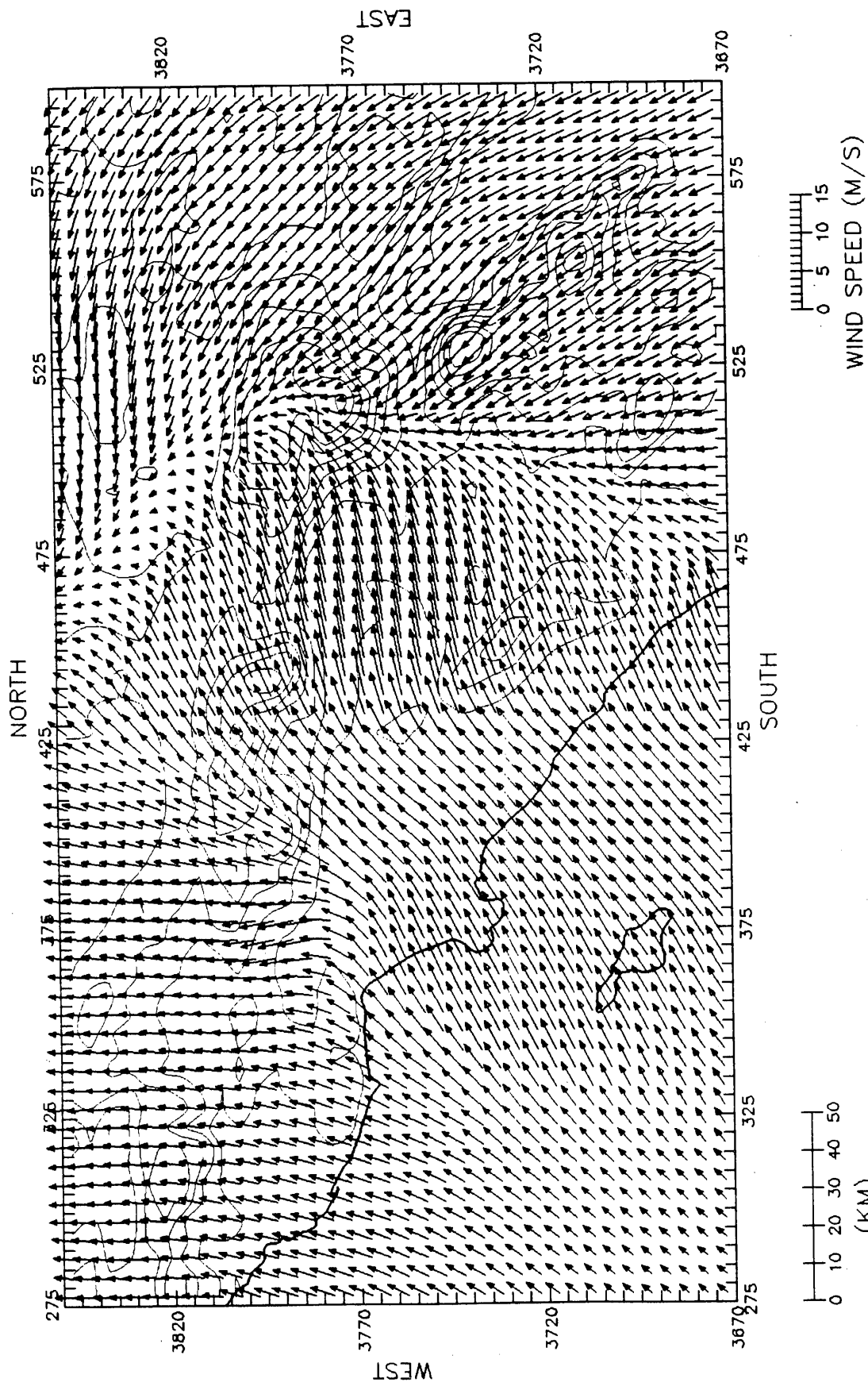


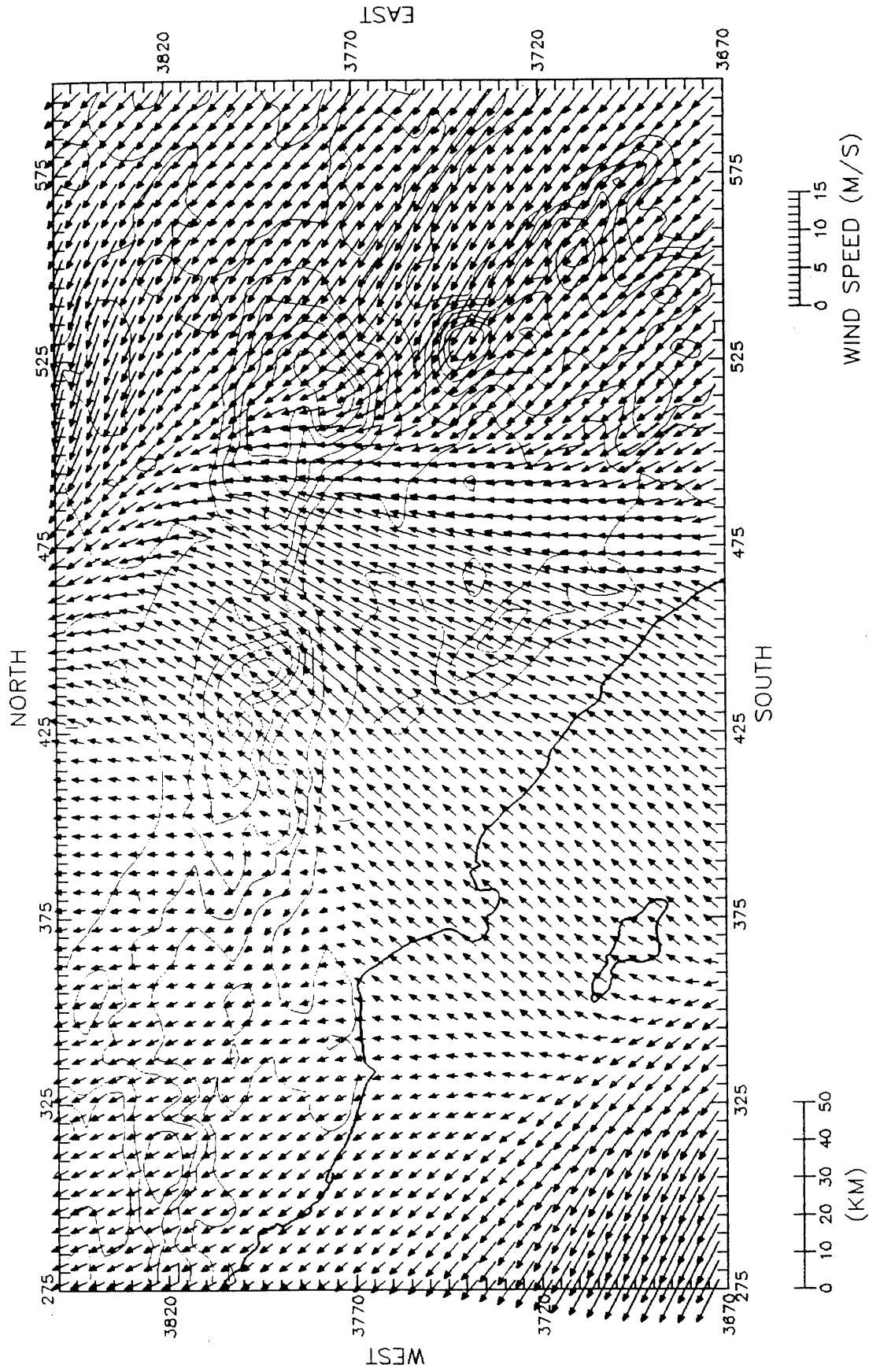
DWM WINDS AT LEVEL 3 (300M)  
 1000 PST 25JUN87

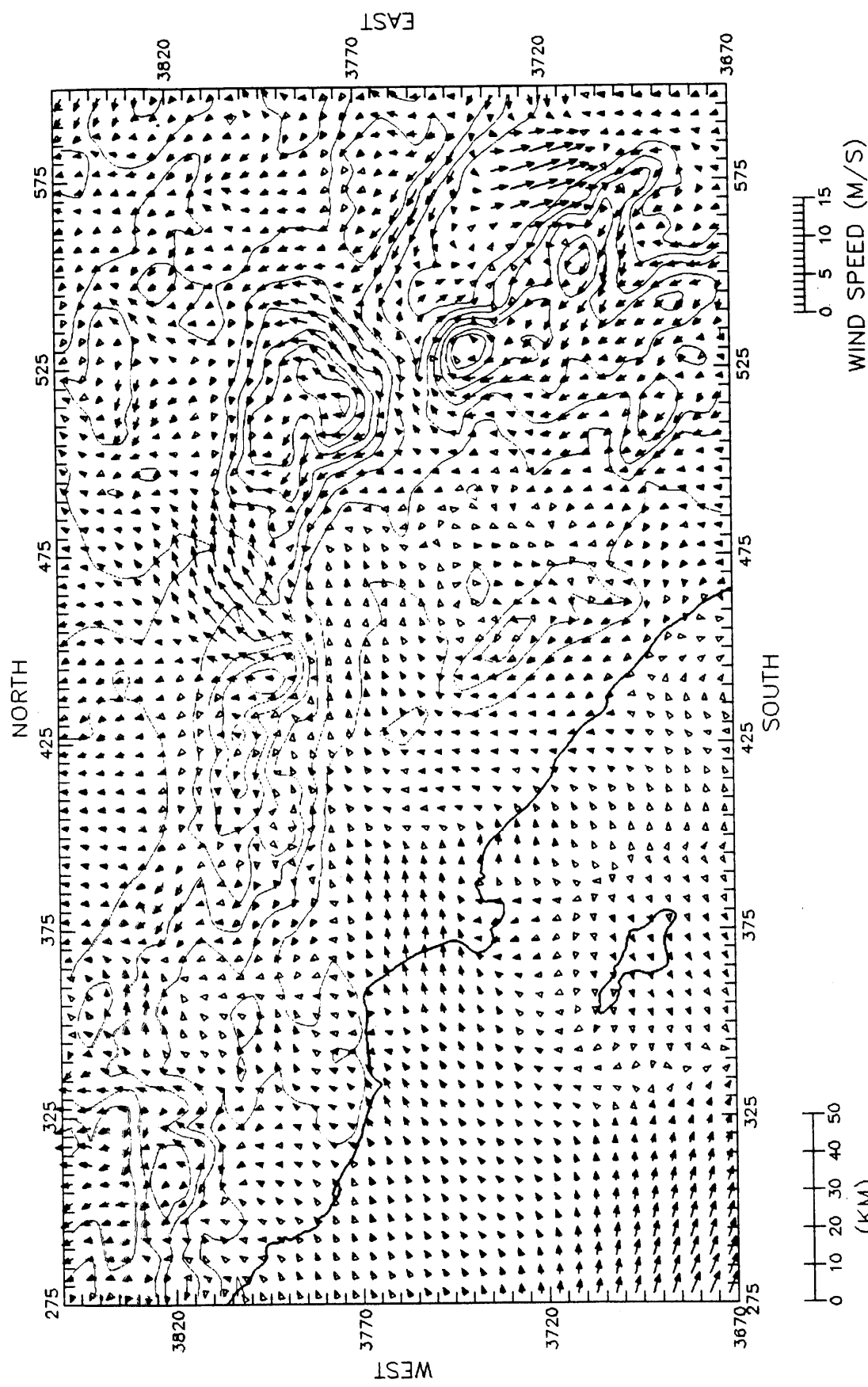


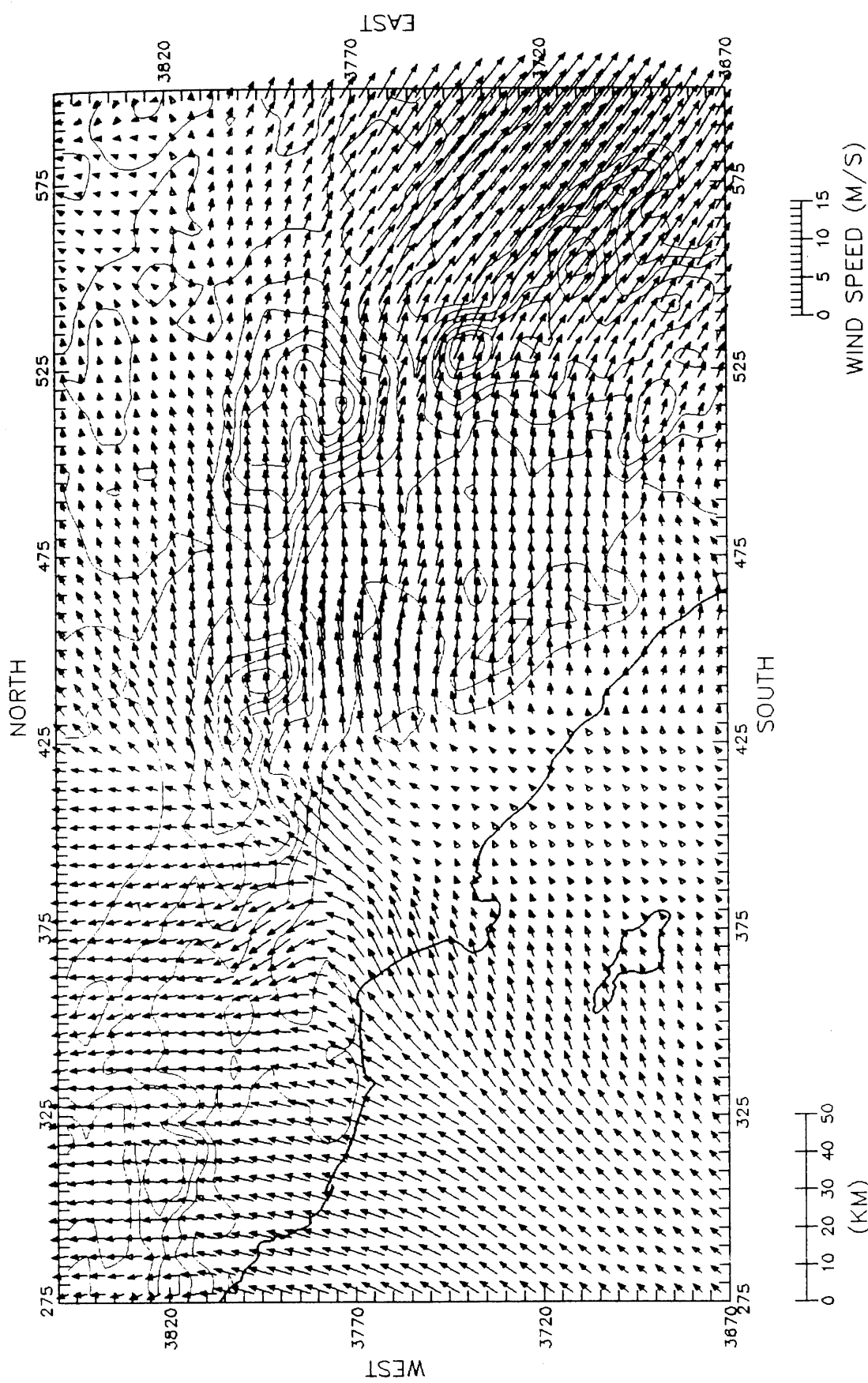
DWM WINDS AT LEVEL 5 (1000M)  
 1000 PST 25JUN87











DWM WINDS AT LEVEL 3 (300M)  
 2200 PST 25JUN87

